1989

A modular nodal method for solving the neutron transport equation using spherical harmonics in two dimensions

Feyzi Inanc
Iowa State University

Order Number 8920145

A modular nodal method for solving the neutron transport equation using spherical harmonics in two dimensions

Inanc, Feyzi, Ph.D.

Iowa State University, 1989

U·M·I
300 N. Zeeb Rd.
Ann Arbor, MI 48106

A modular nodal method for solving the neutron transport equation using spherical harmonics in two dimensions

by

Feyzi Inanc

A Dissertation Submitted to the
Graduate Faculty in Partial Fulfillment of the
Requirements for the Degree of
DOCTOR OF PHILOSOPHY

Major: Nuclear Engineering

Approved:

Signature was redacted for privacy.

In Charge of Major Work

Signature was redacted for privacy.

For the Major Department

Signature was redacted for privacy.

For the Graduate College

Members of the Committee:

Signature was redacted for privacy.

Signature was redacted for privacy.

Signature was redacted for privacy.

Signature was redacted for privacy.

Iowa State University
Ames, Iowa
1989

TABLE OF CONTENTS

LIST OF TABLES

LIST OF FIGURES

1 INTRODUCTION

The purpose of this dissertation project is to develop a coarse mesh nodal method which can be used for solving the multigroup neutron transport equation in two dimensions. The solution technique which uses a least squares minimization principle is based upon the spherical harmonics approximation to the neutron transport equation. A modular approach which can use different orders of the spherical harmonics approximation to the transport equation in the different nodes is also investigated.

Reactor physics problems usually require solution of the diffusion equation and the neutron transport equation in a rigorous manner. Except for very ideal cases, both of these equations can be solved only by numerical means. Since the early times of nuclear engineering, the traditional techniques implemented for solving the transport and the diffusion equation numerically has been finite difference methods. These methods require discretization of the problem domain into very small mesh points. Both the abundance of the variables which require consideration in the solutions and the discretization of the domain into very small mesh points usually make these fine mesh methods impractical to implement for a large majority of the problems. This problem which persists in spite of rapid developments in computer hardware has prompted efforts for developing new alternatives to fine mesh methods.

The common goal in this new research area is to improve the efficiency in both computer storage requirements and computational speeds. Although the early efforts have been directed toward achieving only these two goals, the recent developments show that the new methods compete with the fine mesh methods in the accuracy area too. The important point in the success of all of these new methods is that they all use homogenous neutronic parameters for describing the finite volumes into which the reactor cores are divided. Due to the ability of implementing relatively large mesh sizes through these methods, they are also called coarse mesh numerical methods. Two major groups which form these coarse mesh methods are the finite element methods and the nodal methods.

The finite element methods usually enjoy flexibility in solving problems in irregular domains. In contrast with that, the nodal methods usually require discretization of the problem domain into rectangular volumes. The advantage of the nodal methods is that they usually ensure neutron balance in the nodes. The earlier trends in the nodal methods have been to calculate only the average fluxes in the nodes and the multiplication factors. The recently developed nodal methods also provide local distributions of the fluxes.

The method developed in this project aims at providing the local flux distributions as well as the average nodal fluxes and the multiplication factors. It uses a least squares minimization principle for achieving its purpose. The neutron balance is provided through implementation of the boundary conditions in an integral sense. The local distributions of the fluxes are expressed in terms of fourth order Legendre polynomials. The nodal method developed for solving the neutron transport equation uses the spherical harmonics expansion for approximating the

angular dependency of the neutron flux. Although this angular dependency can be approximated by various approaches, the spherical harmonics approach offers some advantages. If the even-parity form of the transport equation is used, the spherical harmonics approach provides a set of second order differential equations analogous to the diffusion equation for which the solution techniques are well established. One other advantage is that the spherical harmonics approach does not suffer from the ray effects that the common discrete ordinates methods suffer. Although the spherical harmonics method for approximating the neutron transport equation poses difficulties in developing the higher order differential equations, an alternative way for easing this difficulty is proposed in this dissertation.

2 LITERATURE REVIEW

The modular nodal method developed in this dissertation has been constructed by utilizing the recent developments in related areas of nuclear engineering. This literature review section is intended to cover the major developments in the field. The material to be reviewed is classified into two groups. One group covers the developments in the spherical harmonics approximation to the neutron transport theory. Since the nodal method uses the spherical harmonics approximation to the neutron transport equation, the way the spherical harmonics are implemented gains importance. The other group of the reviewed literature covers the major works in the evolution of the nodal methods. The first part of that section is devoted to the progress in the nodal methods for the diffusion equation. In general, the nodal methods used for the transport equation are extensions of the methods developed for the diffusion equation. Therefore, the review of the diffusion theory methods becomes important. Finally some insight is given to the methods developed for the transport theory.

2.1 The Spherical Harmonic Methods

Although the spherical harmonic expansions have been used in other engineering fields before nuclear engineering, the first implementation of these expansions

for approximating the angular part of the angular neutron flux was done by C. Mark in 1944 [1,2]. He also proposed approximations for the boundary conditions for the spherical harmonics approach, called the Mark boundary conditions. Another important contribution to the spherical harmonics method came from R. E. Marshak in 1947 [3]. He proposed another type of approximate boundary conditions for the spherical harmonics method called the Marshak boundary conditions. They became alternatives to the Mark conditions. B. Davison has clarified some points necessary for developing the boundary conditions and he showed the relation between the order of the spherical harmonics approximation and the number of the necessary boundary conditions for a general geometry [4].

Researchers kept working to develop the generalized boundary conditions for the spherical harmonics method. Pomraning and Clark attempted to develop the right boundary conditions by using variational methods [5]. J. A. Davis developed another variational principle providing the unique boundary conditions for the spherical harmonics approximation to the neutron transport equation [6]. Another variational principle developed by Vladimirov previously surfaced about the same time as the J. A. Davis's variational principle was published [7]. This same work also introduced the even parity form of the transport equation which is utilized in this dissertation. S. Kaplan and J. A. Davis have unified the various variational principles proposed for the transport equation through some transformations and showed that these variational principles in fact are related to each other [8].

Along with the developments at the theoretical front, the practical applications also began to surface in the form of the computer codes. One of the earlier codes, which solved the P_n and double P_n equations in slab geometry, was reported by

B. Anderson [9]. Another computer code for two dimensional Cartesian geometry for the third order approximation was developed by E. Gelbard in 1962 [10]. The code reported by R. Gast had the ability to go up to ninth order approximation in slab geometry [11]. P. Daitch reported another code developed for cylindrical geometry [12]. These first generation computer codes employing the spherical harmonics approach were limited to a certain order. The complexity in developing the higher order equations for the multidimensional cases has been difficult. Due to this problem, the interest in the method has faded. A recent solution to that problem came from Fletcher [13-17]. He developed a computer routine for providing the second order spherical harmonic equations. For doing that, he assumed that the all scattering cross section terms higher than the first order are equal. Another recent work which also has the ability to generate the second order forms of the spherical harmonic equations automatically was reported by Kobayashi et al. [18].

2.2 Nodal Methods

A new era in nuclear engineering started with the introduction of analyses of the reactor cores through computer simulations. The first real computer code in this new era was the PDQ program which was developed in 1957 [19]. That computer code was based on a finite difference method. The experience in the new era of computers showed that the analyses of large reactor cores in three dimensions through the computational techniques using fine mesh discretization would be impractical. That prompted researchers to look at other alternatives which could give the means to analyze a large core in three dimensions.

The first coarse mesh method which was developed as an alternative was the

FLARE code [20]. In this code, neutronic parameters of each fuel assembly was homogenized and each node also was used as a single node which in turn was coupled to the other nodes through coupling coefficients. These coupling coefficients were obtained by using experimental data from specific reactors for which the code was used. More information about these first generation nodal methods can be found in a review paper by Gupta [21].

A new generation of the nodal methods emerged in the early 1970s. Although these new modern nodal methods have been developed at different centers, they all have some common features. The unknowns in these methods are usually the nodal average fluxes and the net or the partial currents at the nodal surfaces. The relationship between the average nodal fluxes and the surface currents are obtained through one-dimensional calculations. These one-dimensional equations are obtained through transverse integrations. The pioneer among these new methods has been the Nodal Synthesis Method developed by M. R. Wagner [22]. In this method, the flux has been assumed to be separable in a node. Then the one dimensional fine mesh calculations have been used for determining the coupling coefficients. A modification to this method later gave rise to the Nodal Expansion Method [23]. In this approach, the one-dimensional fine mesh calculations were replaced by a polynomial approximation to the one dimensional flux. The real differences between the various nodal methods have been in choosing the method for solving the one dimensional equations. A nodal method which has been developed by R. A. Shober et al. used an analytical method for solving the one dimensional equation [24]. One other method which was reported by R. D. Lawrence has implemented the Green's function method for solving the one dimensional differential equation which was

obtained through a transverse integration [25]. The review papers by Wagner and Koebke [26] and R. D. Lawrence [27] can be used for locating more information about these new generation nodal methods.

Another nodal method which does not share common features with the methods mentioned above has been developed by A. F. Rohach [28-31]. This nodal method has been used as the basis for developing the nodal method used in this dissertation. That nodal method uses a least squares minimization technique while expanding the neutron flux into Legendre polynomials. This minimization procedure provides the local flux distributions as well as the average nodal fluxes. The nodal methods have been reported to be quite successful in determining the average flux distributions and the multiplication factors with considerable efficiency when computer storage and computational speeds were considered.

The general successes of these diffusion nodal methods have prompted extension of these methods into the neutron transport equation computations. Although there are some nodal methods based upon the spherical harmonics approach, the most of the current transport nodal methods use discrete ordinate approximation to the neutron transport equation as the starting point. The first of these transport nodal methods was developed by Wagner [32]. In the method, the transport equation is reduced to one dimension by transverse integration over the node. Also the azimuthal angle is integrated out. The transverse leakage terms coming from that transverse integration is approximated by a quadratic fit over the nodal surfaces. That quadratic leakage term is assumed to be free from angular dependency as in the diffusion equation. In another group of the transport nodal methods, the transverse leakage terms are approximated by expressions which are angular depen-

dent. Methods which can be included in this class are reported by Lawrence and Dorning [33], Walters and O'Dell [34] and R. E. Pevey [35]. In addition to these nodal methods, which use the discrete-ordinates approach, there are also some nodal methods using the spherical harmonics approximation. A variational nodal method using the spherical harmonics approximations has been developed by Dilber and Lewis [36]. Another spherical harmonics nodal method based upon least squares minimization and Legendre polynomials has been developed for one-dimensional transport equation by M. Feiz [37] and Feiz and Rohach [38].

3 NEUTRON TRANSPORT THEORY

This chapter introduces the neutron transport equation and the relevant concepts. The introduction starts with the major concepts used in transport theory and then the neutron transport equation itself is introduced in the conventional integro-differential form. The transport equation can be rearranged into more than one form such as the integro-differential form, the integral transport form or the even, odd-parity transport equation form. In this dissertation project, the even-parity form of the neutron transport equation is more useful than the other forms of the transport equation. The spherical harmonics approximation to the neutron transport equation is based on the second order form of the even-parity neutron transport equation. Therefore, the even-parity form of the neutron transport equation is derived for further reference in this dissertation. The derivation of the transport equation and the definition of the concepts can be found in any major nuclear engineering textbook [39,40,41]. The following section uses the derivations and the concepts as given by Bell and Glasstone [40].

3.1 The Concepts and the Derivation of the Transport Equation

The ultimate goal in solving the neutron transport equation is to determine the distribution of the neutron population in reactor core. One important property of

the neutrons is that they are not stationary particles. They move around in different directions with various speeds as determined by their energies. In general, the number of neutrons at a given location moving in a specific direction is different from the number of neutrons heading in another direction. That directional dependency of the neutron population is affected by factors such as their location in the reactor core and the neutronic parameters of the core material. One other concept, which is also a function of the direction, is the scattering behavior of the core materials. The scattering of the neutrons from some nuclei may be oriented toward some preferable direction. In other words, we can say that the neutron population and the neutron scattering in a reactor core are functions of the direction. That direction of motion is usually expressed through a direction unit vector $\vec{\Omega}$. The general convention is to express that unit vector the spherical coordinates which are shown in the Figure 3.1. If the azimuthal angle φ and the polar angle θ are defined as in the Figure 3.1, then the unit vector $\vec{\Omega}$ is expressed by the equation 3.1 as below.

$$\vec{\Omega} = sin\theta cos\varphi\vec{i} + sin\theta sin\varphi\vec{j} + cos\theta\vec{k} \tag{3.1}$$

Another concept which comes with the direction vector $\vec{\Omega}$ is the solid angle $d\Omega$. The definition of the solid angle is given by the equation 3.2.

$$d\Omega = sin\theta d\theta d\varphi \tag{3.2}$$

The first physical concept to be introduced is the neutron angular density. The neutron angular density is basically the neutron population density at given locations and direction. That neutron angular density, the determination of which is the ultimate goal of solving the neutron transport equation, is represented by

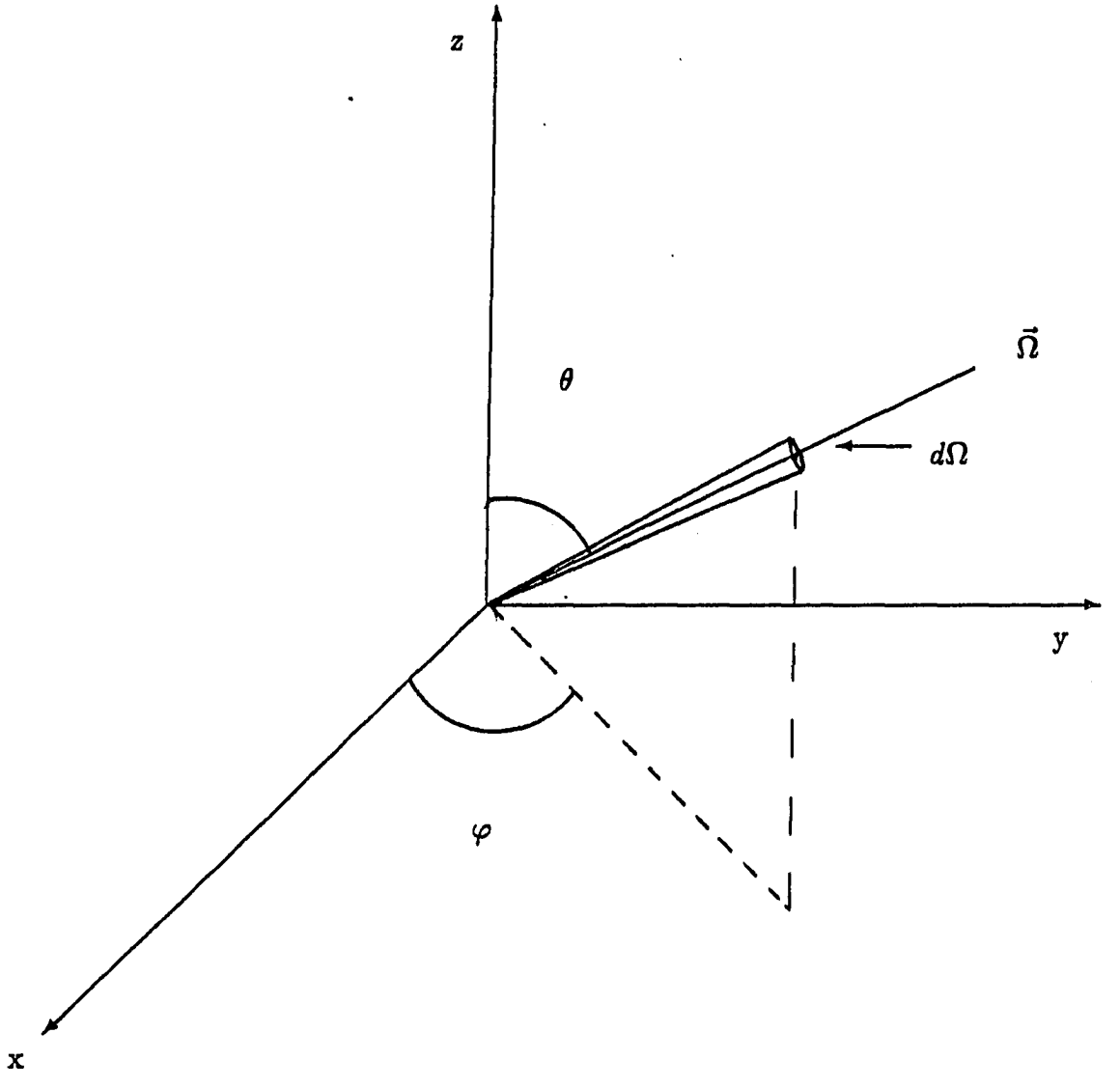

Figure 3.1: The spherical coordinates

$N(\vec{r},\vec{\Omega},E,t)$. The formal definition of that concept can be given as the probable number of neutrons at the position $\vec{r}$ with direction $\vec{\Omega}$ and energy E at time t, per unit volume per unit solid angle per unit energy. The expression $N(\vec{r},\vec{\Omega},E,t)dVd\Omega dE$ is the number of neutrons in the volume dV about $\vec{r}$, having directions within $d\Omega$ about $\vec{\Omega}$ and energies in dE about E at time t.

If the angular dependency of the angular neutron density is integrated out, we get another quantity which is known as the neutron density. This quantity is given by $n(\vec{r},E,t)$. In physical terms, this operation is basically the same as lumping together all the neutrons moving in different directions, i.e.,

$$n(\vec{r},E,t) = \int_{4\pi} N(\vec{r},\vec{\Omega},E,t)d\Omega \tag{3.3}$$

where 4π implies that the integration is over all directions.

One other quantity which also plays a major role in this discussion is the interaction cross section, σ_α. It is the probability that a neutron will have an α type interaction with the nucleus of a specific isotope, and it is known as the microscopic cross section. In practical applications, macroscopic interaction cross sections are used. The macroscopic cross section is the probability that a neutron will undergo a particular reaction in a medium in unit distance. The macroscopic cross section Σ_α is obtained by summing the microscopic cross sections for the all nuclei in a cubic centimeter. The macroscopic cross sections are usually expressed as functions of space and energy as it will be seen in equation 3.4. The unit of the macroscopic cross section is cm^{-1}. The interaction types which play major roles in the determination of the neutron populations are the fission, absorption and scattering interactions. The total cross section usually stands for the summation of all possible interaction types.

Once the interaction cross sections and the angular neutron density are defined, the angular interaction rates can be defined easily. The angular interaction rates, which determine the angular neutron density in the medium, can be defined as the product of the macroscopic cross section, the neutron speed, and the angular neutron population for the given volume dV around $\vec{r}$, in the $d\Omega$ about $\vec{\Omega}$ in the energy interval dE around E. This is defined mathematically by the following expression.

$$F_\alpha(\vec{r},\vec{\Omega},E,t) = \Sigma_\alpha(\vec{r},E)v(E)N(\vec{r},\vec{\Omega},E,t)dV\,d\Omega dE \tag{3.4}$$

The product of the neutron speed and the angular neutron density in the above expression is known as the angular neutron flux density $\Psi(\vec{r},\vec{\Omega},E,t)$. The physical meaning of $\Psi(\vec{r},\vec{\Omega},E,t)dAd\Omega dE$ is the number of neutrons passing through the area dA in $d\Omega$ about $\vec{\Omega}$ within dE at E at time t. If the angular part of that angular neutron flux density is integrated out as it done with the angular neutron density, the result is known as the total flux. Both the angular and the total neutron fluxes are scalar quantities. Although they are densities as explained above, they are usually referred as the angular neutron flux and the neutron flux.

The neutron transport equation, which uses the basic concepts given above, is given as

$$\frac{1}{v}\frac{\partial\Psi}{\partial t} + \vec{\Omega}.\nabla\Psi(\vec{r},\vec{\Omega},E,t) + \Sigma_t(\vec{r},E)\Psi(\vec{r},\vec{\Omega},E,t) = S(\vec{r},\vec{\Omega},E,t) + \int d\acute{E}\int d\acute{\Omega}\Sigma(\vec{r},\acute{E}\rightarrow E,\acute{\vec{\Omega}}\rightarrow\vec{\Omega})\Psi(\vec{r},\acute{\vec{\Omega}},\acute{E},t) \tag{3.5}$$

As is seen from equation 3.5, the dependent variable, angular neutron flux $\Psi(\vec{r},\vec{\Omega},E,t)$, is a function of space, direction, energy and time. The first term

on the left side of the transport equation exists only for the dynamic cases and it defines the change of the angular neutron density at the given location. This term is dropped for static problems as is the case in this dissertation. The second term on the left hand side is known as the streaming term. That term usually represents the moving neutrons at given directions. The third term is the total interaction density for the given location, direction, energy and time. The first term on the right side of the transport equation is the source term. This source term can be either an external source or a fission source. For the external source cases, the emitted neutrons are independent of the neutron density. In contrast with that, the fission source, which results from the fission interaction between the neutrons and the fissile nuclei, is determined by the neutron density. The second term on the right side is the contribution from the neutron scattering events. The neutrons with different directions and energies prior to the scattering may be born into the energy level E and the direction $\vec{\Omega}$ after the collision. The scattering cross section is thus actually a transfer cross section.

The usual boundary condition used with the neutron transport equation is the vacuum condition which assumes that there are no incoming neutrons from exterior regions to the problem domain. If the transport equation is solved in a volume V with the surface Γ, then the vacuum boundary condition is expressed in the following form.

$$\Psi(\vec{r},\vec{\Omega},E,t) = 0 \quad for\ \vec{n}.\vec{\Omega} < 0 \quad at\ \vec{r} \in \Gamma \tag{3.6}$$

3.2 The Even-Parity Form of the Neutron Transport Equation

The nodal method developed in this project uses the second order form of the differential equations derived through the spherical harmonics approximation to the transport equation. These second order differential equations correspond to the second order even-parity form of the neutron transport equation [7,8,42]. The formal procedure for deriving the even-parity form of the neutron transport equation is illustrated using the monoenergetic and the steady state case as given by equation 3.7.

$$\vec{\Omega}.\nabla\Psi(\vec{r},\vec{\Omega}) + \Sigma_t(\vec{r})\Psi(\vec{r},\vec{\Omega}) = \int d\acute{\Omega}\Sigma(\vec{r},\acute{\vec{\Omega}} \rightarrow \vec{\Omega})\Psi(\vec{r},\acute{\vec{\Omega}}) + S(\vec{r},\vec{\Omega}) \tag{3.7}$$

$$\Psi(\vec{r},\vec{\Omega}) = 0 \quad for\ \vec{n}.\vec{\Omega} < 0 \quad at\ \vec{r} \in \Gamma \tag{3.8}$$

The neutron transport equation given by 3.7 is valid for all directions. Since the equation is valid for all $\vec{\Omega}$'s, then the same equation should also be valid for $-\vec{\Omega}$. The neutron transport equation for this reverse direction case is expressed by equation 3.9.

$$-\vec{\Omega}.\nabla\Psi(\vec{r},-\vec{\Omega}) + \Sigma_t(\vec{r})\Psi(\vec{r},-\vec{\Omega}) = \int d\acute{\Omega}\Sigma(\vec{r},-\acute{\vec{\Omega}} \rightarrow -\vec{\Omega})\Psi(\vec{r},-\acute{\vec{\Omega}}) + S(\vec{r},-\vec{\Omega}) \tag{3.9}$$

At this point, some new quantities are introduced into the even and odd-parity equations resulting from this derivation procedure. The first two of these quantities are the even and odd-parity angular fluxes.

$$\Psi^{+}(\vec{r},\vec{\Omega}) = \frac{1}{2}\left[\Psi(\vec{r},\vec{\Omega}) + \Psi(\vec{r},-\vec{\Omega})\right] \quad even\ parity \tag{3.10}$$

$$\Psi^{-}(\vec{r},\vec{\Omega}) = \frac{1}{2}\left[\Psi(\vec{r},\vec{\Omega}) - \Psi(\vec{r},-\vec{\Omega})\right] \quad odd\ parity \tag{3.11}$$

Some important properties of these even and odd-parity fluxes are defined by the following four identities.

$$\Psi^+(\vec{r},\vec{\Omega}) = \Psi^+(\vec{r},-\vec{\Omega}) \tag{3.12}$$

$$\Psi^-(\vec{r},\vec{\Omega}) = -\Psi^-(\vec{r},-\vec{\Omega}) \tag{3.13}$$

$$\int_{4\pi} \Psi^+(\vec{r},\vec{\Omega})d\Omega = \Phi(\vec{r}) \tag{3.14}$$

$$\int_{4\pi} \Psi^-(\vec{r},\vec{\Omega})d\Omega = 0 \tag{3.15}$$

where $\Phi(\vec{r})$ is the total flux.

The even and the odd parities are defined also for the source term and the scattering cross section in the same manner as was done with the angular flux.

$$S^+(\vec{r},\vec{\Omega}) = \frac{1}{2}\left[S(\vec{r},\vec{\Omega}) + S(\vec{r},-\vec{\Omega})\right] \tag{3.16}$$

$$S^-(\vec{r},\vec{\Omega}) = \frac{1}{2}\left[S(\vec{r},\vec{\Omega}) - S(\vec{r},-\vec{\Omega})\right] \tag{3.17}$$

$$\Sigma^+(\vec{r},\dot{\vec{\Omega}} \rightarrow \vec{\Omega}) = \frac{1}{2}\left[\Sigma(\vec{r},\dot{\vec{\Omega}} \rightarrow \vec{\Omega}) + \Sigma(\vec{r},-\dot{\vec{\Omega}} \rightarrow -\vec{\Omega})\right] \tag{3.18}$$

$$\Sigma^-(\vec{r},\dot{\vec{\Omega}} \rightarrow \vec{\Omega}) = \frac{1}{2}\left[\Sigma(\vec{r},\dot{\vec{\Omega}} \rightarrow \vec{\Omega}) - \Sigma(\vec{r},-\dot{\vec{\Omega}} \rightarrow -\vec{\Omega})\right] \tag{3.19}$$

If the transport equations for the normal and the reverse directions given by 3.7 and 3.9 are added and subtracted, two new equations are obtained. The substitution of the newly defined quantities into these equations results in the two new equations given below. The first of these equations is known as the even-parity transport equation while the second one is called the odd-parity equation.

$$\vec{\Omega}.\nabla\Psi^{-}(\vec{r},\vec{\Omega}) + \Sigma_t(\vec{r})\Psi^{+}(\vec{r},\vec{\Omega}) = \int d\acute{\Omega}\Sigma^{+}(\vec{r},\acute{\vec{\Omega}} \rightarrow \vec{\Omega})\Psi^{+}(\vec{r},\acute{\vec{\Omega}}) + S^{+}(\vec{r},\vec{\Omega}) \quad (3.20)$$

$$\vec{\Omega}.\nabla\Psi^{+}(\vec{r},\vec{\Omega}) + \Sigma_t(\vec{r})\Psi^{-}(\vec{r},\vec{\Omega}) = \int d\acute{\Omega}\Sigma^{-}(\vec{r},\acute{\vec{\Omega}} \rightarrow \vec{\Omega})\Psi^{-}(\vec{r},\acute{\vec{\Omega}}) + S^{-}(\vec{r},\vec{\Omega}) \quad (3.21)$$

As can be seen from the equations 3.20 and 3.21, both the even and the odd-parity transport equations contain both the even and the odd-parity angular fluxes. At this point, we will eliminate the odd-parity angular flux from the even-parity neutron transport equation. This can be achieved by expressing $\Psi^{-}(\vec{r},\vec{\Omega})$ in terms of the even-parity quantities using equation 3.21. Then that odd angular flux is substituted into equation 3.20. The substitution results in the second order form of the even-parity neutron transport equation. Before going through the process, a new operator is defined.

$$K = \Sigma_t(\vec{r}) - \int d\acute{\Omega}\Sigma^{-}(\vec{r},\acute{\vec{\Omega}} \rightarrow \vec{\Omega}) \quad (3.22)$$

If this operator is used in the odd-parity transport equation, equation 3.21 can be rearranged as

$$\vec{\Omega}.\nabla\Psi^{+}(\vec{r},\vec{\Omega}) + K\Psi^{-}(\vec{r},\vec{\Omega}) = S^{-}(\vec{r},\vec{\Omega}) \quad (3.23)$$

If equation 3.23 is solved for the odd angular flux, the following expression is obtained.

$$\Psi^{-}(\vec{r},\vec{\Omega}) = K^{-1}\left[S^{-}(\vec{r},\vec{\Omega}) - \vec{\Omega}.\nabla\Psi^{+}(\vec{r},\vec{\Omega})\right] \quad (3.24)$$

If this expression for the odd-parity flux is substituted into equation 3.20, the second order form of the even parity neutron transport equation is obtained.

$$-\vec{\Omega}.\nabla K^{-1}\vec{\Omega}.\nabla\Psi^{+}(\vec{r},\vec{\Omega}) + \Sigma_t(\vec{r})\Psi^{+}(\vec{r},\vec{\Omega}) =$$

$$\int d\acute{\Omega}\Sigma^{+}(\vec{r},\acute{\vec{\Omega}} \rightarrow \vec{\Omega})\Psi^{+}(\vec{r},\acute{\vec{\Omega}}) + \left[S^{+}(\vec{r},\vec{\Omega}) - \vec{\Omega}.\nabla K^{-1}S^{-}(\vec{r},\vec{\Omega})\right] \tag{3.25}$$

In the even-odd parity transport equation form, the vacuum boundary conditions are also expressed in terms of the even and the odd-parity fluxes as below.

$$\left[\Psi^{+}(\vec{r},\vec{\Omega}) + \Psi^{-}(\vec{r},\vec{\Omega})\right] = 0 \quad for\ \vec{n}.\vec{\Omega} < 0 \quad at\ \vec{r} \in \Gamma \tag{3.26}$$

4 REVIEW OF THE SPHERICAL HARMONICS

The solution techniques of the neutron transport equation usually involves some kind of approximations. The spherical harmonics approximation is used in this dissertation. In this method, the angular neutron flux is approximated by the spherical harmonics. This chapter gives a short review of the spherical harmonics. A more detailed discussion of the spherical harmonics can be found in the book by Morse and Feshbach [43].

The origin of the spherical harmonic expansion lies with the solution of the Laplace equation in spherical coordinates

$$\frac{1}{r^2}\frac{\partial}{\partial r}\left(r^2\frac{\partial f}{\partial r}\right)+\frac{1}{r^2\sin\theta}\frac{\partial}{\partial\theta}\left(\sin\theta\frac{\partial f}{\partial\theta}\right)+\frac{1}{r^2\sin^2\theta}\frac{\partial^2 f}{\partial\varphi^2}=0 \tag{4.1}$$

The Laplace equation is a separable equation and the dependent variable $f(\vec{r},\theta,\varphi)$ can be expressed as the product of the three separate quantities which are functions of the space vector $\vec{r}$, the axial angle θ and the azimuthal angle φ in the spherical coordinates.

$$f(r,\theta,\varphi)=R(r)P(\theta)G(\varphi) \tag{4.2}$$

If the expression 4.2 is substituted into equation 4.1 and the separation procedure is performed, the Laplace equation in the spherical coordinates gives rise to the three following ordinary differential equations

$$\frac{1}{\sin\theta}\frac{d}{d\theta}\left(\sin\theta\frac{dP}{d\theta}\right)+\left(n(n+1)-\frac{m^2}{\sin^2\theta}\right)P(\theta)=0 \tag{4.3}$$

$$\frac{d^2G}{d\varphi^2}+m^2G(\varphi)=0 \tag{4.4}$$

$$\frac{1}{r^2}\frac{d}{dr}\left(r^2\frac{dR}{dr}\right)-\frac{n(n+1)}{r^2}R(r)=0 \tag{4.5}$$

The nature of the problem requires both n and m in equations 4.3-4.5 to be integers. For the cases where both n and m are integers and $n \geq m$, a solution to equation 4.3 is known as the associated Legendre function and it is given as

$$P_{nm}(\cos\theta)=\left(1-\cos^2\theta\right)^{\left(\frac{m}{2}\right)}\frac{d^m}{d(\cos\theta)^m}P_n(\cos\theta) \tag{4.6}$$

where:

$$P_n(\cos\theta)=\frac{1}{2^n n!}\frac{d^n}{d(\cos\theta)}\left(\cos^2\theta-1\right)^n \tag{4.7}$$

The second and the third differential equations 4.4 and 4.5 are very common in type and their solutions are given by equations 4.8 and 4.9.

$$G(\varphi)=c_1\sin m\varphi+c_2\cos m\varphi \tag{4.8}$$

$$R(r)=d_1r^n+d_2r^{-(n+1)} \tag{4.9}$$

where d_2 in equation 4.9 is zero due to the boundary conditions.

Special solutions to the Laplace equation are expressed as the product of the associated Legendre functions and the solutions of the differential differential equations 4.4 and 4.5. These are called spherical harmonics. Superposition of these solutions gives

$$f(r,\theta,\varphi) = \sum_{n=0}^{\infty} \sum_{m=0}^{n} (A_{nm} \cos m\varphi + B_{nm} \sin m\varphi) P_{nm}(\cos\theta)(\frac{r}{a})^n \qquad (4.10)$$

While any solution of differential equation 4.1 inside a sphere with a radius a can be approximated by equation 4.10, the boundary values defined over the surface of the sphere can be approximated by

$$g(\theta,\varphi) = \sum_{n=0}^{\infty} \sum_{m=0}^{n} (A_{nm} \cos m\varphi + B_{nm} \sin m\varphi) P_{nm}(cos\theta) \qquad (4.11)$$

The series given by equation 4.11 is complete in the sense that any function can be represented through that expression in an exact manner as the number of the terms goes to infinity. One of the important properties of spherical harmonics is the orthogonality property. This property introduces a considerable amount of simplification in the procedures implemented for determining the moments of the series given by equation 4.11.

5 THE SPHERICAL HARMONICS APPROXIMATION TO THE NEUTRON TRANSPORT EQUATION

Spherical harmonics, which have been reviewed previously, play an important role in nuclear reactor calculations. One of the methods used for solving the neutron transport equation is based upon these spherical harmonics. In this approach, the angular neutron flux is approximated by a spherical harmonics expansion. The method then gives rise to a set of differential equations which use the moments of the spherical harmonics expansion as the dependent variables. This chapter gives an insight into the conventional application of the spherical harmonics approximation in reactor calculations.

The conventional application of the spherical harmonics method usually results in a set of first order partial differential equations. The implementation of the spherical harmonics approximation in this dissertation deviates from that conventional approach and uses a second order form. This method is becoming popular as shown in recent publications [13-17,18,44].

5.1 The Conventional Application of the Spherical Harmonics

As has been reiterated, the spherical harmonics are used for approximating the angular dependency of the neutron flux. In this section, some details are given

about the application of this method. In order to keep the equations in a simple form, the approach used in the third section is repeated and the equations are shown for the monoenergetic and the steady state cases. The extension of the method to the multigroup form of the neutron transport equation is very straightforward and it will be shown for the recurrence relations which will be developed in this section.

The first step in the spherical harmonics method is to expand the angular neutron flux in the unnormalized spherical harmonics. This expansion represents the angular flux in an exact manner.

$$\Psi(\vec{r},\theta,\varphi) = \sum_{l=0}^{\infty}(2l+1)\sum_{m=0}^{l}\left[\Phi_{lm}(\vec{r})\cos m\varphi + \gamma_{lm}(\vec{r})\sin m\varphi\right]P_{lm}(\cos\theta) \qquad (5.1)$$

The moments Φ_{lm} and γ_{lm} in the equation 5.1 are functions of space. In the cases where the neutron transport equation is used for time and energy dependent problems, these moments are functions of time and energy as well. In usual applications, a few terms in the expansion are adequate to approximate the angular neutron flux. Therefore, the upper limit of the first summation is picked as a finite number. One important point in determining the upper limit of that first summation is to pick it as an odd number[45]. Another point, which is also worthy of some attention, is the meaning of some moments in expansion 5.1. The moment $\Phi_{00}(\vec{r})$ is known as the scalar flux. The moments $\Phi_{10}(\vec{r})$, $\Phi_{11}(\vec{r})$ and $\gamma_{11}(\vec{r})$ also correspond to some physical quantities and they represent the net neutron currents in the x, y and z directions. The match between these lower order moments and the scalar flux and the net currents is an important property of the spherical harmonics approximation. Once these moments are determined through a computational procedure, no additional calculations are required for obtaining the scalar flux and the net neutron

currents. As a result of the finite approximation, the angular neutron flux will be represented by

$$\Psi(\vec{r},\theta,\varphi) \doteq \sum_{l=0}^{N}(2l+1)\sum_{m=0}^{l}\left[\Phi_{lm}(\vec{r})\cos m\varphi + \gamma_{lm}(\vec{r})\sin m\varphi\right] P_{lm}(\cos\theta) \qquad (5.2)$$

As can be seen from equation 5.2, if the moments can be determined then the approximate angular neutron flux can be easily computed for any location and direction. The usual practice in the determination of the spherical harmonic moments is to implement a Galerkin weighted-residual scheme. In this procedure, the approximate angular neutron flux expression given by 5.2 is substituted into the neutron transport equation and then the neutron transport equation is weighted by the spherical harmonic polynomials over the whole ranges of the spherical angles θ and φ. This procedure which is shown by the following two equations

$$\int\int_{4\pi} P_{lm}(\cos\theta)\cos m\varphi\left[\vec{\Omega}.\nabla\Psi(\vec{r},\vec{\Omega}) + \Sigma_t(\vec{r})\Psi(\vec{r},\vec{\Omega})\right]\sin\theta d\theta d\varphi$$
$$-\int\int_{4\pi} P_{lm}(\cos\theta)\cos m\varphi\left[\int d\acute{\Omega}\Sigma(\vec{r},\acute{\vec{\Omega}}\rightarrow\vec{\Omega})\Psi(\vec{r},\acute{\vec{\Omega}}) + S(\vec{\Omega})\right]\sin\theta d\theta d\varphi = 0 \qquad (5.3)$$

$$\int\int_{4\pi} P_{lm}(\cos\theta)\sin m\varphi\left[\vec{\Omega}.\nabla\Psi(\vec{r},\vec{\Omega}) + \Sigma_t(\vec{r})\Psi_g(\vec{r},\vec{\Omega})\right]\sin\theta d\theta d\varphi$$
$$-\int\int_{4\pi} P_{lm}(\cos\theta)\sin m\varphi\left[\int d\acute{\Omega}\Sigma(\vec{r},\acute{\vec{\Omega}}\rightarrow\vec{\Omega})\Psi(\vec{r},\acute{\vec{\Omega}}) + S(\vec{\Omega})\right]\sin\theta d\theta d\varphi = 0 \qquad (5.4)$$

provide the correct number of equations for determining the spherical harmonic moments. One important point, which distinguishes this procedure from the common weighted-residual applications, is that the resulting expressions are first order partial differential equations while the common applications result in algebraic equations.

In the spherical harmonics method, the source on the right hand side of the neutron transport equation is also expanded into the spherical harmonics in a similar manner to the neutron flux.

$$S(\vec{r},\theta,\varphi) \doteq \sum_{l=0}^{N}(2l+1)\sum_{m=0}^{l}\left[\bar{S}_{lm}(\vec{r})\cos m\varphi + \hat{S}_{lm}(\vec{r})\sin m\varphi\right]P_{lm}(\cos\theta) \qquad (5.5)$$

One other quantity, which also requires a treatment in the spherical harmonics method, is the scattering cross section. Since the scattering cross section represents a transfer from one direction to the other, it is a function of the two different directions and as a result of that, it is approximated by an expansion which implements the addition theorem. The expansion of the scattering cross section is given

$$\Sigma(\vec{r},\vec{\Omega}' \rightarrow \vec{\Omega}) = \frac{1}{4\pi}\sum_{l=0}^{\infty}(2l+1)\Sigma_s^l(\vec{r})P_l(\vec{\Omega}'.\vec{\Omega}) \qquad (5.6)$$

where :

$$P_l(\vec{\Omega}'.\vec{\Omega}) = \sum_{m=0}^{l}[2-\delta(0-m)]\frac{(l-m)!}{(l+m)!}P_{lm}(cos\theta)P_{lm}(cos\acute{\theta})cos(m(\varphi-\acute{\varphi})) \qquad (5.7)$$

The implementation of the Galerkin weighted-residual scheme leads to recurrence relations which allow the generation of the first order differential equations for the spherical harmonic moments without going through all the derivation procedure for each weighing function separately. The development of these recurrence relations are made possible by two recurrence relations.

$$(2l+1)cos\theta P_{lm}(cos\theta) = (l-m+1)P_{l+1,m}(cos\theta) + (l+m)P_{l-1,m}(cos\theta) \qquad (5.8)$$

$$(2l+1)sin\theta P_{lm}(cos\theta) = (l+m)(l+m-1)P_{l-1,m-1}(cos\theta) - (l-m+1)(l-m+2)P_{l+1,m-1}(cos\theta) \quad (5.9)$$

If the procedure described here in general terms is carried out for Cartesian coordinates, the following two recurrence relations are obtained.

$$\begin{aligned}
&2(l+m+1)\frac{\partial\Phi_{l+1,m}}{\partial z} + 2(l-m)\frac{\partial\Phi_{l-1,m}}{\partial z} \\
&+[1+\delta(1-m)]\left[\frac{\partial\Phi_{l-1,m-1}}{\partial x} - \frac{\partial\Phi_{l+1,m-1}}{\partial x} + \frac{\partial\gamma_{l+1,m-1}}{\partial y} - \frac{\partial\gamma_{l-1,m-1}}{\partial y}\right] \\
&+(l+m+2)(l+m+1)\left[\frac{\partial\Phi_{l+1,m+1}}{\partial x} + \frac{\partial\gamma_{l+1,m+1}}{\partial y}\right] \\
&-(l-m-1)(l-m)\left[\frac{\partial\Phi_{l-1,m+1}}{\partial x} + \frac{\partial\gamma_{l-1,m+1}}{\partial y}\right] + 2(2l+1)\Sigma_t\Phi_{l,m}(x,y,z) \\
&= 2(2l+1)\Sigma_s^l\Phi_{l,m}(x,y,z) + 2(2l+1)\bar{S}_{lm}(x,y,z) \quad (5.10)
\end{aligned}$$

$$\begin{aligned}
&2(l+m+1)\frac{\partial\gamma_{l+1,m}}{\partial z} + 2(l-m)\frac{\partial\gamma_{l-1,m}}{\partial z} \\
&+[1+\delta(1-m)]\left[\frac{\partial\Phi_{l-1,m-1}}{\partial y} + \frac{\partial\gamma_{l-1,m-1}}{\partial x} - \frac{\partial\Phi_{l+1,m-1}}{\partial y} - \frac{\partial\gamma_{l+1,m-1}}{\partial x}\right] \\
&+(l+m+2)(l+m+1)\left[-\frac{\partial\Phi_{l+1,m+1}}{\partial y} + \frac{\partial\gamma_{l+1,m+1}}{\partial x}\right] \\
&-(l-m-1)(l-m)\left[\frac{\partial\gamma_{l-1,m+1}}{\partial x} - \frac{\partial\Phi_{l-1,m+1}}{\partial y}\right] + 2(2l+1)\Sigma_t\gamma_{l,m}(x,y,z) \\
&= 2(2l+1)\Sigma_s^l\gamma_{l,m}(x,y,z) + 2(2l+1)\hat{S}_{l,m}(x,y,z) \quad (5.11)
\end{aligned}$$

These two relations allow one to generate as many equations as one desires. Since the derivation of the recurrence relations is not of direct interest to this

project, it is not demonstrated. One important point which is worthy of mention is that if the moment operated on by Σ_t is an even moment where l is even, then the recurrence relations given by the equations 5.10 and 5.11 generate the spherical harmonic differential equations for the even-parity transport equation. If that moment is an odd moment, then the recurrence formulas generate the spherical harmonic differential equations for the odd-parity transport equations given by 3.21.

The recurrence relations as given by equations 5.10 and 5.11 are only for the monoenergetic case. The conversion of these relations to the multigroup form is very straightforward. In the multigroup form, the right sides of equations 5.10 and 5.11 are modified to include scattering from the other energy groups. The multigroup form of the spherical harmonic recurrence relations are given as

$$
\begin{aligned}
&2(l+m+1)\frac{\partial \Phi^g_{l+1,m}}{\partial z} + 2(l-m)\frac{\partial \Phi^g_{l-1,m}}{\partial z} + [1+\delta(1-m)]\cdot \\
&\left[\frac{\partial \Phi^g_{l-1,m-1}}{\partial x} - \frac{\partial \Phi^g_{l+1,m-1}}{\partial x} + \frac{\partial \gamma^g_{l+1,m-1}}{\partial y} - \frac{\partial \gamma^g_{l-1,m-1}}{\partial y}\right] \\
&\quad +(l+m+2)(l+m+1)\left[\frac{\partial \Phi^g_{l+1,m+1}}{\partial x} + \frac{\partial \gamma^g_{l+1,m+1}}{\partial y}\right] - \\
&\quad (l-m-1)(l-m)\left[\frac{\partial \Phi^g_{l-1,m+1}}{\partial x} + \frac{\partial \gamma^g_{l-1,m+1}}{\partial y}\right] + \\
&\quad 2(2l+1)\Sigma_{tg}\Phi^g_{l,m}(x,y,z) = \\
&2(2l+1)\sum_{h=1}^{G}\Sigma^l_{s,h\to g}\Phi^h_{l,m}(x,y,z) + 2(2l+1)\bar{S}^g_{lm}(x,y,z)
\end{aligned}
\tag{5.12}
$$

$$
2(l+m+1)\frac{\partial \gamma^g_{l+1,m}}{\partial z} + 2(l-m)\frac{\partial \gamma^g_{l-1,m}}{\partial z} + [1+\delta(1-m)]\cdot
$$

$$\left[\frac{\partial\Phi^g_{l-1,m-1}}{\partial y}+\frac{\partial\gamma^g_{l-1,m-1}}{\partial x}-\frac{\partial\Phi^g_{l+1,m-1}}{\partial y}-\frac{\partial\gamma^g_{l+1,m-1}}{\partial x}\right]$$

$$+(l+m+2)(l+m+1)\left[-\frac{\partial\Phi^g_{l+1,m+1}}{\partial y}+\frac{\partial\gamma^g_{l+1,m+1}}{\partial x}\right]-$$

$$(l-m-1)(l-m)\left[\frac{\partial\gamma^g_{l-1,m+1}}{\partial x}-\frac{\partial\Phi^g_{l-1,m+1}}{\partial y}\right]+$$

$$2(2l+1)\Sigma_{tg}\gamma^g_{l,m}(x,y,z)=$$

$$2(2l+1)\sum_{h=1}^{G}\Sigma^l_{s,h\to g}\gamma^h_{l,m}(x,y,z)+2(2l+1)\hat{S}^g_{l,m}(x,y,z) \tag{5.13}$$

where g gives the energy group number. The $\Phi^g_{lm}(x,y)$ and $\gamma^g_{lm}(x,y)$ in the above equations define the group moments. $\Sigma^l_{s,h\to g}$ is the lth coefficient of the Legendre polynomial expansion for scattering probability from group h to g.

Equations 5.12 and 5.13 generate the spherical harmonic differential equations for the three-dimensional case. The reduction of the resulting equations to the two-dimensional case is done in the following manner. The first step in the modification of these recurrence relations which provide $(N+1)^2$ partial differential equations is to eliminate all the terms which involves derivatives with respect to the z direction. Once this is done, then the symmetry condition is used for eliminating the other moments which are not to be used in the X-Y geometry. The rule of thumb which results from that condition, is that all moments with odd m when l = *even* and all moments with even m when l = *odd* are eliminated from the three-dimensional equations. In the following part, the conventional P_3 approximation differential equations are shown for demonstrating the idea described above. As it is done here, the P_3 approximation will be used for demonstrating the ideas described.

$$\frac{\partial \Phi_{11}}{\partial x} + \frac{\partial \gamma_{11}}{\partial y} + \Sigma_t \Phi_{00} = \Sigma_s^0 \Phi_{00} + \bar{S}_{00} \tag{5.14}$$

$$\frac{\partial \Phi_{00}}{\partial x} - \frac{\partial \Phi_{20}}{\partial x} + 6\frac{\partial \Phi_{22}}{\partial x} + 6\frac{\partial \gamma_{22}}{\partial y} + 3\Sigma_t \Phi_{11} = 3\Sigma_s^1 \Phi_{11} + 3\bar{S}_{11} \tag{5.15}$$

$$\frac{\partial \Phi_{00}}{\partial y} - \frac{\partial \Phi_{20}}{\partial y} - 6\frac{\partial \Phi_{22}}{\partial y} + 6\frac{\partial \gamma_{22}}{\partial x} + 3\Sigma_t \gamma_{11} = 3\Sigma_s^1 \gamma_{11} + 3\hat{S}_{11} \tag{5.16}$$

$$6\frac{\partial \Phi_{31}}{\partial x} + 6\frac{\partial \gamma_{31}}{\partial y} - \frac{\partial \Phi_{11}}{\partial x} - \frac{\partial \gamma_{11}}{\partial y} + 5\Sigma_t \Phi_{20} = 5\Sigma_s^2 \Phi_{20} + 5\bar{S}_{20} \tag{5.17}$$

$$\frac{\partial \Phi_{11}}{\partial x} - \frac{\partial \Phi_{31}}{\partial x} + \frac{\partial \gamma_{31}}{\partial y} - \frac{\partial \gamma_{11}}{\partial y} + 30\frac{\partial \Phi_{33}}{\partial x} + 30\frac{\partial \gamma_{33}}{\partial y} + 10\Sigma_t \Phi_{22} = 10\Sigma_s^2 \Phi_{22} + 10\bar{S}_{22} \tag{5.18}$$

$$\frac{\partial \Phi_{11}}{\partial y} - \frac{\partial \Phi_{31}}{\partial y} - \frac{\partial \gamma_{31}}{\partial x} + \frac{\partial \gamma_{11}}{\partial x} - 30\frac{\partial \Phi_{33}}{\partial y} + 30\frac{\partial \gamma_{33}}{\partial x} + 10\Sigma_t \gamma_{22} = 10\Sigma_s^2 \gamma_{22} + 10\hat{S}_{22} \tag{5.19}$$

$$\frac{\partial \Phi_{20}}{\partial x} - \frac{\partial \Phi_{22}}{\partial x} - \frac{\partial \gamma_{22}}{\partial y} + 7\Sigma_t \Phi_{31} = 7\Sigma_s^3 \Phi_{31} + 7\bar{S}_{31} \tag{5.20}$$

$$\frac{\partial \Phi_{20}}{\partial y} + \frac{\partial \Phi_{22}}{\partial y} - \frac{\partial \gamma_{22}}{\partial x} + 7\Sigma_t \gamma_{31} = 7\Sigma_s^3 \gamma_{31} + 7\hat{S}_{31} \tag{5.21}$$

$$\frac{\partial \Phi_{22}}{\partial x} - \frac{\partial \gamma_{22}}{\partial y} + 14\Sigma_t \Phi_{33} = 14\Sigma_s^3 \Phi_{33} + 14\bar{S}_{33} \tag{5.22}$$

$$\frac{\partial \Phi_{22}}{\partial y} + \frac{\partial \gamma_{22}}{\partial x} + 14\Sigma_t \gamma_{33} = 14\Sigma_s^3 \gamma_{33} + 14\hat{S}_{33} \tag{5.23}$$

The differential equations 5.14, 5.17, 5.18 and 5.19 in the above differential equation set represent the even-parity transport equation while the rest of the six differential equations represent the odd-parity transport equation.

5.2 The Second Order Form of the Spherical Harmonics Method

In this section, the second order form of the spherical harmonics method is introduced. The approach used is to manipulate the spherical harmonic equations into a form which corresponds to the second order form of the even-parity neutron transport equations as shown by equation 3.25. The second order form of the spherical harmonic equations offers some important advantages. In the second order form, only the even moments are determined through the computational procedure. If the odd moments are needed, they can be computed by using the approach described by equation 3.24. This introduces a significant amount of reduction in the number of the spherical harmonic moments to be determined. Another important advantage is that the second order form of the spherical harmonic equations is a familiar differential equation. In this second order form, only four types of operators are seen. One of these operators is the Laplace operator. When the coupled differential equations are decoupled and solved iteratively in the manner which will be described below, the left side of the differential equations become analogous to the neutron diffusion equation. The solution techniques for that type of equation are readily available. One other advantage is that the second order form allows the generation of any order equations in an automatic manner.

The even spherical harmonic moments can be used to form the spherical harmonic approximation to the even-parity angular flux. The spherical harmonic expansions approximating the even and the odd-parity angular neutron fluxes are given by equations 5.24 and 5.25. If the odd-parity angular flux needs to be known, the odd moments can be determined by using the recurrence formulas 5.12 and 5.13. The procedure of solving the second order form of the spherical harmonic

equations and then determining the odd moments by using equations 5.12 and 5.13 corresponds to solving equation 3.25 for the even-parity angular flux and then determining the odd-parity angular flux by using equation 3.24.

$$\Psi^{+}(\vec{r},\vec{\Omega}) = \sum_{\substack{l=0 \\ l=even}}^{\infty} (2l+1) \cdot \sum_{m=0}^{l} \left[\Phi(\vec{r})_{lm} \cos m\varphi + \gamma(\vec{r})_{lm} \sin m\varphi\right] P_{lm}(\cos\theta) \tag{5.24}$$

$$\Psi^{-}(\vec{r},\vec{\Omega}) = \sum_{\substack{l=1 \\ l=odd}}^{\infty} (2l+1) \sum_{m=0}^{l} \left[\Phi(\vec{r})_{lm} \cos m\varphi + \gamma(\vec{r})_{lm} \sin m\varphi\right] P_{lm}(\cos\theta) \tag{5.25}$$

If the expansions are truncated at some odd N, then the approximate expressions are given by the following two forms.

$$\Psi^{+}(\vec{r},\vec{\Omega}) \doteq \sum_{\substack{l=0 \\ l=even}}^{N-1} (2l+1) \sum_{m=0}^{l} \left[\Phi(\vec{r})_{lm} \cos m\varphi + \gamma(\vec{r})_{lm} \sin m\varphi\right] P_{lm}(\cos\theta) \tag{5.26}$$

$$\Psi^{-}(\vec{r},\vec{\Omega}) \doteq \sum_{\substack{l=1 \\ l=odd}}^{N} (2l+1) \sum_{m=0}^{l} \left[\Phi(\vec{r})_{lm} \cos m\varphi + \gamma(\vec{r})_{lm} \sin m\varphi\right] P_{lm}(\cos\theta) \tag{5.27}$$

The main idea in developing the second order form spherical harmonic procedure is to strip off the odd moments from the spherical harmonic equations. This would reduce the amount of required storage for a computer code which will implement the numerical method to be used for solving the equations. One way to develop such a procedure is to go through the same Galerkin weighted-residual method as has been done for the conventional spherical harmonics method. The conventional form of the neutron transport equation in equations 5.3 and 5.4 would have been replaced by the second order even-parity form of the transport equation given by 3.25. Such a procedure has been reported by Kobayashi et al. [18] and Kobayashi [44] for space dependent neutronic parameters case. In our application, instead of going through that weighted-residual scheme, which would prove to be quite time consuming in its development stage, a short cut was used. In this project, the conventional forms of the spherical harmonic recurrence relations were used for deriving the second order form of the spherical harmonic equations for the isotropic source and the homogenous regions. If the first order differential equations are generated for the case (l, m) where l is even, the recurrence formulas 5.12 and 5.13 would contain the moments Φ's and γ's for $(l+1, m+1)$, $(l+1, m-1)$, $(l-1, m+1)$ and $(l-1, m-1)$. These would make up the odd moments in the equations. In the development of the second order form, the first order equations were generated for these eight odd moments and then they were substituted into the equation generated for (l, m) where l is even. Although this procedure is a very tedious operation, it has been achieved easily by utilizing the symbolic processor MACSYMA [46] and the recurrence relations developed for the conventional spherical harmonics approach gave rise to the two recurrence relations for the sec-

ond order spherical harmonic equations. These recurrence relations are valid for all cases for $l > 0$. The differential equation for $l = 0$ can not be generated through the recurrence formulas developed here. As a result, the equations which will be used in the determination of the even order spherical harmonic moments can be given by the following expressions for the monoenergetic case.

$$L_0\Phi_{00}(x,y) + \nabla^2\Phi_{20} - 6\left[\frac{\partial^2}{\partial x^2} - \frac{\partial^2}{\partial y^2}\right]\Phi_{22} - 12\frac{\partial^2}{\partial x \partial y}\gamma_{22} = 3\Sigma_1 S_{00}(x,y) \tag{5.28}$$

$$L_1\Phi_{lm}(x,y) - \nabla^2\,[B]\,[\Phi]_1 - \left[\frac{\partial^2}{\partial x^2} - \frac{\partial^2}{\partial y^2}\right][C]\,[\Phi]_2 - \frac{\partial^2}{\partial x \partial y}\left[\acute{D}\right][\gamma]_1 = 0 \tag{5.29}$$

$$L_2\gamma_{lm}(x,y) - \nabla^2\left[\acute{B}\right][\gamma]_2 - \left[\frac{\partial^2}{\partial x^2} - \frac{\partial^2}{\partial y^2}\right]\left[\acute{C}\right][\gamma]_3 - \frac{\partial^2}{\partial x \partial y}[D]\,[\Phi]_3 = 0 \tag{5.30}$$

The operators L_0, L_1 and L_2 which were used in the equations 5.28, 5.29 and 5.30, are given by the following expressions.

$$L_0 = -\nabla^2 + 3\Sigma_0\Sigma_1 \tag{5.31}$$

$$L_1 = (A_1\Sigma_{l-1} + A_2\Sigma_{l+1})\nabla^2 + A_3\Sigma_{l-1}\Sigma_l\Sigma_{l+1} \tag{5.32}$$

$$L_2 = (\acute{A}_1\Sigma_{l-1} + \acute{A}_2\Sigma_{l+1})\nabla^2 + \acute{A}_3\Sigma_{l-1}\Sigma_l\Sigma_{l+1} \tag{5.33}$$

where :

$$\Sigma_l = \Sigma_t - \dot{\Sigma}_s^l \tag{5.34}$$

The $[B]$, $[C]$, $[D]$, $\left[\dot{B}\right]$, $\left[\dot{C}\right]$, $\left[\dot{D}\right]$, $[\Phi]_1^T$, $[\Phi]_2^T$, $[\Phi]_3^T$, $[\gamma]_1^T$, $[\gamma]_2^T$, $[\gamma]_3^T$ are column vectors. Their products $[B][\Phi]_1$, $[C][\Phi]_2$, $[D][\Phi]_3$, $\left[\dot{B}\right][\gamma]_1$, $\left[\dot{C}\right][\gamma]_2$ and $\left[\dot{D}\right][\gamma]_3$ used in 5.28, 5.29 and 5.30 are defined as

$$[B][\Phi]_1 = B_1\Sigma_{l+1}\Phi_{l-2,m}(x,y) + B_2\Sigma_{l-1}\Phi_{l+2,m}(x,y) \tag{5.35}$$

$$\begin{aligned}
[C][\Phi]_2 \;=\; & C_1\Sigma_{l+1}\Phi_{l-2,m-2}(x,y) + C_2\Sigma_{l+1}\Phi_{l-2,m+2}(x,y) + \\
& (C_3\Sigma_{l-1} + C_4\Sigma_{l+1})\Phi_{l,m-2}(x,y) + \\
& (C_5\Sigma_{l-1} + C_6\Sigma_{l+1})\Phi_{l,m+2}(x,y) + \\
& C_7\Sigma_{l-1}\Phi_{l+2,m-2}(x,y) + C_8\Sigma_{l-1}\Phi_{l+2,m+2}(x,y)
\end{aligned} \tag{5.36}$$

$$\begin{aligned}
[D][\Phi]_3 \;=\; & D_1\Sigma_{l+1}\Phi_{l-2,m-2}(x,y) + D_2\Sigma_{l+1}\Phi_{l-2,m+2}(x,y) + \\
& (D_3\Sigma_{l-1} + D_4\Sigma_{l+1})\Phi_{l,m-2}(x,y) + \\
& (D_5\Sigma_{l-1} + D_6\Sigma_{l+1})\Phi_{l,m+2}(x,y) + \\
& D_7\Sigma_{l-1}\Phi_{l+2,m-2}(x,y) + D_8\Sigma_{l-1}\Phi_{l+2,m+2}(x,y)
\end{aligned} \tag{5.37}$$

$$\left[\dot{B}\right][\gamma]_1 = \dot{B}_1\Sigma_{l+1}\gamma_{l-2,m}(x,y) + \dot{B}_2\Sigma_{l-1}\gamma_{l+2,m}(x,y) \tag{5.38}$$

$$
\begin{aligned}
\left[\acute{C}\right][\gamma]_2 \;=\; & \acute{C}_1\Sigma_{l+1}\gamma_{l-2,m-2}(x,y) + \acute{C}_2\Sigma_{l+1}\gamma_{l-2,m+2}(x,y) + \\
& (\acute{C}_3\Sigma_{l-1} + \acute{C}_4\Sigma_{l+1})\gamma_{l,m-2}(x,y) + \\
& (\acute{C}_5\Sigma_{l-1} + \acute{C}_6\Sigma_{l+1})\gamma_{l,m+2}(x,y) + \\
& \acute{C}_7\Sigma_{l-1}\gamma_{l+2,m-2}(x,y) + \acute{C}_8\Sigma_{l-1}\gamma_{l+2,m+2}(x,y)
\end{aligned} \tag{5.39}
$$

$$
\begin{aligned}
\left[\acute{D}\right][\gamma]_2 \;=\; & \acute{D}_1\Sigma_{l+1}\gamma_{l-2,m-2}(x,y) + \acute{D}_2\Sigma_{l+1}\gamma_{l-2,m+2}(x,y) + \\
& (\acute{D}_3\Sigma_{l-1} + \acute{D}_4\Sigma_{l+1})\gamma_{l,m-2}(x,y) + \\
& (\acute{D}_5\Sigma_{l-1} + \acute{D}_6\Sigma_{l+1})\gamma_{l,m+2}(x,y) + \\
& \acute{D}_7\Sigma_{l-1}\gamma_{l+2,m-2}(x,y) + \acute{D}_8\Sigma_{l-1}\gamma_{l+2,m+2}(x,y)
\end{aligned} \tag{5.40}
$$

The constants A_i's, B_i's, C_i's, $\acute{A}_i$'s, $\acute{B}_i$'s, $\acute{C}_i$'s in the recurrence relations above can be generated as functions of spherical harmonic indices l and m by using the expressions given in the Appendix.

In the two-dimensional Cartesian geometry, the number of second order simultaneous differential equations is defined by the following expression.

$$
\textit{Number of the Equations} \;=\; \sum_{\substack{l=1 \\ l=odd}}^{N} l \tag{5.41}
$$

As it can be seen from the above formula, the number of the differential equations which will be solved simultaneously increase very rapidly. Although the lower order approximations do not pose any problem, the higher order approximations may result in very large matrices if simultaneous solution techniques are adapted.

The solution technique adapted in this research is an iterative scheme which resembles the Gauss-Seidel method if the differential equations are assumed to be linear algebraic equations. In that iterative scheme, the first step is to assume that all the moments, which are not operated on by the operators L_0, L_1 or L_2, are known quantities. As a result, all of the moments assumed to be known can be transferred to the right side of the equations. Once this is done, a set of initial guesses was formed for all the moments for which we are seeking a solution. The equations were solved by starting with the ones which have the lower order moments as the dependent variables. The values of the moments obtained from the last iteration were substituted into the equations for the following iterations. The final forms of the spherical harmonic differential equations which allow the described iterative scheme to be implemented are

$$L_0\Phi_{00}(x,y) = 3\Sigma_1 S_{00}(x,y) - \nabla^2\Phi_{20} + 6\left[\frac{\partial^2}{\partial x^2} - \frac{\partial^2}{\partial y^2}\right]\Phi_{22} + 12\frac{\partial^2}{\partial x \partial y}\gamma_{22} \tag{5.42}$$

$$L_1\Phi_{lm}(x,y) = \nabla^2\,[B]\,[\Phi]_1 + \left[\frac{\partial^2}{\partial x^2} - \frac{\partial^2}{\partial y^2}\right][C]\,[\Phi]_2 + \frac{\partial^2}{\partial x \partial y}\left[\acute{D}\right][\gamma]_1 \tag{5.43}$$

$$L_2\gamma_{lm}(x,y) = \nabla^2\left[\acute{B}\right][\gamma]_2 + \left[\frac{\partial^2}{\partial x^2} - \frac{\partial^2}{\partial y^2}\right]\left[\acute{C}\right][\gamma]_3 + \frac{\partial^2}{\partial x \partial y}[D]\,[\Phi]_3 \tag{5.44}$$

The following four equations constitute the second order form of P_3 approximation to the monoenergetic neutron transport equation.

$$-\nabla^2\Phi_{00} + 3\Sigma_0\Sigma_1\Phi_{00}(x,y) = 3\Sigma_1 S_{00}(x,y) - \nabla^2\Phi_{20} + 6\left[\frac{\partial^2}{\partial x^2} - \frac{\partial^2}{\partial y^2}\right]\Phi_{22} + 12\frac{\partial^2}{\partial x\partial y}\gamma_{22} \tag{5.45}$$

$$-(36\Sigma_1 + 14\Sigma_3)\nabla^2\Phi_{20} + 210\Sigma_1\Sigma_2\Sigma_3\Phi_{20}(x,y) = -14\Sigma_3\nabla^2\Phi_{00} - (36\Sigma_1 + 84\Sigma_3)\left[\frac{\partial^2}{\partial x^2} - \frac{\partial^2}{\partial y^2}\right]\Phi_{22} - (72\Sigma_1 + 168\Sigma_3)\frac{\partial^2}{\partial x\partial y}\gamma_{22} \tag{5.46}$$

$$-(48\Sigma_1 + 42\Sigma_3)\nabla^2\Phi_{22} + 210\Sigma_1\Sigma_2\Sigma_3\Phi_{22}(x,y) = 7\Sigma_3\left[\frac{\partial^2}{\partial x^2} - \frac{\partial^2}{\partial y^2}\right]\Phi_{00} - (3\Sigma_1 + 7\Sigma_3)\left[\frac{\partial^2}{\partial x^2} - \frac{\partial^2}{\partial y^2}\right]\Phi_{20} \tag{5.47}$$

$$-(48\Sigma_1 + 42\Sigma_3)\nabla^2\gamma_{22} + 210\Sigma_1\Sigma_2\Sigma_3\gamma_{22}(x,y) = 14\Sigma_3\frac{\partial^2}{\partial x\partial y}\Phi_{00} - (6\Sigma_1 + 14\Sigma_3)\frac{\partial^2}{\partial x\partial y}\Phi_{20} \tag{5.48}$$

If the four equations are compared to the ten equations given for the P_3 approximation in the conventional spherical harmonics section, the advantage of using the second order form over the conventional method becomes apparent.

6 THE BOUNDARY CONDITIONS FOR THE SPHERICAL HARMONICS METHOD

The spherical harmonic boundary conditions used in this project differs from the main stream application of the spherical harmonic boundary conditions. The idea used in this work is to manipulate the boundary conditions into such a form that they can be used both for external and internal boundaries without any modification. In contrast with that, the usual applications of the boundary conditions for the second order form of the spherical harmonic method in the available literature do not allow such an approach. The technique which will be summarized here is one of the most common implementations of the spherical harmonics boundary conditions [13-16,18]. As will be seen from this summary, the external and the internal boundary conditions will be implemented in different ways.

The simulation of the reflective external boundary conditions is carried out by setting the derivatives of the even moments at normal direction to the boundaries equal to zero. The odd moments at the reflective boundaries are set equal to zero. This usually allows the reflective boundary conditions to be represented in an exact manner. The simulation of the vacuum conditions can not be done in an exact manner and it poses difficulties. What is commonly done for representing the vacuum boundary conditions is to set all the moments except Φ_{00} equal to zero

at the vacuum boundaries. For Φ_{00}, the diffusion equation boundary condition incoming partial current is set equal to zero. This method is reported to work fine if the values of the moments at the boundaries are not needed. If the values of the moments at the vacuum boundaries need to be known, then the vacuum boundary is surrounded by a pure absorber material and all moments are set equal to zero at the outer boundary. The drawback of this application is that this treatment introduces an extra region for which all the calculations must be done in addition to the real problem domain calculations. The treatment of the internal boundary conditions or the interface conditions are done by making all the moments, both even and odd, continuous across these material interfaces. As can be seen from this summary, the treatment involves the utilization of the odd moments. This requires that these odd moments are to be computed at some points in the computational procedure. This introduces some extra computations which will increase overall execution time for any given problem.

The boundary condition used in this work is based upon the variational principle derived by Davis [6]. He derives the following boundary condition from that variational principle for the vacuum boundary condition.

$$\int_{\vec{n}.\vec{\Omega}<0} \vec{n}.\vec{\Omega} Y_{lm}(\Psi + \chi) d\Omega = 0 \tag{6.1}$$

If the notation is converted to the one used in this dissertation, that boundary condition can be expressed by

$$\int_{\vec{n}.\vec{\Omega}<0} \vec{n}.\vec{\Omega} \left[\Psi^{+}(\vec{r},\vec{\Omega}) + \Psi^{-}(\vec{r},\vec{\Omega})\right] P_{lm}(cos\theta)cos(m\varphi)sin\theta d\theta d\varphi = 0 \tag{6.2}$$

$$\int_{\vec{n}.\vec{\Omega}<0} \vec{n}.\vec{\Omega} \left[\Psi^{+}(\vec{r},\vec{\Omega}) + \Psi^{-}(\vec{r},\vec{\Omega})\right] P_{lm}(cos\theta)sin(m\varphi)sin\theta d\theta d\varphi = 0 \tag{6.3}$$

In the rest of this dissertation, the boundary conditions based upon the expression given by the equation 6.2 will be called the first type boundary conditions, while the ones based on the equation 6.3 will be called the second type conditions.

Although the vacuum condition is the most common boundary condition for the neutron transport equation, we can generalize that boundary condition by assuming that the condition is actually equal to a function f at the boundary as given below.

$$\Psi(\vec{r},\vec{\Omega}) = f(\vec{r},\vec{\Omega}) \quad for\ \vec{n}.\vec{\Omega} < 0 \quad at\ \vec{r} \in \Gamma \tag{6.4}$$

Since the function f in equation 6.4 can take any value, it allows us to use that boundary condition at the material interfaces as well as the external boundaries. As a result, the generalized forms of the boundary conditions to be used are given as

$$\int_{\vec{n}.\vec{\Omega}<0} \vec{n}.\vec{\Omega} \left[\Psi^{+}(\vec{r},\vec{\Omega}) + \Psi^{-}(\vec{r},\vec{\Omega})\right] P_{lm}(cos\theta)cos(m\varphi)sin\theta d\theta d\varphi = f_{lm} \tag{6.5}$$

$$\int_{\vec{n}.\vec{\Omega}<0} \vec{n}.\vec{\Omega} \left[\Psi^{+}(\vec{r},\vec{\Omega}) + \Psi^{-}(\vec{r},\vec{\Omega})\right] P_{lm}(cos\theta)sin(m\varphi)sin\theta d\theta d\varphi = g_{lm} \tag{6.6}$$

The first step in the manipulation of the boundary conditions is to replace the even and the odd-parity angular fluxes in equations 6.5 and 6.6 by the spherical harmonic expansions 5.26 and 5.27. This gives rise to boundary condition expressions involving both the even and the odd moments of the spherical harmonic expansion. As was described in Chapter 5, the general approach in the spherical harmonics method is to eliminate all the odd moments from the calculations. This same approach is adapted for the manipulation of the boundary conditions. The odd moments in the boundary conditions 6.5 and 6.6 can be eliminated by using the recurrence relations 5.10 and 5.11 for the isotropic source case. If the boundary

conditions given by 6.5 and 6.6 are evaluated for the boundary of a square region perpendicular to the x direction, the following expressions are obtained.

$$\int_{\vec{n}.\vec{\Omega}<0} \vec{n}.\vec{\Omega}\left[\Psi^{+}(\vec{r},\vec{\Omega})+\Psi^{-}(\vec{r},\vec{\Omega})\right] P_{lm}(cos\theta)cos(m\varphi)sin\theta d\theta d\varphi =$$
$$\sum_{\substack{j=0 \\ j=even}}^{N-1} \sum_{k=0}^{j} \left(b_{1,jk}\Phi_{jk} + b_{2,jk}\frac{\partial \Phi_{jk}}{\partial x} \right) + \sum_{\substack{j=2 \\ j=even}}^{N-1} \sum_{k=1}^{j} c_{jk}\frac{\partial \gamma_{jk}}{\partial y} \tag{6.7}$$

$$\int_{\vec{n}.\vec{\Omega}<0} \vec{n}.\vec{\Omega}\left[\Psi^{+}(\vec{r},\vec{\Omega})+\Psi^{-}(\vec{r},\vec{\Omega})\right] P_{lm}(cos\theta)sin(m\varphi)sin\theta d\theta d\varphi =$$
$$\sum_{\substack{j=2 \\ j=even}}^{N-1} \sum_{k=1}^{j} \left(\acute{b}_{1,jk}\gamma_{jk} + \acute{b}_{2,jk}\frac{\partial \gamma_{jk}}{\partial x} \right) + \sum_{\substack{j=0 \\ j=even}}^{N-1} \sum_{k=0}^{j} \acute{c}_{jk}\frac{\partial \Phi_{jk}}{\partial y} \tag{6.8}$$

If these expressions are modified for the two dimensional Cartesian coordinates, then the following two final forms are obtained.

$$\int_{\vec{n}.\vec{\Omega}<0} \vec{n}.\vec{\Omega}\left[\Psi^{+}(\vec{r},\vec{\Omega})+\Psi^{-}(\vec{r},\vec{\Omega})\right] P_{lm}(cos\theta)cos(m\varphi)sin\theta d\theta d\varphi =$$
$$\sum_{\substack{j=0 \\ j=even}}^{N-1} \sum_{\substack{k=0 \\ k=even}}^{j} \left(b_{1,jk}\Phi_{jk} + b_{2,jk}\frac{\partial \Phi_{jk}}{\partial x} \right) + \sum_{\substack{j=2 \\ j=even}}^{N-1} \sum_{\substack{k=2 \\ k=even}}^{j} c_{jk}\frac{\partial \gamma_{jk}}{\partial y} \tag{6.9}$$

$$\int_{\vec{n}.\vec{\Omega}<0} \vec{n}.\vec{\Omega}\left[\Psi^{+}(\vec{r},\vec{\Omega})+\Psi^{-}(\vec{r},\vec{\Omega})\right] P_{lm}(cos\theta)sin(m\varphi)sin\theta d\theta d\varphi =$$
$$\sum_{\substack{j=2 \\ j=even}}^{N-1} \sum_{\substack{k=2 \\ k=even}}^{j} \left(\acute{b}_{1,jk}\gamma_{jk} + \acute{b}_{2,jk}\frac{\partial \gamma_{jk}}{\partial x} \right) + \sum_{\substack{j=0 \\ j=even}}^{N-1} \sum_{\substack{k=0 \\ k=even}}^{j} \acute{c}_{jk}\frac{\partial \Phi_{jk}}{\partial y} \tag{6.10}$$

The boundary conditions for the surfaces perpendicular to the y direction can be derived in a similar manner. The coefficients $b_{1,jk}$'s, $b_{2,jk}$'s and c_{jk}'s contain the odd order cross sections Σ_j's.

As can be seen from the two boundary conditions 6.9 and 6.10 given above, they are combinations of the mixed type boundary conditions for each moment. One problem with these boundary conditions is that they have derivatives with respect to the directions tangent to the surface at which the boundary conditions are to be evaluated. Since the tangential terms coming from two sides of the material interfaces can not be set equal to each other due to the physical considerations, these terms are dropped from the boundary conditions.

$$\int_{\vec{n}.\vec{\Omega}<0} \vec{n}.\vec{\Omega} \left[\Psi^+(\vec{r},\vec{\Omega}) + \Psi^-(\vec{r},\vec{\Omega})\right] P_{lm}(cos\theta)cos(m\varphi)sin\theta d\theta d\varphi \doteq \sum_{\substack{j=0 \\ j=even}}^{N-1} \sum_{\substack{k=0 \\ k=even}}^{j} \left(b_{1,jk}\Phi_{jk} + b_{2,jk}\frac{\partial \Phi_{jk}}{\partial x}\right) \tag{6.11}$$

$$\int_{\vec{n}.\vec{\Omega}<0} \vec{n}.\vec{\Omega} \left[\Psi^+(\vec{r},\vec{\Omega}) + \Psi^-(\vec{r},\vec{\Omega})\right] P_{lm}(cos\theta)sin(m\varphi)sin\theta d\theta d\varphi \doteq \sum_{\substack{j=2 \\ j=even}}^{N-1} \sum_{\substack{k=2 \\ k=even}}^{j} \left(\acute{b}_{1,jk}\gamma_{jk} + \acute{b}_{2,jk}\frac{\partial \gamma_{jk}}{\partial x}\right) \tag{6.12}$$

+ These boundary conditions 6.11 and 6.12 can be used with the spherical harmonics method. They consist of only the even moments and their derivatives. In addition to that, the final forms can be used both for the external and the internal boundaries. In our implementation, one further step was taken before these boundary conditions were implemented. As was shown in Chapter 5, the second order

governing equations were decoupled and an iterative scheme was implemented for solving the simultaneous equations. A similar approach is required for the boundary conditions in order to solve the simultaneous differential equations with an iterative method. One way for achieving this is to follow the same procedure used in Chapter 5. The moments, which are assumed to be known, can be transferred to the right side of the boundary conditions. The drawback of this approach is that as the approximation order increases, the number of terms in the boundary conditions rises rapidly. As a result, the evaluation of these boundary conditions during the computations requires a considerable amount of time. The alternative scheme implemented here is to drop all the moments that have indices different from the weighing harmonics in the boundary conditions. Once this is done, we obtain the final form which was implemented in this project. This approach is shown by the two following expressions.

$$\int_{\vec{n}.\vec{\Omega}<0} \vec{n}.\vec{\Omega}\left[\Psi^{+}(\vec{r},\vec{\Omega})+\Psi^{-}(\vec{r},\vec{\Omega})\right] P_{lm}(cos\theta)cos(m\varphi)sin\theta d\theta d\varphi \doteq b_{1,lm}\Phi_{lm}+b_{2,lm}\frac{\partial\Phi_{lm}}{\partial x} \tag{6.13}$$

$$\int_{\vec{n}.\vec{\Omega}<0} \vec{n}.\vec{\Omega}\left[\Psi^{+}(\vec{r},\vec{\Omega})+\Psi^{-}(\vec{r},\vec{\Omega})\right] P_{lm}(cos\theta)sin(m\varphi)sin\theta d\theta d\varphi \doteq \acute{b}_{1,lm}\gamma_{lm}+\acute{b}_{2,lm}\frac{\partial\gamma_{lm}}{\partial x} \tag{6.14}$$

In the nodal method which is developed here, the nodes are rectangular as shown in Figure 6.1. As a result, the intervals of the angles over which the equations 6.13 and 6.14 will be integrated are known. The integration over the axial angle

is carried from π to 0 for all sides of the nodes. In contrast, the intervals for the azimuthal angle vary over each side. For the right side where the node (i,j) interfaces the node $(i,j+1)$, this range is given as $0.5\pi \leq \varphi \leq 1.5\pi$. The interval is given as $\pi \leq \varphi \leq 2\pi$ for the top of the node (i,j) which faces node $(i-1,j)$. For the left side of the nodes, the integration is done over $1.5\pi \leq \varphi \leq 2.5\pi$. The integration interval for the bottom side is $0 \leq \varphi \leq \pi$. Equations 6.15-6.18 give the boundary conditions for a rectangular node. The boundary conditions are given in counter clockwise order by starting from the right side surface. The first set is provided by the conditions which use $P_{lm}(cos\theta)cos(m\varphi)$ as the weighing function. The second set comes from the condition which uses $P_{lm}(cos\theta)sin(m\varphi)$. In the following boundary condition expressions, the terms f_{lm} and g_{lm} have one more index in addition to the indices which designate the weighing function. That extra index is used only if the boundary conditions are discussed specifically for the nodal geometry. If the discussion is for the general geometry, that index is dropped from the f_{lm}'s and g_{lm}'s.

$$b_{1,lm}\Phi_{lm} + b_{2,lm}\frac{\partial \Phi_{lm}}{\partial x} = f_{r,lm} \tag{6.15}$$

$$b_{1,lm}\Phi_{lm} + b_{2,lm}\frac{\partial \Phi_{lm}}{\partial y} = f_{t,lm} \tag{6.16}$$

$$b_{1,lm}\Phi_{lm} - b_{2,lm}\frac{\partial \Phi_{lm}}{\partial x} = f_{l,lm} \tag{6.17}$$

$$b_{1,lm}\Phi_{lm} - b_{2,lm}\frac{\partial \Phi_{lm}}{\partial y} = f_{b,lm} \tag{6.18}$$

The second set of boundary conditions are only for the γ_{lm}'s.

$$\acute{b}_{1,lm}\gamma_{lm} + \acute{b}_{2,lm}\frac{\partial \gamma_{lm}}{\partial x} = g_{r,lm} \tag{6.19}$$

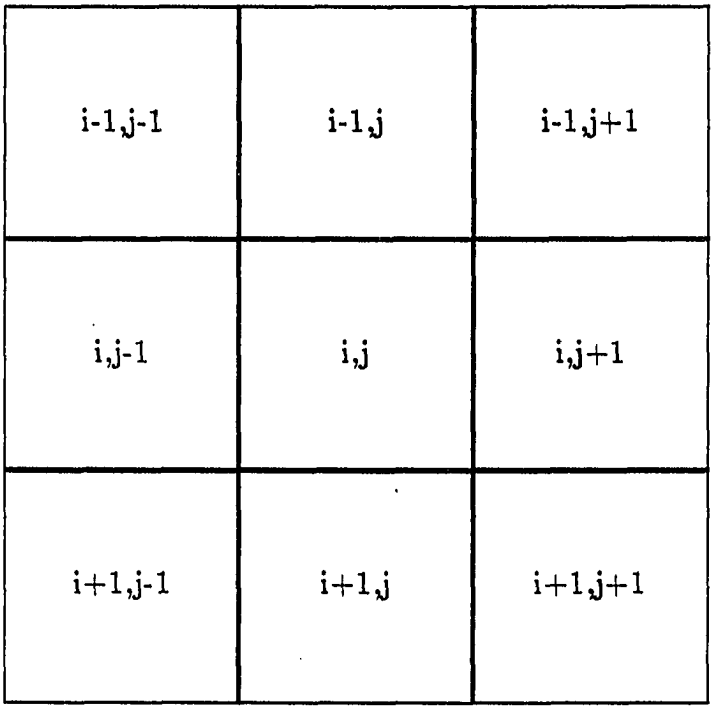

Figure 6.1: The nodal geometry

$$\acute{b}_{1,lm}\gamma_{lm} + \acute{b}_{2,lm}\frac{\partial\gamma_{lm}}{\partial y} = g_{t,lm} \tag{6.20}$$

$$\acute{b}_{1,lm}\gamma_{lm} - \acute{b}_{2,lm}\frac{\partial\gamma_{lm}}{\partial x} = g_{l,lm} \tag{6.21}$$

$$\acute{b}_{1,lm}\gamma_{lm} - \acute{b}_{2,lm}\frac{\partial\gamma_{lm}}{\partial y} = g_{b,lm} \tag{6.22}$$

In the preceding equations, the subscripts r, t, l and b stand for the right side, top, left side and bottom respectively. As can be seen from the above boundary conditions, the $b_{1,lm}$ and $b_{2,lm}$'s are the same for all four sides of the nodes. When all these four conditions are compared, there can be only two parameters changing in these conditions. The first one is that the derivatives are with respect to the x variable for the first and the third conditions while these derivatives are with respect to y for the second and the fourth conditions. The second difference is that of the sign in front of the $b_{2,lm}$'s. As a result, the generation of these boundary conditions can be done automatically. The four coefficients for a rectangular region, $b_{1,lm}$, $b_{2,lm}$, $\acute{b}_{1,lm}$ and $\acute{b}_{2,lm}$ are calculated from the following expressions.

$$b_{1,lm} = (2l+1)\int_{\frac{\pi}{2}}^{\frac{3\pi}{2}} cos^2(m\varphi)cos\varphi \left[\int_0^{\pi} P_{lm}^2(cos\theta)sin^2\theta d\theta\right] d\varphi \tag{6.23}$$

$$
\begin{aligned}
b_{2,lm} = & \left[\int_{\frac{\pi}{2}}^{\frac{3\pi}{2}} -\frac{(l+m)(l+m-1)}{2\Sigma_{l-1}} cos(m\varphi)cos[(m-1)\varphi]cos\varphi d\varphi\right] . \\
& \left[\int_0^{\pi} P_{lm}(cos\theta)P_{l-1,m-1}(cos\theta)sin^2\theta d\theta\right] + \\
& \left[\int_{\frac{\pi}{2}}^{\frac{3\pi}{2}} \frac{(1+\delta(0-m))}{2\Sigma_{l-1}} cos[(m+1)\varphi]cos(m\varphi)d\varphi\right] . \\
& \left[\int_0^{\pi} P_{lm}(cos\theta)P_{l-1,m+1}(cos\theta)sin^2\theta d\theta\right] + \\
& \left[\int_{\frac{\pi}{2}}^{\frac{3\pi}{2}} \frac{(l-m+1)(l-m+2)}{2\Sigma_{l+1}} cos(m\varphi)cos[(m-1)\varphi]cos\varphi d\varphi\right] . \\
& \left[\int_0^{\pi} P_{lm}(cos\theta)P_{l+1,m-1}(cos\theta)sin^2\theta d\theta\right] - \\
& \left[\int_{\frac{\pi}{2}}^{\frac{3\pi}{2}} \frac{(1+\delta(0-m))}{2\Sigma_{l+1}} cos[(m+1)\varphi]cos(m\varphi)cos\varphi d\varphi\right] . \\
& \left[\int_0^{\pi} P_{lm}(cos\theta)P_{l+1,m+1}(cos\theta)sin^2\theta d\theta\right] \qquad (6.24)
\end{aligned}
$$

In this last equation, $\delta(0-m)$ is the dirac delta function and it is nonzero only for the cases where $m = 0$. If the equation 6.24 is studied, it seen that this expression is a summation of four terms. The second, the third and the fourth of these terms vanish for certain cases.

If $l = 0$ *or* $m = 0$ *or* $l = m = 0$, *then Term* $2 = 0$

If $l = m$, *then Term* $3 = 0$

If $m = 0$, *then Term* $4 = 0$

The $\acute{b}$'s used in equations 6.19-6.22 are determined in a similar manner to the b's in the following two expressions.

$$
\acute{b}_{1,lm} = (2l+1)\int_{\frac{\pi}{2}}^{\frac{3\pi}{2}} sin^2(m\varphi)cos\varphi \left[\int_0^{\pi} P_{lm}^2(cos\theta)sin^2\theta d\theta\right] d\varphi \qquad (6.25)
$$

$$
\begin{aligned}
b_{2,lm} = & \left[\int_{\frac{\pi}{2}}^{\frac{3\pi}{2}} -\frac{(l+m)(l+m-1)}{2\Sigma_{l-1}} sin(m\varphi)sin[(m-1)\varphi]cos\varphi d\varphi\right] \cdot \\
& \left[\int_0^{\pi} P_{lm}(cos\theta)P_{l-1,m-1}(cos\theta)sin^2\theta d\theta\right] + \\
& \left[\int_{\frac{\pi}{2}}^{\frac{3\pi}{2}} \frac{(1+\delta(0-m))}{2\Sigma_{l-1}} sin[(m+1)\varphi]sin(m\varphi)cos\varphi d\varphi\right] \cdot \\
& \left[\int_0^{\pi} P_{lm}(cos\theta)P_{l-1,m+1}(cos\theta)sin^2\theta d\theta\right] + \\
& \left[\int_{\frac{\pi}{2}}^{\frac{3\pi}{2}} \frac{(l-m+1)(l-m+2)}{2\Sigma_{l+1}} sin(m\varphi)sin[(m-1)\varphi]cos\varphi d\varphi\right] \cdot \\
& \left[\int_0^{\pi} P_{lm}(cos\theta)P_{l+1,m-1}(cos\theta)sin^2\theta d\theta\right] - \\
& \left[\int_{\frac{\pi}{2}}^{\frac{3\pi}{2}} \frac{(1+\delta(0-m))}{2\Sigma_{l+1}} sin[(m+1)\varphi]sin(m\varphi)cos\varphi d\varphi\right] \cdot \\
& \left[\int_0^{\pi} P_{lm}(cos\theta)P_{l+1,m+1}(cos\theta)sin^2\theta d\theta\right] \qquad (6.26)
\end{aligned}
$$

This second type boundary condition varies from the first type condition in an important aspect. It does not exist for $m = 0$. In addition to that, the third term vanishes for the cases where $l = m$.

Now we can look at the right sides of the boundary conditions f_{lm} and g_{lm}. The expressions f_{lm} and g_{lm} depend on the type of boundary surrounding the node. The types of boundaries used in this dissertation are classified into three groups. The first type is the external boundary. The second type is an interface between two adjacent nodes. The last one is again an interface. The last type differs from the second type in one important aspect. The order of the P_n approximation in the current node is higher than the adjacent node.

For the external boundaries, we tried to manipulate the boundary conditions into albedo type boundary conditions. In doing so, we used the principles given by

the equations 6.27 and 6.28. The principles are basically the same as Davis's variational principle. The only difference is the integration interval.We also multiplied that expression by the albedo α. If α takes the value 1.0, the external condition becomes a full reflective condition. If α takes the value 0.0, the condition becomes a vacuum boundary condition. By changing the α, we can impose any condition on the external boundaries. The spherical harmonic moments and the neutronic parameters used in calculating these boundary conditions are taken from the node where the external boundary will be implemented.

$$f_{lm} = \alpha \int_{\vec{n}.\vec{\Omega}>0} \vec{n}.\vec{\Omega} \left[\Psi^{+}(\vec{r},\vec{\Omega}) + \Psi^{-}(\vec{r},\vec{\Omega})\right] P_{lm}(cos\theta)cos(m\varphi)sin\theta d\theta d\varphi \qquad (6.27)$$

$$g_{lm} = -\alpha \int_{\vec{n}.\vec{\Omega}>0} \vec{n}.\vec{\Omega} \left[\Psi^{+}(\vec{r},\vec{\Omega}) + \Psi^{-}(\vec{r},\vec{\Omega})\right] P_{lm}(cos\theta)sin(m\varphi)sin\theta d\theta d\varphi \qquad (6.28)$$

As can be seen from the second type of the external boundary condition, it is multiplied by a minus sign. The reason is that the integrand of the second type condition is in fact the component tangent to the surface of the domain. Therefore, the signs of the derivative terms in the left and the right hand sides of the boundary conditions should be the same. The minus sign multiplying the albedo α in the expression for g_{lm} is used for that consideration. Without that minus sign, the derivatives in both sides of the boundary conditions would have opposite signs. The rest of the manipulation of the external boundary conditions are exactly the same as for the left sides of the boundary conditions.

$$f_{r,lm} = \alpha_r \left[b_{1,lm}\Phi_{lm} - b_{2,lm}\frac{\partial \Phi_{lm}}{\partial x}\right] \qquad (6.29)$$

$$f_{t,lm} = \alpha_t \left[b_{1,lm}\Phi_{lm} - b_{2,lm}\frac{\partial \Phi_{lm}}{\partial y}\right] \qquad (6.30)$$

$$f_{l,lm} = \alpha_l \left[b_{1,lm} \Phi_{lm} + b_{2,lm} \frac{\partial \Phi_{lm}}{\partial x} \right] \tag{6.31}$$

$$f_{b,lm} = \alpha_b \left[b_{1,lm} \Phi_{lm} + b_{2,lm} \frac{\partial \Phi_{lm}}{\partial y} \right] \tag{6.32}$$

As with for the left hand sides of the boundary conditions, the second set is again for the second type of boundary conditions. If the following expressions are compared to the left sides, one point can be observed easily. Since the signs of the γ's are opposite at the boundaries, the only condition which can satisfy that type of boundary conditions is that all γ's should be zero at the boundaries.

$$g_{r,lm} = -\alpha_r \left[b_{1,lm} \gamma_{lm} - b_{2,lm} \frac{\partial \gamma_{lm}}{\partial x} \right] \tag{6.33}$$

$$g_{t,lm} = -\alpha_t \left[b_{1,lm} \gamma_{lm} - b_{2,lm} \frac{\partial \gamma_{lm}}{\partial y} \right] \tag{6.34}$$

$$g_{l,lm} = -\alpha_l \left[b_{1,lm} \gamma_{lm} + b_{2,lm} \frac{\partial \gamma_{lm}}{\partial x} \right] \tag{6.35}$$

$$g_{b,lm} = -\alpha_b \left[b_{1,lm} \gamma_{lm} + b_{2,lm} \frac{\partial \gamma_{lm}}{\partial y} \right] \tag{6.36}$$

The second type of boundary is the nodal interface type. In that type, the materials on both sides of the interface may be the same or different. In this case, the right sides of both boundary conditions are given by the same expressions as the left sides of the equations below. The only difference in this case is that the moments and the neutronic parameters which will be used in forming the right side term are taken from the adjacent node.

$$f_{lm} = \int_{\vec{n}.\vec{\Omega}<0} \vec{n}.\vec{\Omega} \left[\Psi^+(\vec{r},\vec{\Omega}) + \Psi^-(\vec{r},\vec{\Omega}) \right] P_{lm}(cos\theta) cos(m\varphi) sin\theta d\theta d\varphi \tag{6.37}$$

$$g_{lm} = \int_{\vec{n}.\vec{\Omega}<0} \vec{n}.\vec{\Omega} \left[\Psi^{+}(\vec{r},\vec{\Omega}) + \Psi^{-}(\vec{r},\vec{\Omega})\right] P_{lm}(cos\theta)sin(m\varphi)sin\theta d\theta d\varphi \qquad (6.38)$$

If these two expressions are manipulated as in the other cases, we get the following conditions, which are exactly the same as the left sides of the boundary conditions. Although they are not shown explicitly, the $b_{1,lm}$ and $b_{2,lm}$ will be using different neutronic parameters if the materials in two adjacent nodes are not the same.

$$f_{r,lm} = b_{1,lm}\Phi_{lm} + b_{2,lm}\frac{\partial \Phi_{lm}}{\partial x} \qquad (6.39)$$

$$f_{t,lm} = b_{1,lm}\Phi_{lm} + b_{2,lm}\frac{\partial \Phi_{lm}}{\partial y} \qquad (6.40)$$

$$f_{l,lm} = b_{1,lm}\Phi_{lm} - b_{2,lm}\frac{\partial \Phi_{lm}}{\partial x} \qquad (6.41)$$

$$f_{b,lm} = b_{1,lm}\Phi_{lm} - b_{2,lm}\frac{\partial \Phi_{lm}}{\partial y} \qquad (6.42)$$

The second set of boundary conditions are for the γ_{lm}'s in the previous cases.

$$g_{r,lm} = b_{1,lm}\gamma_{lm} + b_{2,lm}\frac{\partial \gamma_{lm}}{\partial x} \qquad (6.43)$$

$$g_{t,lm} = b_{1,lm}\gamma_{lm} + b_{2,lm}\frac{\partial \gamma_{lm}}{\partial y} \qquad (6.44)$$

$$g_{l,lm} = b_{1,lm}\gamma_{lm} - b_{2,lm}\frac{\partial \gamma_{lm}}{\partial x} \qquad (6.45)$$

$$g_{b,lm} = b_{1,lm}\gamma_{lm} - b_{2,lm}\frac{\partial \gamma_{lm}}{\partial y} \qquad (6.46)$$

The last of the boundary types to be investigated is the interfaces where two nodes, which use different order P_n approximations, intersect. That type of boundary condition becomes important when the modular approach is adapted for solving

the neutron transport equation. In the modular approach, the neutron transport equation is approximated by different orders of the P_n approximation in different nodes. In such a case, the moments utilized in one node may not be used in the adjacent node because the order of the approximation in that adjacent node is lower. If the current node uses a higher order than the neighboring node, then all the boundary conditions for the moments which are not utilized in the adjacent node are set equal to zero. In other words, for these higher moments the boundary conditions are the same as the vacuum condition where the inbound weighted fluxes are set equal to zero. The practical application of that is done by setting all f_{lm}'s and g_{lm}'s equal to zero.

The following equations give the P_3 boundary conditions for the right side of a rectangular region. The boundary conditions for the top, left and bottom sides can be determined by using equations 6.16-6.18.

$$\Phi_{00} + \frac{2}{3\Sigma_1}\frac{\partial \Phi_{00}}{\partial x} = f_{r,00} \tag{6.47}$$

$$250\Phi_{20} + \left[\frac{128}{3\Sigma_1} + \frac{768}{7\Sigma_3}\right]\frac{\partial \Phi_{20}}{\partial x} = f_{r,20} \tag{6.48}$$

$$350\Phi_{22} + \left[\frac{128}{\Sigma_1} + \frac{1024}{7\Sigma_3}\right]\frac{\partial \Phi_{22}}{\partial x} = f_{r,22} \tag{6.49}$$

$$25\gamma_{22} + \left[\frac{8}{\Sigma_1} + \frac{64}{7\Sigma_3}\right]\frac{\partial \gamma_{22}}{\partial x} = g_{r,22} \tag{6.50}$$

7 THE DEVELOPMENT OF THE NODAL METHOD

This chapter introduces the development of the nodal method. The nodal method developed here uses the principles previously laid down for the multigroup diffusion theory by Rohach [28-31]. The method is based on a least squares minimization principle. The spherical harmonic moments are expanded into fourth order Legendre polynomials. The boundary conditions are used in the determination of the coefficients of the Legendre polynomials in an integral sense, so that the neutron balances in the nodes are preserved.

Since the Legendre polynomials are used in an interval from 1.0 to -1.0, the equations 5.42, 5.43 and 5.44, which give the governing equations in general terms, should be transformed into the new coordinate system. In this coordinate transformation, the node shown in the Figure 7.1a is taken as the starting point. As can be seen from that figure, the width of the node is 2ζ while the height is 2η. The intersection point of the diagonals is taken as the center of the coordinates. The node with new coordinates is shown in Figure 7.1b. In that new system, the x-coordinate is now transformed to the u-coordinate while the y-coordinate is transformed to the w-coordinate. That transformation is reflected to the equations 5.42, 5.43 and 5.44 by modifying the three operators used in these equations in the following way.

$$\nabla^2 = \frac{1}{\zeta^2}\frac{\partial^2}{\partial u^2} + \frac{1}{\eta^2}\frac{\partial^2}{\partial w^2} \tag{7.1}$$

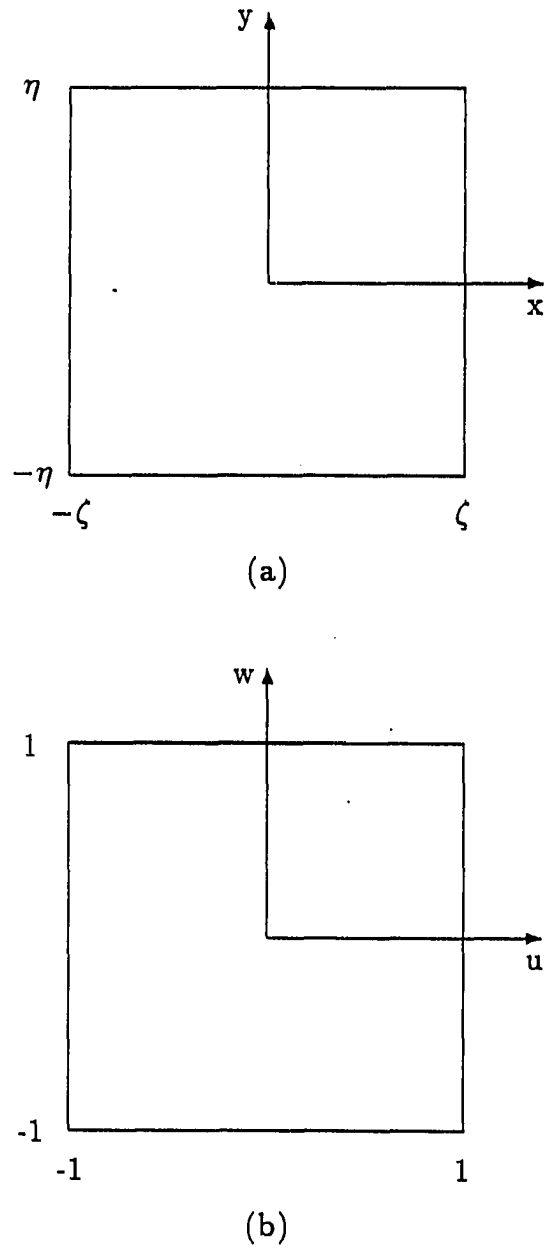

Figure 7.1: The coordinate transformation

$$\frac{\partial^2}{\partial x^2} - \frac{\partial^2}{\partial y^2} = \frac{1}{\zeta^2}\frac{\partial^2}{\partial u^2} - \frac{1}{\eta^2}\frac{\partial^2}{\partial w^2} \tag{7.2}$$

$$\frac{\partial^2}{\partial x \partial y} = \frac{1}{\zeta\eta}\frac{\partial^2}{\partial u \partial w} \tag{7.3}$$

After the three modifications made above, equations 5.42, 5.43 and 5.44 are rearranged as the following three equations.

$$L_0\Phi_{00}(u,w) = 3\Sigma_1 S_{00}(u,w) - \left[\frac{1}{\zeta^2}\frac{\partial^2}{\partial u^2} + \frac{1}{\eta^2}\frac{\partial^2}{\partial w^2}\right]\Phi_{20} + 12\frac{1}{\zeta\eta}\frac{\partial^2}{\partial u \partial w}\gamma_{22} + 6\left[\frac{1}{\zeta^2}\frac{\partial^2}{\partial u^2} - \frac{1}{\eta^2}\frac{\partial^2}{\partial w^2}\right]\Phi_{22} \tag{7.4}$$

$$L_1\Phi_{lm}(u,w) = \left[\frac{1}{\zeta^2}\frac{\partial^2}{\partial u^2} + \frac{1}{\eta^2}\frac{\partial^2}{\partial w^2}\right][B][\Phi]_1 + \left[\frac{1}{\zeta^2}\frac{\partial^2}{\partial u^2} - \frac{1}{\eta^2}\frac{\partial^2}{\partial w^2}\right][C][\Phi]_2 + \frac{1}{\zeta\eta}\frac{\partial^2}{\partial u \partial w}\left[\acute{B}\right][\gamma]_1 \tag{7.5}$$

$$L_2\gamma_{lm}(x,y) = \left[\frac{1}{\zeta^2}\frac{\partial^2}{\partial u^2} + \frac{1}{\eta^2}\frac{\partial^2}{\partial w^2}\right]\left[\acute{C}\right][\gamma]_2 + \left[\frac{1}{\zeta^2}\frac{\partial^2}{\partial u^2} - \frac{1}{\eta^2}\frac{\partial^2}{\partial w^2}\right]\left[\acute{D}\right][\gamma]_3 + \frac{1}{\zeta\eta}\frac{\partial^2}{\partial u \partial w}[D][\Phi]_3 \tag{7.6}$$

where :

$$L_0 = -\left[\frac{1}{\zeta^2}\frac{\partial^2}{\partial u^2} + \frac{1}{\eta^2}\frac{\partial^2}{\partial w^2}\right] + 3\Sigma_0\Sigma_1 \tag{7.7}$$

$$L_1 = (A_1\Sigma_{l-1} + A_2\Sigma_{l+1})\left[\frac{1}{\zeta^2}\frac{\partial^2}{\partial u^2} + \frac{1}{\eta^2}\frac{\partial^2}{\partial w^2}\right] + A_3\Sigma_{l-1}\Sigma_l\Sigma_{l+1} \tag{7.8}$$

$$L_2 = (\acute{A}_1\Sigma_{l-1} + \acute{A}_2\Sigma_{l+1})\left[\frac{1}{\zeta^2}\frac{\partial^2}{\partial u^2} + \frac{1}{\eta^2}\frac{\partial^2}{\partial w^2}\right] + \acute{A}_3\Sigma_{l-1}\Sigma_l\Sigma_{l+1} \tag{7.9}$$

The first step in the development of the nodal method is to approximate the spherical harmonic moments by fourth order Legendre polynomial expansions. Since the number of the spherical harmonic moments, in other words the dependent variables, vary with respect to the order of the spherical harmonic approximation, we will show the development of the nodal method for a generic moment $\Phi(u,w)$. Since all the governing equations will assume the same form as shown by equations 7.4, 7.5 and 7.6, the development introduced in the following section is valid for all the spherical harmonic differential equations. The Legendre polynomial expansion for the generic moment is given by the following expression.

$$\Phi(u,w) \doteq \sum_{i=0}^{4}\sum_{j=0}^{4-i} a_{ij}P_i(u)P_j(w) \tag{7.10}$$

Once this approximation is made, the problem of solving the neutron transport equation is reduced to determining the fifteen coefficients a_{ij}'s of the expansion 7.10. This goal can be achieved by forming fifteen algebraic conditions for each spherical harmonic moment. These conditions are provided by both the least squares minimization scheme to be implemented for the governing equations and the boundary conditions. The procedure for determining these conditions is given in the following sections.

7.1 The Least Squares Minimization Technique

The least square minimization technique which provides some of the conditions for determining the coefficients of the Legendre polynomials for the spherical

harmonic moments is a variation of the conventional least squares method. Therefore, some insight is given for the conventional implementation of the least squares method. For describing the least squares technique, we can use the following differential equation.

$$Au(\vec{r}) = f(\vec{r}) \tag{7.11}$$

where A is a differential operator.

For solving that differential equation, the dependent variable u is approximated by an expansion which also satisfies the boundary conditions.

$$\acute{u} \doteq \sum_{i=0}^{N} b_i Q_i(\vec{r}) \tag{7.12}$$

The substitution of the above expansion into the differential equation 7.11 does not satisfy the equality and results in a residual.

$$R(\vec{r}) = A\acute{u}(\vec{r}) - f(\vec{r}) \tag{7.13}$$

For a proper representation of the dependent variable $u(\vec{r})$ by the approximation $\acute{u}(\vec{r})$, the residual should be minimized. This is achieved by the following procedure.

$$\frac{\partial}{\partial b_i} \int_V R^2 dV = 0 \quad for\ i = 0, .., N \tag{7.14}$$

As is seen from the conventional application of the least squares method summarized above, the method is based upon the fact that the expansion $\acute{u}(\vec{r})$ satisfies the boundary conditions exactly. As was discussed in the sixth chapter, the boundary conditions to be used here are mixed type conditions. The Legendre polynomial expansions used in that project do not satisfy these mixed type boundary conditions

explicitly. Therefore, the least squares method can not be used in its conventional form. The least squares minimization technique which was used in this project is based on the following procedure. Since the right hand sides of the spherical harmonic differential equations will be known from the previous iterations, we will demonstrate the development of that technique for the following generalized form of the differential equations.

$$A\left[\frac{1}{\zeta^2}\frac{\partial^2}{\partial u^2}+\frac{1}{\eta^2}\frac{\partial^2}{\partial w^2}\right]\Phi(u,w)+B\Phi(u,w)=g(u,w) \tag{7.15}$$

where the descriptions of the constants A and B are given by the following expressions for equation 7.5. If the A_i's are replaced by the $\acute{A}_i$'s in these expressions, the constants for the equation 7.6 are obtained.

$$A=(A_1\Sigma_{l-1}+A_2\Sigma_{l+1}) \tag{7.16}$$

$$B=A_3\Sigma_{l-1}\Sigma_l\Sigma_{l+1} \tag{7.17}$$

The development of the minimization conditions starts by substituting the Legendre expansion 7.10 into the differential equation 7.15 as was done with the conventional method. At that point, the Laplace operator in the equation reduces the fourth order moment expansion by two orders. That resulting polynomial can be rearranged into a second order Legendre polynomial with new coefficients. These new coefficients are combinations of the coefficients of the original expansion. Since the resulting expression does not satisfy the differential equation exactly, we end up with a residual. That residual is given by the following expression.

$$R(u,w)=A\sum_{i=0}^{2}\sum_{j=0}^{2-i}c_{ij}P_i(u)P_j(w)+B\sum_{i=0}^{4}\sum_{j=0}^{4-i}c_{ij}P_i(u)P_j(w)-g(u,w) \tag{7.18}$$

As can be seen from the equation 7.18, the residual is a combination of two polynomials and $g(u,w)$. The first polynomial is a second order Legendre polynomial while the second one is still a fourth order polynomial. The coefficients of the first polynomial are combinations of the coefficients of the original spherical harmonic expansions. These newly defined coefficients for the first polynomial are given by the following six expressions.

$$c_{00} = \frac{1}{\zeta^2}(3a_{20} + 10a_{40}) + \frac{1}{\eta^2}(3a_{02} + 10a_{04}) \tag{7.19}$$

$$c_{01} = \frac{1}{\zeta^2}3a_{21} + \frac{1}{\eta^2}15a_{03} \tag{7.20}$$

$$c_{02} = \frac{1}{\zeta^2}3a_{22} + \frac{1}{\eta^2}35a_{04} \tag{7.21}$$

$$c_{10} = \frac{1}{\zeta^2}15a_{30} + \frac{1}{\eta^2}3a_{12} \tag{7.22}$$

$$c_{11} = \frac{1}{\zeta^2}15a_{31} + \frac{1}{\eta^2}15a_{13} \tag{7.23}$$

$$c_{20} = \frac{1}{\zeta^2}35a_{40} + \frac{1}{\eta^2}3a_{22} \tag{7.24}$$

At this point, we carry out the minimization procedure. If the conventional application is studied carefully, it seen that the minimization is actually done by forcing the two polynomials close to each other. Since the right hand side of the differential equation is not approximated, the degree of the agreement between the two polynomials will determine the success of the minimization procedure. In our approach, instead of tuning up both of the polynomials in the residual, we keep one of these polynomials fixed while adjusting the other polynomial for minimizing the error. This is done by manipulating the coefficients of the first polynomial so

that the difference between the first and the second polynomial is minimized. This approach can be expressed mathematically by the following expression.

$$\int_{-1}^{1}\int_{-1}^{1}\frac{\partial R}{\partial c_{i,j}}R(u,w)dudw = 0 \tag{7.25}$$

where: $i = 0,1,2$ and $j = 0,..,2-i$

When these integrations are carried out, the following six conditions are obtained.

$$A\left[\frac{1}{\zeta^2}(3a_{20}+10a_{40})+\frac{1}{\eta^2}(3a_{02}+10a_{04})\right]+Ba_{00}=\frac{1}{4}G_{00} \tag{7.26}$$

$$A\left[\frac{1}{\zeta^2}3a_{21}+\frac{1}{\eta^2}15a_{03}\right]+Ba_{01}=\frac{3}{4}G_{01} \tag{7.27}$$

$$A\left[\frac{1}{\zeta^2}3a_{22}+\frac{1}{\eta^2}35a_{04}\right]+Ba_{02}=\frac{5}{4}G_{02} \tag{7.28}$$

$$A\left[\frac{1}{\zeta^2}15a_{30}+\frac{1}{\eta^2}3a_{12}\right]+Ba_{10}=\frac{3}{4}G_{10} \tag{7.29}$$

$$A\left[\frac{1}{\zeta^2}15a_{31}+\frac{1}{\eta^2}15a_{13}\right]+Ba_{11}=\frac{9}{4}G_{11} \tag{7.30}$$

$$A\left[\frac{1}{\zeta^2}35a_{40}+\frac{1}{\eta^2}3a_{22}\right]+Ba_{20}=\frac{5}{4}G_{20} \tag{7.31}$$

where the right hand sides of the above equations are given by the following expression.

$$G_{ij}=\int_{-1}^{1}\int_{-1}^{1}\left[g(u,w)P_i(u)P_j(w)\right]dudw \tag{7.32}$$

The manipulation of the function $g(u,w)$, the right hand side of the equation, is done in a manner similar to the treatment of the moment operated on by the Laplace operator. The $g(u,w)$ is usually a combination of the various terms which are in fact spherical harmonic moments operated on by one of the three differential operators given by 7.1, 7.2 and 7.3. We designate the known moment as $\bar{\Phi}$ and expand that moment in the following fashion.

$$\bar{\Phi}(u,w) = \sum_{i=0}^{4} \sum_{j=0}^{4-i} \acute{a}_{ij} P_i(u) P_j(w) \tag{7.33}$$

If the moment $\bar{\Phi}(u,w)$ is operated on by $\left[\frac{1}{\zeta^2}\frac{\partial^2}{\partial u^2} + \frac{1}{\eta^2}\frac{\partial^2}{\partial w^2}\right]$, it contributes to the G_{ij} through the following six expressions.

$$d_{00} = 4\left[\frac{1}{\zeta^2}(3\acute{a}_{20} + 10\acute{a}_{40}) + \frac{1}{\eta^2}(3\acute{a}_{02} + 10\acute{a}_{04})\right] \tag{7.34}$$

$$d_{01} = \frac{4}{3}\left[\frac{1}{\zeta^2}3\acute{a}_{21} + \frac{1}{\eta^2}15\acute{a}_{03}\right] \tag{7.35}$$

$$d_{02} = \frac{4}{5}\left[\frac{1}{\zeta^2}3\acute{a}_{22} + \frac{1}{\eta^2}35\acute{a}_{04}\right] \tag{7.36}$$

$$d_{10} = \frac{4}{3}\left[\frac{1}{\zeta^2}15\acute{a}_{30} + \frac{1}{\eta^2}3\acute{a}_{12}\right] \tag{7.37}$$

$$d_{11} = \frac{4}{9}\left[\frac{1}{\zeta^2}15\acute{a}_{31} + \frac{1}{\eta^2}15\acute{a}_{13}\right] \tag{7.38}$$

$$d_{20} = \frac{4}{5}\left[\frac{1}{\zeta^2}35\acute{a}_{40} + \frac{1}{\eta^2}3\acute{a}_{22}\right] \tag{7.39}$$

If this operator is $\left[\frac{1}{\zeta^2}\frac{\partial^2}{\partial u^2} - \frac{1}{\eta^2}\frac{\partial^2}{\partial w^2}\right]$, then the contribution of $\bar{\Phi}(u,w)$ is given by the following six expressions.

$$e_{00} = 4\left[\frac{1}{\zeta^2}(3\acute{a}_{20} + 10\acute{a}_{40}) - \frac{1}{\eta^2}(3\acute{a}_{02} + 10\acute{a}_{04})\right] \tag{7.40}$$

$$e_{01} = \frac{4}{3}\left[\frac{1}{\zeta^2}3\acute{a}_{21} - \frac{1}{\eta^2}15\acute{a}_{03}\right] \tag{7.41}$$

$$e_{02} = \frac{4}{5}\left[\frac{1}{\zeta^2}3\acute{a}_{22} - \frac{1}{\eta^2}35\acute{a}_{04}\right] \tag{7.42}$$

$$e_{10} = \frac{4}{3}\left[\frac{1}{\zeta^2}15\acute{a}_{30} - \frac{1}{\eta^2}3\acute{a}_{12}\right] \tag{7.43}$$

$$e_{11} = \frac{4}{9}\left[\frac{1}{\zeta^2}15\acute{a}_{31} - \frac{1}{\eta^2}15\acute{a}_{13}\right] \tag{7.44}$$

$$e_{20} = \frac{4}{5}\left[\frac{1}{\zeta^2}35\acute{a}_{40} - \frac{1}{\eta^2}3\acute{a}_{22}\right] \tag{7.45}$$

The last type of contribution comes from the $\frac{1}{\zeta\eta}\frac{\partial^2}{\partial u \partial w}$. The equations for that group is listed below.

$$f_{00} = \frac{4}{\zeta\eta}\left[\acute{a}_{11} + \acute{a}_{13} + \acute{a}_{31}\right] \tag{7.46}$$

$$f_{01} = \frac{4}{\zeta\eta}\acute{a}_{12} \tag{7.47}$$

$$f_{02} = \frac{4}{\zeta\eta}\acute{a}_{13} \tag{7.48}$$

$$f_{10} = \frac{4}{\zeta\eta}\acute{a}_{21} \tag{7.49}$$

$$f_{11} = \frac{4}{\zeta\eta}\acute{a}_{22} \tag{7.50}$$

$$f_{20} = \frac{4}{\zeta\eta}\acute{a}_{31} \tag{7.51}$$

The right hand sides G_{ij}'s are formed by combining the contributions from d_{ij}'s, e_{ij}'s and f_{ij}'s for which the full expressions were given above. As can be seen from these minimization conditions, they provide only six of the fifteen conditions which are required for determining all of the coefficients for the moment expansions. The rest of the conditions must be provided by the boundary conditions.

7.2 The Implementation of the Boundary Conditions

The introduction of the boundary conditions into the nodal scheme is done in a way such that the neutron balance is conserved in the nodes. In fact, this is the reason why the overall scheme can be classified as a nodal method. As was done in the least squares section above, the equations for the boundary conditions will also be derived for a generalized form of the equations. For doing that, the indices designating the moments will be dropped from the equations. In doing so, the boundary conditions are expressed by four equations. As is always the case, the first and the second types of equations have the same form.

$$b_1\Phi + \frac{b_2}{\zeta}\frac{\partial\Phi}{\partial u} = f_r \tag{7.52}$$

$$b_1\Phi + \frac{b_2}{\eta}\frac{\partial\Phi}{\partial w} = f_t \tag{7.53}$$

$$b_1\Phi - \frac{b_2}{\zeta}\frac{\partial\Phi}{\partial u} = f_l \tag{7.54}$$

$$b_1\Phi - \frac{b_2}{\eta}\frac{\partial\Phi}{\partial w} = f_b \tag{7.55}$$

The indices r, t, l and b in the above equations stand for the right, top, left and bottom sides of the nodes. The boundary conditions for each side is integrated over the half ranges of the nodal surfaces. That integration procedure results in eight conditions which are shown below.

$$\begin{aligned} b_1 a_{00} + (b_1 + \frac{b_2}{\zeta})a_{10} + (b_1 + 3\frac{b_2}{\zeta})a_{20} + (b_1 + 6\frac{b_2}{\zeta})a_{30} + (b_1 + 10\frac{b_2}{\zeta})a_{40} \\ + \frac{1}{2}\left[b_1 a_{01} + (b_1 + \frac{b_2}{\zeta})a_{11} + (b_1 + 3\frac{b_2}{\zeta})a_{21} + (b_1 + 6\frac{b_2}{\zeta})a_{31}\right] \\ - \frac{1}{8}\left[b_1 a_{03} + (b_1 + \frac{b_2}{\zeta})a_{13}\right] = \int_0^1 f_r(w)dw \end{aligned} \tag{7.56}$$

$$b_1 a_{00} + (b_1 + \frac{b_2}{\zeta})a_{10} + (b_1 + 3\frac{b_2}{\zeta})a_{20} + (b_1 + 6\frac{b_2}{\zeta})a_{30} + (b_1 + 10\frac{b_2}{\zeta})a_{40}$$
$$-\frac{1}{2}\left[b_1 a_{01} + (b_1 + \frac{b_2}{\zeta})a_{11} + (b_1 + 3\frac{b_2}{\zeta})a_{21} + (b_1 + 6\frac{b_2}{\zeta})a_{31}\right]$$
$$+\frac{1}{8}\left[b_1 a_{03} + (b_1 + \frac{b_2}{\zeta})a_{13}\right] = \int_{-1}^{0} f_r(w)dw \quad (7.57)$$

$$b_1 a_{00} + (b_1 + \frac{b_2}{\eta})a_{01} + (b_1 + 3\frac{b_2}{\eta})a_{02} + (b_1 + 6\frac{b_2}{\eta})a_{03} + (b_1 + 10\frac{b_2}{\eta})a_{04}$$
$$+\frac{1}{2}\left[b_1 a_{10} + (b_1 + \frac{b_2}{\eta})a_{11} + (b_1 + 3\frac{b_2}{\eta})a_{12} + (b_1 + 6\frac{b_2}{\eta})a_{13}\right]$$
$$-\frac{1}{8}\left[b_1 a_{30} + (b_1 + \frac{b_2}{\eta})a_{31}\right] = \int_{0}^{1} f_t(u)du \quad (7.58)$$

$$b_1 a_{00} + (b_1 + \frac{b_2}{\eta})a_{01} + (b_1 + 3\frac{b_2}{\eta})a_{02} + (b_1 + 6\frac{b_2}{\eta})a_{03} + (b_1 + 10\frac{b_2}{\eta})a_{04}$$
$$-\frac{1}{2}\left[b_1 a_{10} + (b_1 + \frac{b_2}{\eta})a_{11} + (b_1 + 3\frac{b_2}{\eta})a_{12} + (b_1 + 6\frac{b_2}{\eta})a_{13}\right]$$
$$+\frac{1}{8}\left[b_1 a_{30} + (b_1 + \frac{b_2}{\eta})a_{31}\right] = \int_{-1}^{0} f_t(u)du \quad (7.59)$$

$$b_1 a_{00} - (b_1 + \frac{b_2}{\zeta})a_{10} + (b_1 + 3\frac{b_2}{\zeta})a_{20} - (b_1 + 6\frac{b_2}{\zeta})a_{30} + (b_1 + 10\frac{b_2}{\zeta})a_{40}$$
$$+\frac{1}{2}\left[b_1 a_{01} - (b_1 + \frac{b_2}{\zeta})a_{11} + (b_1 + 3\frac{b_2}{\zeta})a_{21} - (b_1 + 6\frac{b_2}{\zeta})a_{31}\right]$$
$$-\frac{1}{8}\left[b_1 a_{03} - (b_1 + \frac{b_2}{\zeta})a_{13}\right] = \int_{0}^{1} f_l(w)dw \quad (7.60)$$

$$b_1 a_{00} - (b_1 + \frac{b_2}{\zeta})a_{10} + (b_1 + 3\frac{b_2}{\zeta})a_{20} - (b_1 + 6\frac{b_2}{\zeta})a_{30} + (b_1 + 10\frac{b_2}{\zeta})a_{40}$$
$$-\frac{1}{2}\left[b_1 a_{01} - (b_1 + \frac{b_2}{\zeta})a_{11} + (b_1 + 3\frac{b_2}{\zeta})a_{21} - (b_1 + 6\frac{b_2}{\zeta})a_{31}\right]$$
$$+\frac{1}{8}\left[b_1 a_{03} - (b_1 + \frac{b_2}{\zeta})a_{13}\right] = \int_{-1}^{0} f_l(w)dw \quad (7.61)$$

$$b_1 a_{00} - (b_1 + \frac{b_2}{\eta})a_{01} + (b_1 + 3\frac{b_2}{\eta})a_{02} - (b_1 + 6\frac{b_2}{\eta})a_{03} + (b_1 + 10\frac{b_2}{\eta})a_{04}$$
$$+\frac{1}{2}\left[b_1 a_{10} - (b_1 + \frac{b_2}{\eta})a_{11} + (b_1 + 3\frac{b_2}{\eta})a_{12} - (b_1 + 6\frac{b_2}{\eta})a_{13}\right]$$
$$-\frac{1}{8}\left[b_1 a_{30} - (b_1 + \frac{b_2}{\eta})a_{31}\right] = \int_{0}^{1} f_b(u)du \quad (7.62)$$

$$b_1 a_{00} - (b_1 + \frac{b_2}{\eta})a_{01} + (b_1 + 3\frac{b_2}{\eta})a_{02} - (b_1 + 6\frac{b_2}{\eta})a_{03} + (b_1 + 10\frac{b_2}{\eta})a_{04}$$
$$-\frac{1}{2}\left[b_1 a_{10} - (b_1 + \frac{b_2}{\eta})a_{11} + (b_1 + 3\frac{b_2}{\eta})a_{12} - (b_1 + 6\frac{b_2}{\eta})a_{13}\right]$$
$$+\frac{1}{8}\left[b_1 a_{30} - (b_1 + \frac{b_2}{\eta})a_{31}\right] = \int_{-1}^{0} f_b(u)du \quad (7.63)$$

When the minimization conditions given by 7.26-7.31 and the boundary conditions 7.56-7.63 are added, it is seen that they total up to fourteen which is one short for determining all fifteen coefficients. This problem is bypassed by setting the coefficient a_{22} equal to zero. This specific coefficient is chosen to be zero because the affect of elimination of a_{22} on the accuracy of the method is negligible [31]. Before the formulation of the nodal method is finished, a last step is introduced for simplifying the final forms of the equations.

7.3 The Simplification of the Equations

If a problem is solved for only a single node, then the simultaneous solution of the fourteen algebraic equations introduced above would provide the coefficients used in the Legendre polynomial expansions of the spherical harmonic moments. The fourteen coefficients can be determined by solving a 14 by 14 matrix. If steps which will be used in the solution of the matrix are introduced into the equations analytically, the 14 by 14 matrix can be arranged into smaller matrices which would speed up the solution process considerably. One other advantage of doing this is to conserve storage space on a computer. When the fourteen algebraic equations are manipulated, the set of simultaneous equations can be broken into four smaller matrices. One of these matrices is 5 by 5 while the other three matrices are 3 by 3. The first group of the equations which form the 5 by 5 matrix are given below.

$$Ba_{00} + \frac{3A}{\eta^2}a_{02} + \frac{10A}{\eta^2}a_{04} + \frac{3A}{\zeta^2}a_{20} + \frac{10A}{\zeta^2}a_{40} = \frac{1}{4}G_{00} \tag{7.64}$$

$$Ba_{02} + \frac{35A}{\eta^2}a_{04} = \frac{5}{4}G_{02} \tag{7.65}$$

$$Ba_{20} + \frac{35A}{\zeta^2}a_{40} = \frac{5}{4}G_{20} \tag{7.66}$$

$$b_1 a_{00} + (b_1 + \frac{3b_2}{\zeta})a_{20} + (b_1 + \frac{10b_2}{\zeta})a_{40} = \frac{1}{4}\int_{-1}^{1}\left[f_r(w) + f_l(w)\right]dw \tag{7.67}$$

$$b_1 a_{00} + (b_1 + \frac{3b_2}{\eta})a_{02} + (b_1 + \frac{10b_2}{\eta})a_{04} = \frac{1}{4}\int_{-1}^{1}\left[f_t(u) + f_b(u)\right]du \tag{7.68}$$

The second set of simultaneous equations is given by the following expressions.

$$Ba_{11} + \frac{15A}{\eta^2}a_{13} + \frac{15A}{\zeta^2}a_{31} = \frac{9}{4}G_{11} \tag{7.69}$$

$$(b_1+\frac{b_2}{\zeta})a_{11}-\frac{1}{4}(b_1+\frac{b_2}{\zeta})a_{13} + (b_1+\frac{6b_2}{\zeta})a_{31}=\frac{1}{2}\int_0^1\left[f_r(w)-f_l(w)\right]dw - \frac{1}{2}\int_{-1}^0\left[f_r(w)-f_l(w)\right]dw \tag{7.70}$$

$$(b_1+\frac{b_2}{\eta})a_{11}+(b_1+\frac{6b_2}{\eta})a_{13} - \frac{1}{4}(b_1+\frac{b_2}{\eta})a_{31}=\frac{1}{2}\int_0^1\left[f_t(u)-f_b(u)\right]du - \frac{1}{2}\int_{-1}^0\left[f_t(u)-f_b(u)\right]du \tag{7.71}$$

The third 3 by 3 matrix is formed by the following three equations.

$$Ba_{01}+\frac{15A}{\eta^2}a_{03}+\frac{3A}{\zeta^2}a_{21}=\frac{3}{4}G_{01} \tag{7.72}$$

$$b_1a_{01}-\frac{1}{4}b_1a_{03}+(b_1+\frac{3b_2}{\zeta})a_{21} = \frac{1}{2}\int_0^1\left[f_r(w)+f_l(w)\right]dw - \frac{1}{2}\int_{-1}^0\left[f_r(w)+f_l(w)\right]dw \tag{7.73}$$

$$(b_1+\frac{b_2}{\eta})a_{01}+(b_1+\frac{6b_2}{\eta})a_{03}=\frac{1}{4}\int_{-1}^1\left[f_t(u)-f_b(u)\right]du \tag{7.74}$$

The last matrix is formed by the following three equations.

$$Ba_{10}+\frac{3A}{\eta^2}a_{12}+\frac{15A}{\zeta^2}a_{30}=\frac{3}{4}G_{10} \tag{7.75}$$

$$b_1a_{10}+(b_1+\frac{3b_2}{\eta})a_{12}-\frac{1}{4}b_1a_{30}=\frac{1}{2}\int_0^1\left[f_t(u)+f_b(u)\right]du - \frac{1}{2}\int_{-1}^0\left[f_t(u)+f_b(u)\right]du \tag{7.76}$$

$$(b_1+\frac{b_2}{\zeta})a_{10}+(b_1+\frac{6b_2}{\zeta})a_{30}=\frac{1}{4}\int_{-1}^1\left[f_r(w)-f_l(w)\right]dw \tag{7.77}$$

8 IMPLEMENTATION OF THE METHOD

This chapter describes the way the modular nodal method has been implemented. The implementation of the method involves three different tasks. The first task is to generate the governing equations. The second task is to form the boundary conditions for these spherical harmonic equations. The last task is to develop a computer code which would implement the computational procedures described in the previous chapters.

As mentioned above, the first step was to develop a computer code for generating the second order form of the spherical harmonic differential equations. Since the spherical harmonic differential equations will always be the same, for practical reasons it was decided to generate them once and then to save the numbers representing these equations in a library file which can be read by the computer code to be developed as the third task. The program generating the differential equations is based upon the equations 5.43 and 5.44. The first differential equation given by 5.42 will always be solved for any order of approximation. Therefore, that equation has been built into the computer code that does the calculations. As a result, the library file generated for the spherical harmonics differential equations has the information only for $l > 0$. The second task was to generate the boundary conditions. The same approach as done with the generation of the differential equations was used

for that step too. A computer code which was based on equations 6.23-6.26 has been used for generating another library file containing the information for the boundary conditions. As in the first library file, this library also contains information for the equations for $l > 0$. Although the current library files have information for the P_{13} approximation, the developed computer codes can regenerate these libraries for any order if it becomes necessary.

The third task was to develop a computer code which would actually implement the modular nodal method. The developed computer code currently can handle the fixed source and the criticality problems. Both of these problems can be solved for either monoenergetic cases or for multigroup cases. The program can also implement the modular approach for determining the order of the spherical harmonic approximation to the neutron transport equation. In a manual mode, the distribution of the orders of the spherical harmonic approximation in the nodes can be given as input by the user. The modular approach for determining the spherical harmonic approximation can be used for both the fixed source and criticality problems. Therefore, we will first discuss the application of the modular approach. Then the implementation of the method for the fixed source problems will be discussed. The methodology for solving the fixed source problems is a subset of the method for solving the criticality problems. Once the fixed source method has been discussed, the criticality problem method will be discussed by using the information given for the fixed source problems.

8.1 The Implementation of the Modular Approach

As was mentioned in the Introduction, determining the order of the spherical harmonic approximation for a specific problem sometimes may not be easy. The chosen order for a problem may be too low or too high. For some problems, the order may be higher than required in some regions of the problem while it may lower in some other regions. The purpose of implementing the modular approach is to avoid the excessive computations or the lack of accuracy which may arise from inappropriate selection of the spherical harmonic order for the problems. The idea underlying the modular nodal method, which will avoid the inappropriate selection of the spherical harmonic order, is that as long as the neutron currents coming from the neighboring nodes are known, each node can be treated as a small isolated reactor core and can be addressed accordingly. In other words, the amount of directional dependency of the neutron flux in the neighboring nodes would have an impact only on the boundary conditions of the current node. That would allow us to use the proper spherical harmonic order for the specific node.

The implementation of the idea of the modular approach can be summarized as follows. If the spherical harmonics approximation in the adjacent node is of lower order, the boundary conditions for the moments which are not used in that adjacent node is set equal to zero as shown in the sixth chapter. If the approximation in the neighboring node is higher than the current node, we do not need to worry about that because the higher order moments in the current node are already zero. Through this approach, the nodes in which the neutron flux is approximated by different orders of the spherical harmonics expansion can be interfaced. The implementation of the modular approach requires one condition to be satisfied. The

method should be able to go to higher spherical harmonics approximation in an automatic manner. The reason for this condition is that the problem may require very high orders to be used. In such a case, the computer code should be able to use these high orders. Since the number of differential equations increases very rapidly as the order increases, no general computer code can be developed for very high order spherical harmonic approximations due to the complexity and the number of equations involved. Instead, the code should implement a numerical method which is good for all of the spherical harmonic equations for which the coefficients can be read from a library or can be generated in the initialization stage of the code. Since manipulating spherical harmonics equations into the equations 5.42-5.44 has been accompanied by implementation of an iterative scheme, that iterative scheme can be used for comparing two successive orders of the spherical harmonics approximation in an efficient manner. If the problem is solved for a specific order, the results will be the best initial guess for the succeeding order. This will reduce the amount of the computations significantly. The comparison between these two successive orders is used to determine if any further increase in the order is necessary for that specific node. As will be seen from equation 8.1, the change in the scalar flux is observed between two successive spherical harmonics orders. If the change for a specific node is smaller than a convergence criteria, the spherical harmonics order is not increased in that node any more. Even if the orders are increased in the neighboring nodes, the same order calculations are repeated in the specific node.

$$Relative\ Error = \left| \frac{\bar{\Phi}_{n-2} - \bar{\Phi}_n}{\bar{\Phi}_n} \right| \tag{8.1}$$

where n is final order of the approximation in the node.

$$\bar{\Phi} = \frac{1}{4}\int_{-1}^{1}\int_{-1}^{1}\Phi_{00}(u,w)dudw \tag{8.2}$$

An alternate mode which the program can handle is to use predetermined orders in all nodes. These orders, predetermined by the user, may be homogenous in all of the nodes or they may be different in the different nodes. In such a problem, the orders are increased in the nodes up to the specific value for each node. After that order, the orders are not increased as is done in the automatic ordering mode previously described.

8.2 The Fixed Source Problems

The fixed source type problems usually involve a source emitting neutrons into the problem domain. This neutron source is independent of the neutron flux. However the neutron source can be a function of direction and position. As was done in Chapter 5, the external source was here assumed to be isotropic. Therefore, the developed computer code can not handle anisotropic external sources. The external sources, however, can also be spatially dependent. In this work, the external source was assumed to be space dependent over the global domain, while it was taken to be flat at the nodal level. As a result, the computer code has capability for handling only flat sources. This can be satisfied by setting $S_{00}(x,y)$ in equation 5.42 equal to a constant in each node.

The computer code starts with an initialization section. In this section, the information necessary for the problem is read from external sources. Then the necessary coefficients for the equations are computed by using the information read from the external files. The computational part of the computer code is made up

of four nested loops. The implementation of the modular nodal method is done in this part. If we proceed from the outermost loop to the innermost one, the loops can be sequenced as follow. The first loop determines the spherical harmonic approximation which will be used. The second loop is for the neutron energy groups. The loop following that implements an iterative scheme which decouples the nodes from each other. The last and the innermost loop is used for implementing the iterative procedure for solving the spherical harmonic equations in the given nodes.

1. As was pointed out above, the outermost loop determines the order of the spherical harmonics approximation to the neutron transport equation. In the first entry to this loop, the approximation is a P_1 approximation. Every time this loop is accessed, the order of the spherical harmonic approximation is increased by two. If the approximation orders for the nodes are given as input for the problem, this loop is performed until the maximum of these orders is reached. If the modular approach with automatic ordering is used, then this loop is terminated if one of two following conditions is met. One of these conditions is that the ceiling number for the spherical harmonic approximation is reached. That ceiling order is used to keep the computer code from going to excessively high orders and it is determined by the user. The other condition which will stop the performance of the loop is that the spherical harmonic orders do not increase in any of the nodes. In other words, the current distribution of the spherical harmonic orders in the nodes are appropriate to solve the problem with enough accuracy. This is true when the errors computed through equation 8.1 in all of the nodes are smaller than the convergence criterion.

2. The second loop is for solving the multigroup problems. That loop is performed as many times as there are neutron energy groups. This is determined by the user. The current computer code can only handle the downscattering. The downscattering can be either directly coupled or nondirectly coupled.

3. The third loop, or middle iteration, performs a block Gauss-Seidel iteration scheme. In Chapter 7, it was shown that fourteen linear algebraic equations should be solved in each node for determining the coefficients of each spherical harmonic moment. These equations are actually coupled to the equations in the other nodes through the boundary conditions. In other words, the system to be solved is fourteen times the total number of the nodes. Instead of solving that system simultaneously, the equations are solved in each node by using the current values of the coefficients in the neighboring nodes. Once the computations in all the nodes are completed, the values of the spherical harmonic moments are compared to the values from the previous middle iteration and a relative error is computed. If the convergence criterion is met by that relative error, then the iteration is stopped; otherwise the iteration is continued.

4. The innermost loop implements an iterative scheme for solving the coupled spherical harmonic differential equations. This loop is also called the inner iteration. It should not be confused with the inner iteration used in conventional reactor analysis codes. Each of the spherical harmonic differential equation is coupled to the other differential equations as well as to the equations in the other nodes. The middle iteration described above decouples that equation from the other nodes. In addition to that, the inner iteration separates the

equation from the other spherical harmonic differential equations in the same node. In that inner iteration, the equations for the lowest moments are solved first. The results are used in calculating the right sides of the equations for the higher moments. The updated values of the higher moments are used for determining the righthand sides of the equations for the lower moments. The iteration is analogous to the Gauss-Seidel scheme if each differential equation can be likened to an algebraic equation. The iterations are terminated if a maximum iteration number is reached or the relative error computed after each iteration satisfies the convergence criterion.

8.3 Criticality Problems

In criticality problems, the source term is formed by neutrons originating from fission. Therefore, the source is affected by the neutron flux levels. For this case, the source term $S_{00}(x,y)$ is given by the following expression.

$$S_{00}(x,y) = \frac{1}{k}\upsilon\Sigma_f\Phi_{00}(x,y) \tag{8.3}$$

where :

k is the multiplication factor,

Σ_f is the fission cross section.

υ is the number of neutrons emitted per fission

In criticality problems, the determination of the multiplication factor k is an ultimate goal. The scheme used in determining the multiplication factor requires some modifications in the scheme described for the fixed source problems. A new loop is inserted between the first loop and the second loop. This new loop imple-

ments an iteration which is also known as the outer iteration or the source iteration. This iteration is started by assigning an initial guess both for the multiplication factor and for the scalar flux $\Phi_{00}(x,y)$. This forms a problem with a known source just as in the case with the fixed source problem. Therefore, the rest of the scheme is the same as the fixed source problem. When the results are obtained for that initial guess, the multiplication factor is updated by using the following expression.

$$k^n = k^{n-1}\left[\frac{\int_{Area} v\Sigma_f(x,y)\Phi_{00}^n(x,y)dxdy}{\int_{Area} v\Sigma_f(x,y)\Phi_{00}^{n-1}(x,y)dxdy}\right] \tag{8.4}$$

where n in the above equation is the iteration number for the source iteration.

Once the multiplication factor is updated, the new source can be computed by using the new values of the multiplication factor and the scalar flux as was done with the initial guess through equation 8.3. When the relative error computed by using two successive values of the multiplication factor is smaller than the convergence criterion, the source iteration is terminated. If the problem requires higher order spherical harmonics approximations, the same steps are repeated for that higher orders too. One important point in criticality problems is that the middle iteration described for the fixed source problem is not applied for criticality problems. This step is performed only once. The criticality problem requires the same problem to be solved with sources which are not significantly different from each other. This eliminates the need for the middle iteration.

9 RESULTS

The method whose development described in the previous chapters of this dissertation has been used for solving five benchmark problems. This chapter covers these five test problems and their results. The first three of these problems are fixed source problem and the last two are criticality problems. While some of these problems are one group problems, others are multigroup problems. Therefore, the test problems represent a wide spectrum of the problems which can be met in nuclear applications.

One of the important points in the evaluation of test results is the stability of the method. For evaluating this stability, some problems are solved for various node sizes and the results for these various node sizes are compared. One other indicator which was used for observing the performance of the method is the accuracy of the scalar flux. In most of the problems, the scalar flux has been compared to the benchmark results. For some other cases, the integral quantities of the scalar flux were used for evaluation purposes. For criticality problems, the quantity which was used as the performance criteria was the multiplication factor. Since a modular approach has been introduced in this work, some of the problems have also been used for determining how that modular approach performed and how the results provided by that approach have been compared to results where the spherical harmonic

approximation is homogenous throughout the problem domain.

The first test problem is a one group fixed source problem. This problem has been widely used by Fletcher [13-17]. For that problem, Fletcher published his own results and a exact solution. While his results are based on a finite difference method, the details about the solution that he refers as the exact solution can be found in [13]. As can be seen in Figure 9.1, the problem domain is a square with a sidelength of 4.0 cm. The top and the right sides of the problem use vacuum boundary conditions while the other sides are reflective conditions. The material of the problem is a pure absorber and the problem domain is homogenous. The total cross section for the region is $\Sigma_t = 1.0\ cm^{-1}$ and the scattering cross section is $\Sigma_s = 0.0\ cm^{-1}$. The problem has a normalized constant source $S = 0.69444\ neutrons.cm^{-3}.sec^{-1}$ in a 1.44 cm^2 zone at the lower left corner. This problem has been used for studying both the stability and the accuracy of the nodal method.

For testing the numerical stability of the method, the problem has been solved for four different configurations for the P_3 approximation. Since this approximation order also provides the P_1 results, the scalar flux for both P_1 and P_3 have been compared for the various node sizes. These comparisons can be seen in Tables 9.1 and 9.2. Equal size nodes are used in all of the four configurations. A middle iteration convergence criterion of $1.0E-6$ was used for this problem.

If Tables 9.1 and 9.2 are studied, the following trend can be seen. While the differences between the 4x4 node configuration and the 5x5 configuration can go up to the order of 0.1, the differences between the 6x6 configuration and the 8x8 configuration are on the order of $1.0E-3$. As a result of this trend, we can say that

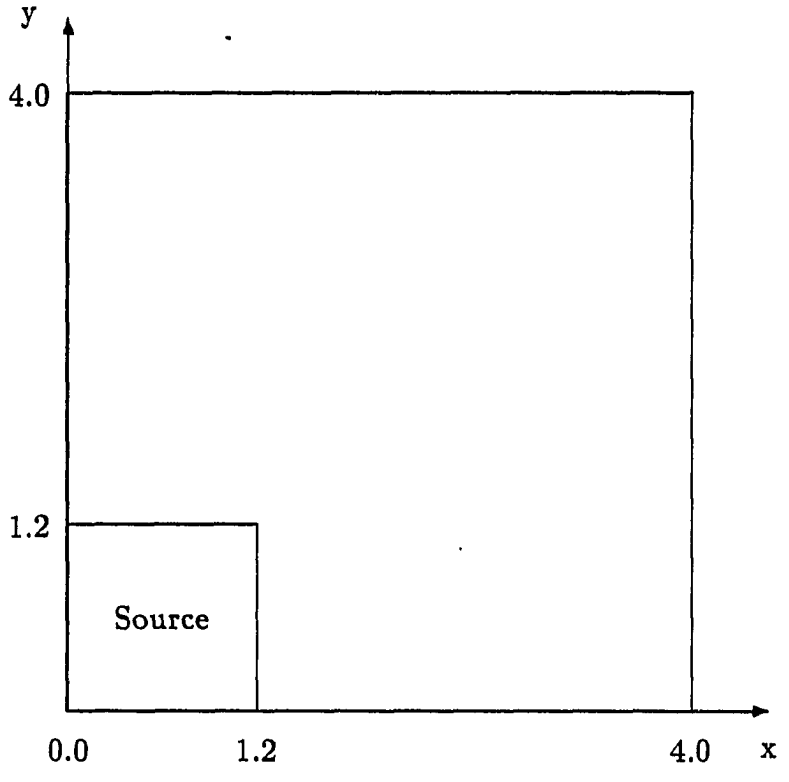

Figure 9.1: The geometry and dimensions for Fletcher's problem

Table 9.1: Comparisons of the P_1 approximation scalar fluxes for Fletcher's problem at $y = 3.9$ cm for various configurations

Distance (cm)	4x4 Nodes	5x5 Nodes	6x6 Nodes	8x8 Nodes	Exact
0.1	2.098E-3	2.062E-3	2.055E-3	2.052E-3	2.603E-3
0.3	2.027E-3	2.020E-3	2.017E-3	2.014E-3	2.569E-3
0.5	1.953E-3	1.953E-3	1.948E-3	1.953E-3	2.502E-3
0.7	1.944E-3	1.864E-3	1.857E-3	1.859E-3	2.408E-3
0.9	1.741E-3	1.731E-3	1.730E-3	1.724E-3	2.286E-3
1.1	1.563E-3	1.586E-3	1.589E-3	1.589E-3	2.143E-3
1.3	1.410E-3	1.436E-3	1.432E-3	1.428E-3	1.985E-3
1.5	1.292E-3	1.275E-3	1.271E-3	1.270E-3	1.818E-3
1.7	1.157E-3	1.111E-3	1.110E-3	1.111E-3	1.646E-3
1.9	1.000E-3	9.492E-4	9.568E-4	9.521E-4	1.475E-3
2.1	8.182E-4	7.907E-4	8.070E-4	8.074E-4	1.307E-3
2.3	6.172E-4	6.714E-4	6.748E-4	6.760E-4	1.149E-3
2.5	4.080E-4	5.579E-4	5.545E-4	5.540E-4	1.000E-3
2.7	4.099E-4	4.535E-4	4.492E-4	4.510E-4	8.652E-4
2.9	3.522E-4	3.577E-4	3.629E-4	3.614E-4	7.426E-4
3.1	2.988E-4	2.831E-4	2.874E-4	2.877E-4	6.335E-4
3.3	2.438E-4	2.258E-4	2.211E-4	2.246E-4	5.369E-4
3.5	1.850E-4	1.776E-4	1.769E-4	1.793E-4	4.528E-4
3.7	1.246E-4	1.360E-4	1.360E-4	1.362E-4	3.802E-4
3.9	6.857E-5	1.000E-4	1.024E-4	1.030E-4	3.179E-4

Table 9.2: Comparisons of the P_3 approximation scalar fluxes for Fletcher's problem at $y = 3.9\ cm$ for various configurations

Distance (cm)	4x4 Nodes	5x5 Nodes	6x6 Nodes	8x8 Nodes	Exact
0.1	2.342E-3	2.414E-3	2.436E-3	2.439E-3	2.603E-3
0.3	2.247E-3	2.376E-3	2.396E-3	2.404E-3	2.569E-3
0.5	2.198E-3	2.315E-3	2.333E-3	2.334E-3	2.502E-3
0.7	1.913E-3	2.209E-3	2.230E-3	2.236E-3	2.408E-3
0.9	1.820E-3	2.091E-3	2.107E-3	2.109E-3	2.286E-3
1.1	1.562E-3	1.952E-3	1.966E-3	1.964E-3	2.143E-3
1.3	1.962E-3	1.810E-3	1.799E-3	1.800E-3	1.985E-3
1.5	1.719E-3	1.646E-3	1.634E-3	1.635E-3	1.818E-3
1.7	1.601E-3	1.492E-3	1.469E-3	1.466E-3	1.646E-3
1.9	1.473E-3	1.327E-3	1.299E-3	1.299E-3	1.475E-3
2.1	1.269E-3	1.152E-3	1.145E-3	1.144E-3	1.307E-3
2.3	9.959E-4	1.006E-3	1.001E-3	9.957E-4	1.149E-3
2.5	7.283E-4	8.813E-4	8.610E-4	8.628E-4	1.000E-3
2.7	6.637E-4	7.537E-4	7.401E-4	7.407E-4	8.652E-4
2.9	6.207E-4	6.260E-4	6.331E-4	6.313E-4	7.426E-4
3.1	5.530E-4	5.266E-4	5.332E-4	5.357E-4	6.335E-4
3.3	4.627E-4	4.515E-4	4.465E-4	4.489E-4	5.369E-4
3.5	3.562E-4	3.742E-4	3.739E-4	3.736E-4	4.528E-4
3.7	2.447E-4	2.980E-4	3.039E-4	3.052E-4	3.802E-4
3.9	1.434E-4	2.265E-4	2.375E-4	2.404E-4	3.179E-4

as the node sizes decreases, the scalar fluxes converge to some limiting values. Due to this convergence and due to the fact that the results are still reasonable for relatively large node sizes, we can say that the nodal method has stable characteristics. In addition to the stability evaluation, Fletcher's test problem has also been used for evaluating the behavior of the method as the spherical harmonic approximation order increases. For a successful application, the scalar fluxes should converge to the exact solution as the spherical harmonic order increases. For this purpose, the problem has been solved for a P_7 approximation. The approximation orders were homogenous in all the nodes. A 6x6 nodal configuration has been used for this problem. The comparison of the results to Fletcher's results is given in the Table 9.3. The same results are also compared to the exact solution in graphic form in Figure 9.2.

If we study the results presented in the Figure 9.2 and Table 9.3, we can make the following observations. The P_5 and P_7 approximations provide results comparable to the exact solution. This can be seen in Figure 9.2. Although it is quantitatively of the right magnitude, the P_7 approximation displays some variations. This points out a convergence problem since the number of spherical harmonic differential equations increases rapidly. The lack of these variations in the lower approximation results supports that conclusion. Other than this perturbation, all of the approximations seem to underestimate the exact solution at the right end of the domain. This same observation is also valid when the comparison is made by taking Fletcher's results as the reference values. The underestimation may arise from the fact that the boundary conditions are implemented in an integral sense. Since the neutron source is at the lower left corner of the domain, the integral im-

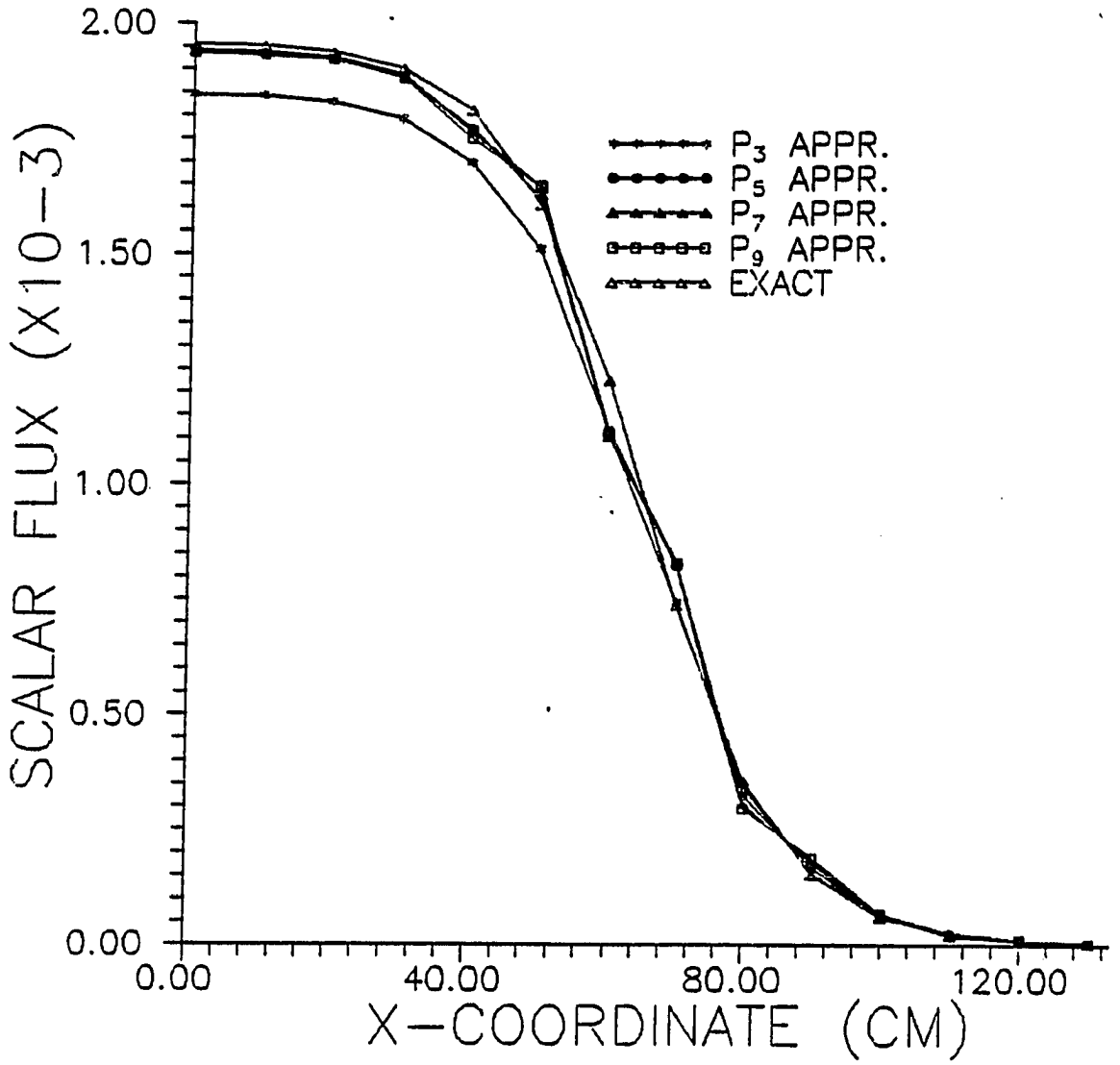

Figure 9.2: The scalar fluxes for Fletcher's problem at y=3.9 cm for various spherical harmonic approximations

Table 9.3: Comparisons of the scalar fluxes to Fletcher's results at y=3.9 cm

Distance (cm)	P_3	P_3 Fletcher	P_5	P_5 Fletcher	P_7	P_7 Fletcher
0.1	2.43E-3	2.53E-3	2.61E-3	2.62E-3	2.61E-3	2.59E-3
0.3	2.39E-3	2.50E-3	2.56E-3	2.59E-3	2.54E-3	2.56E-3
0.5	2.33E-3	2.43E-3	2.48E-3	2.52E-3	2.46E-3	2.49E-3
0.7	2.23E-3	2.34E-3	2.36E-3	2.43E-3	2.30E-3	2.40E-3
0.9	2.10E-3	2.23E-3	2.22E-3	2.30E-3	2.14E-3	2.28E-3
1.1	1.96E-3	2.10E-3	2.06E-3	2.16E-3	1.99E-3	2.13E-3
1.3	1.79E-3	1.95E-3	1.89E-3	2.00E-3	1.87E-3	1.97E-3
1.5	1.63E-3	1.79E-3	1.72E-3	1.83E-3	1.74E-3	1.81E-3
1.7	1.46E-3	1.62E-3	1.54E-3	1.65E-3	1.57E-3	1.63E-3
1.9	1.29E-3	1.46E-3	1.34E-3	1.48E-3	1.34E-3	1.46E-3
2.1	1.14E-3	1.30E-3	1.17E-3	1.31E-3	1.15E-3	1.30E-3
2.3	1.00E-3	1.15E-3	1.02E-3	1.15E-3	9.99E-4	1.14E-3
2.5	8.61E-4	1.01E-3	8.69E-4	1.00E-3	8.33E-4	9.97E-4
2.7	7.40E-4	8.78E-4	7.50E-4	8.72E-4	7.22E-4	8.62E-4
2.9	6.33E-4	7.58E-4	6.49E-4	7.48E-4	6.33E-4	7.40E-4
3.1	5.33E-4	6.51E-4	5.50E-4	6.37E-4	5.48E-4	6.32E-4
3.3	4.46E-4	5.55E-4	4.60E-4	5.40E-4	4.65E-4	5.36E-4
3.5	3.73E-4	4.70E-4	3.79E-4	4.55E-4	3.84E-4	4.53E-4
3.7	3.03E-4	3.97E-4	3.00E-4	3.82E-4	3.04E-4	3.80E-4
3.9	2.37E-4	3.33E-4	2.28E-4	3.19E-4	2.38E-4	3.18E-4

plementation of the boundary conditions may not provide strong enough coupling to the upper right corner. This argument can be supported by the fact that the same underestimation is not observed at the left side of the domain. These results are also compared to Fletcher's results to see if the method is in agreement with the other methods employing the spherical harmonic approximation to the transport equation. The comparison given in the Table 9.3 shows both the nodal method results and Fletcher's results based upon the finite difference method are in agreement in general except at the upper right part of the domain.

A second test problem is also a fixed source problem used by Natelson [47]. As seen from Figure 9.3, the dimensions and the geometry of this one group problem resemble Fletcher's problem. However the problems differ at two points. Natelson's problem uses reflective boundary conditions all around the domain and the domain is not homogenous. The neutronic parameters in the source region and outside the source region are not the same. The total macroscopic cross section both inside and outside the source region has the value $\Sigma_t = 1.0\ cm^{-1}$. The scattering cross section inside the source region is $\Sigma_s = 0.25\ cm^{-1}$ and $\Sigma_s = 0.5\ cm^{-1}$ outside the source region. The strength of the source is $S = 1.0\ neutrons.cm^{-3}.sec^{-1}$. As it was done with Fletcher's problem, the spherical harmonic orders are chosen to be homogenous for all the nodes. In contrast with Fletcher's problem, the exact solution is not available for comparison. The nodal method results are compared to the spherical harmonic approximation results provided by Kobayashi et al. who solved the same problem through a finite difference based method [18]. Kobayashi presents his results in graphical form. The numerical form of the results were obtained through digitization of the graph. The comparisons of both sets of the

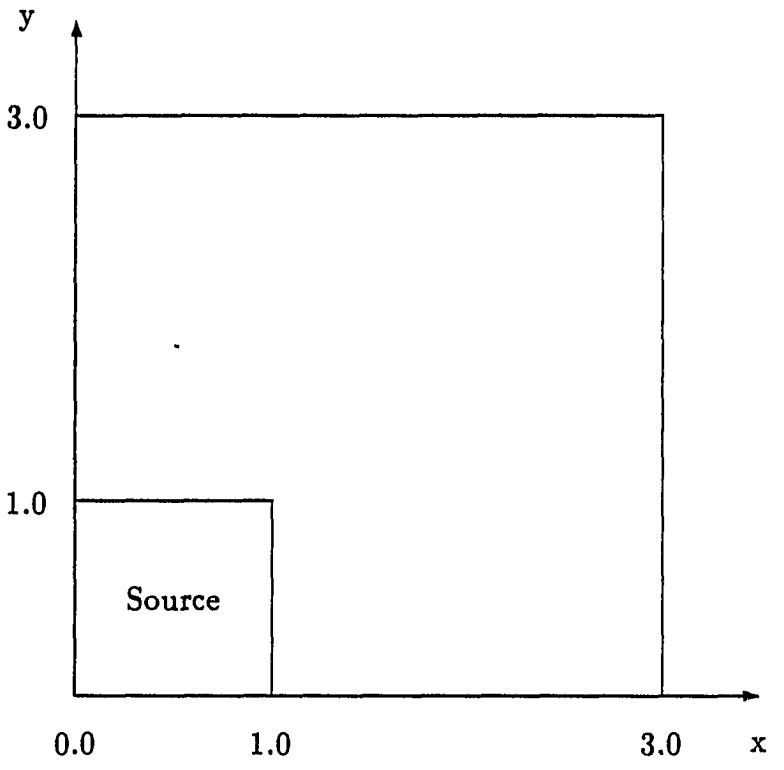

Figure 9.3: The geometry and dimensions for Natelson's problem

results at $y = 3.0$ *cm* are shown in the Table 9.4. A very close agreement is apparent between two the sets of results for all approximation orders. The differences between the two sets of results are on the orders of 1.0%. In Figure 9.4, the scalar fluxes are compared for various orders of spherical harmonic approximations.

A third problem used to test the model is also a fixed source problem formed by Gelbard and Crawford [48]. This problem differs from the previous problems on two important points. One of these differences is that this problem is a two group problem. In addition to that, the dimensions of the problem are very large. As seen from

Table 9.4: The comparison of the scalar fluxes to the Kobayashi's results at y=3.0 cm

Distance (cm)	P-3	P-3 Kobayashi	P-5	P-5 Kobayashi	P-7	P-7 Kobayashi
0.0	3.65E-2	3.65E-2	3.89E-2	3.87E-2	3.94E-2	3.89E-2
0.2	3.61E-2	3.62E-2	3.84E-2	3.83E-2	3.88E-2	3.87E-2
0.4	3.53E-2	3.53E-2	3.75E-2	3.75E-2	3.78E-2	3.77E-2
0.6	3.40E-2	3.42E-2	3.60E-2	3.61E-2	3.61E-2	3.63E-2
0.8	3.23E-2	3.25E-2	3.41E-2	3.42E-2	3.40E-2	3.44E-2
1.0	3.02E-2	3.05E-2	3.19E-2	3.22E-2	3.18E-2	3.22E-2
1.2	2.80E-2	2.81E-2	2.95E-2	2.98E-2	2.96E-2	2.98E-2
1.4	2.57E-2	2.58E-2	2.69E-2	2.70E-2	2.70E-2	2.70E-2
1.6	2.34E-2	2.35E-2	2.45E-2	2.36E-2	2.44E-2	2.46E-2
1.8	2.13E-2	2.14E-2	2.22E-2	2.23E-2	2.22E-2	2.24E-2
2.0	1.94E-2	1.94E-2	2.01E-2	2.01E-2	1.99E-2	2.02E-2
2.2	1.78E-2	1.78E-2	1.84E-2	1.83E-2	1.82E-2	1.83E-2
2.4	1.65E-2	1.65E-2	1.70E-2	1.68E-2	1.69E-2	1.67E-2
2.6	1.56E-2	1.55E-2	1.60E-2	1.57E-2	1.61E-2	1.58E-2
2.8	1.50E-2	1.50E-2	1.54E-2	1.51E-2	1.55E-2	1.51E-2
3.0	1.48E-2	1.47E-2	1.52E-2	1.50E-2	1.53E-2	1.49E-2

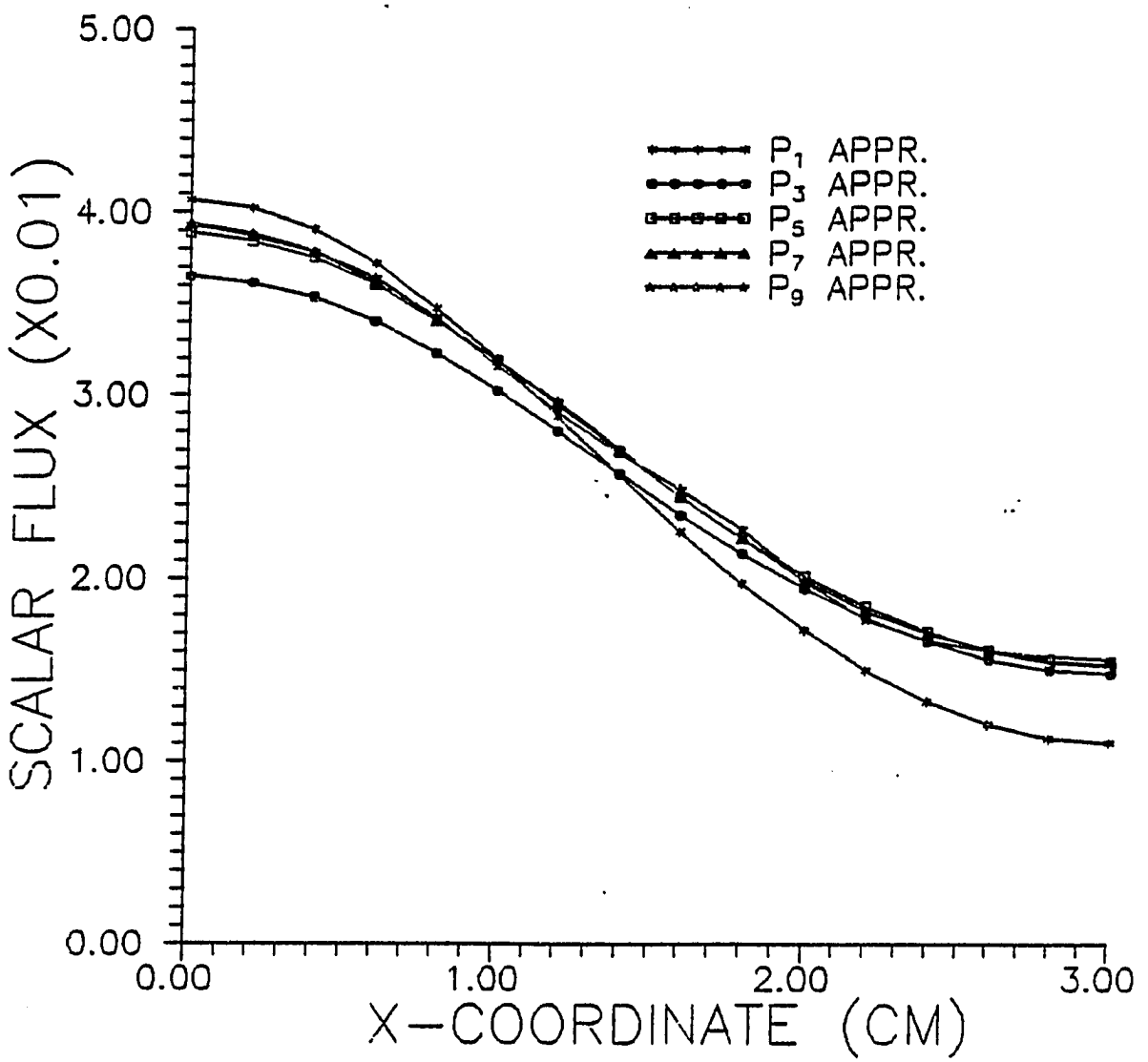

Figure 9.4: The scalar fluxes for Natelson's problem at y=3.0 cm for various spherical harmonic approximations

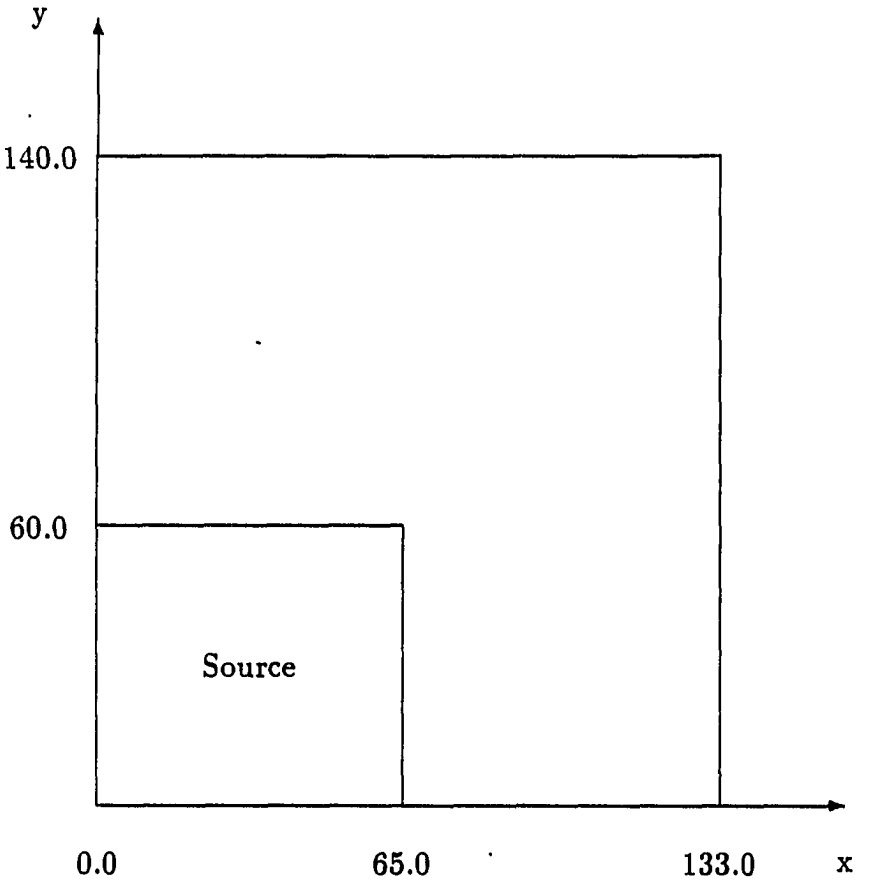

Figure 9.5: The geometry and dimensions for Gelbard and Crawford's problem

Figure 9.5, the geometry of the problem is similar to the first two fixed source problems. The neutronic parameters defining the material to be used is given in the Table 9.5. The neutron normalized sources used are $S = 0.006546\ neutrons.cm^{-3}.sec^{-1}$ for the first group and $S = 0.017701\ neutrons.cm^{-3}.sec^{-1}$ for the second group. Reflective boundary conditions are used all around the problem domain.

Gelbard's problem was solved with a P_9 approximation. The spherical harmonic orders were homogenous all through the nodes. A 10x10 nodal configura-

Table 9.5: Neutronic parameters for Gelbard's problem

Σ_{t1}	Σ_{t2}	$\Sigma_{s,1\rightarrow 1}$	$\Sigma_{s,1\rightarrow 2}$	$\Sigma_{s,2\rightarrow 2}$
0.092104	0.100877	0.006947	0.023434	0.00485

tion was used for solving the problem. The comparisons of the scalar fluxes for $y = 139.0\ cm$ and $y = 80.0\ cm$ for the first group are given in the Table 9.6 and Table 9.7. The exact solutions for this problem are provided in [48]. One important trend in these results is that the convergence problem pointed out for Fletcher's problem is visible for the P_9 approximation. Otherwise the approximations up to P_7 seem to be converging to the exact solution in a smooth manner. This behavior can be observed in Tables 9.6 and 9.7. Except convergence problem for the P_9 approximation, the results seem to be in good agreement with the exact solutions at both locations. This can be observed in Figures 9.6 and 9.7. The P_1 approximation gives nonphysical results for this problem and not listed here.

Gelbard's problem has also been solved by using the modular approach. The maximum order of the program has been chosen as P_9. The convergence criterion for the spherical harmonic was selected as %1.0. Whenever one of the nodes satisfied this convergence criterion, the spherical harmonic order was kept constant for the rest of the calculations. Figure 9.8 shows the final distribution of the spherical harmonic approximation orders in the nodes. The execution time for this problem on the NAS 9160 machine at Iowa State University was 87.1 seconds. This can be compared to the execution time of 167.2 seconds for the homogenous case. If the problem had been solved for a maximum order of P_7, these execution times would have been 82.6 seconds and 68.1 seconds respectively. If Figure 9.8 is studied carefully, we can observe the following trends. The computer code implements the

Table 9.6: The comparison of the scalar fluxes at y=139.0 cm for the first group

Distance (cm)	P_3	P_5	P_7	P_9	Exact
0.0	6.013E-6	6.071E-6	6.103E-6	6.139E-6	6.118E-6
10.0	5.954E-6	6.020E-6	6.042E-6	6.048E-6	6.062E-6
20.0	5.776E-6	5.839E-6	5.839E-6	5.722E-6	5.884E-6
30.0	5.462E-6	5.521E-6	5.586E-6	5.737E-6	5.561E-6
40.0	4.991E-6	5.070E-6	5.057E-6	5.007E-6	5.070E-6
50.0	4.331E-6	4.396E-6	4.349E-6	4.258E-6	4.408E-6
60.0	3.536E-6	3.600E-6	3.630E-6	3.855E-6	3.615E-6
70.0	2.703E-6	2.744E-6	2.727E-6	2.502E-6	2.773E-6
80.0	1.905E-6	1.946E-6	2.014E-6	2.046E-6	1.980E-6
90.0	1.249E-6	1.288E-6	1.328E-6	1.411E-6	1.317E-6
100.0	7.808E-7	8.279E-7	7.890E-7	6.610E-7	8.225E-7
110.0	4.563E-7	4.993E-7	4.933E-7	5.716E-7	4.934E-7
120.0	2.666E-7	3.135E-7	3.077E-7	3.137E-7	3.038E-7
130.0	1.930E-7	2.421E-7	2.402E-7	2.031E-7	2.261E-7

Table 9.7: Comparisons of the scalar fluxes at y=80.0 cm for the first energy group

Distance (cm)	P_3	P_5	P_7	P_9	Exact
0.0	1.844E-3	1.935E-3	1.941E-3	1.937E-3	1.954E-3
10.0	1.842E-3	1.932E-3	1.937E-3	1.931E-3	1.951E-3
20.0	1.828E-3	1.921E-3	1.925E-3	1.921E-3	1.937D-3
30.0	1.791E-3	1.882E-3	1.886E-3	1.879E-3	1.900D-3
40.0	1.695E-3	1.768E-3	1.762E-3	1.748E-3	1.810E-3
50.0	1.510E-3	1.618E-3	1.641E-3	1.644E-3	1.605E-3
60.0	1.114E-3	1.114E-3	1.107E-3	1.102E-3	1.224E-3
70.0	7.442E-4	8.238E-4	8.321E-4	8.277E-4	7.374E-4
80.0	3.482E-4	3.264E-4	3.063E-4	2.969E-4	3.562E-4
90.0	1.551E-4	1.690E-4	1.794E-4	1.875E-4	1.512E-4
100.0	6.404E-5	6.257E-5	6.493E-5	6.719E-5	6.050E-5
110.0	2.565E-5	2.294E-5	2.112E-5	1.954E-5	2.375E-5
120.0	1.041E-5	9.723E-6	1.031E-5	1.147E-5	9.748E-6
130.0	5.473E-6	5.482E-6	5.420E-6	4.946E-6	5.371E-6

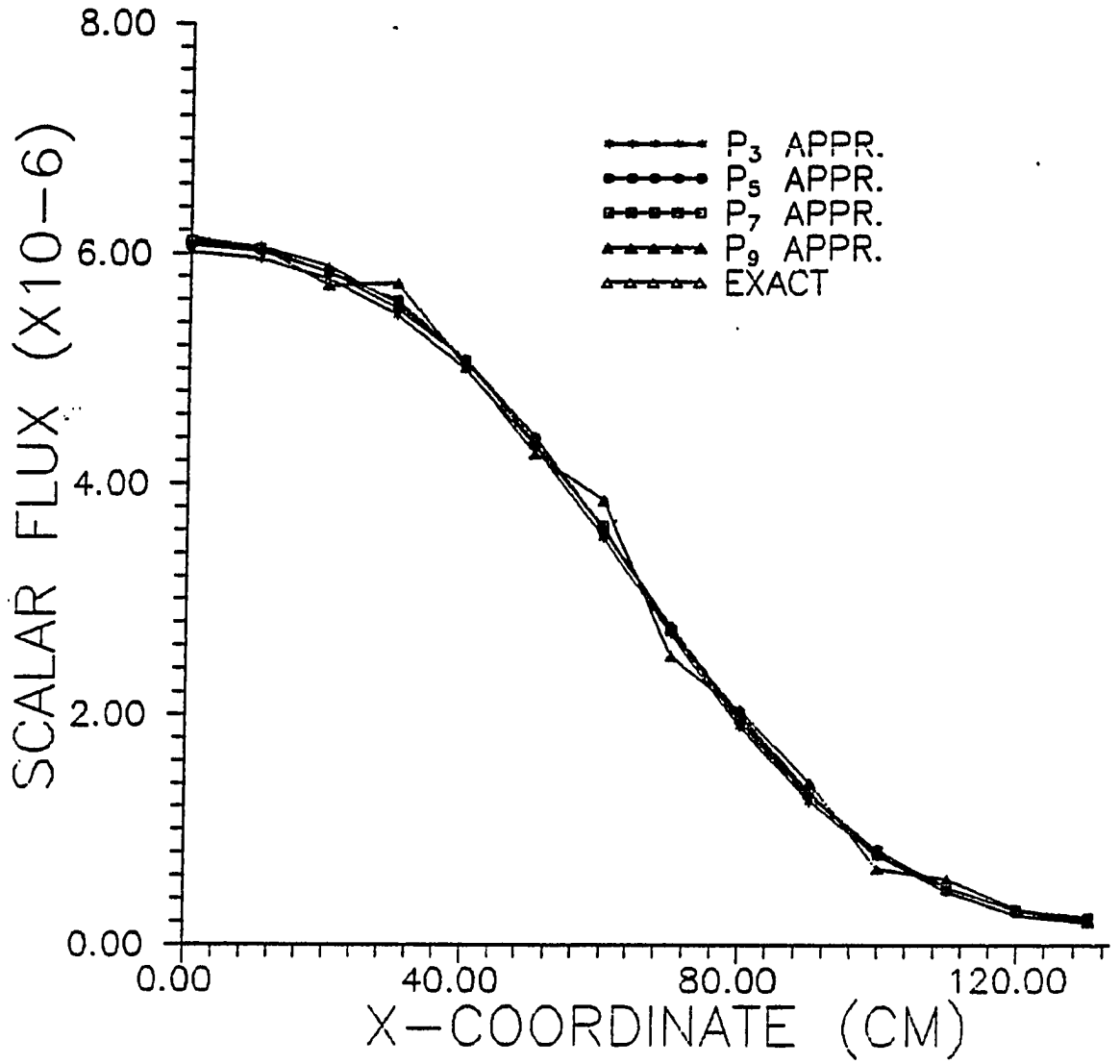

Figure 9.6: Comparisons of the scalar fluxes at y=139.0 cm for the first energy group

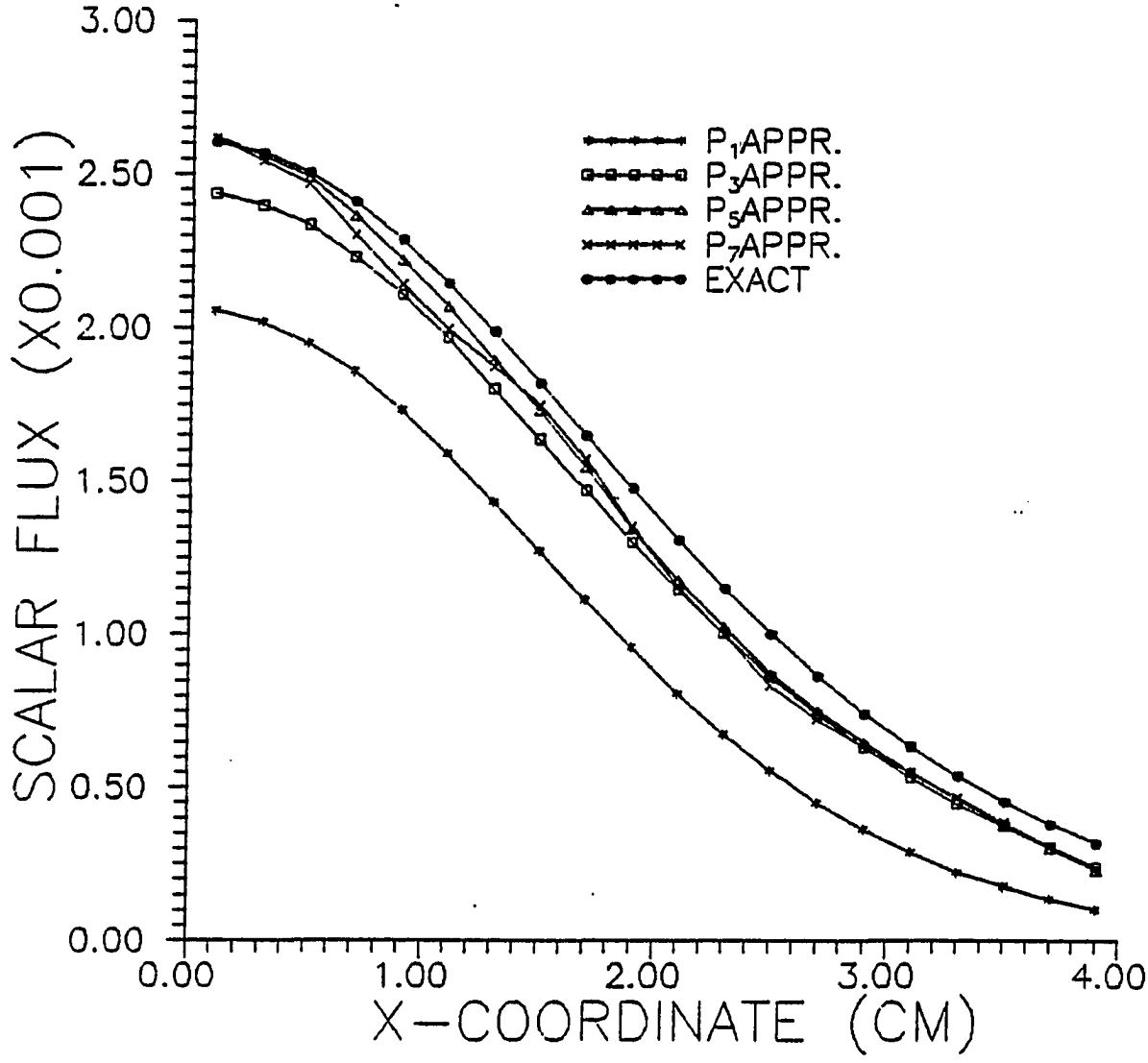

Figure 9.7: Comparisons of the scalar fluxes at y=80.0 cm for the first energy group

P_3 approximation for the left lower corner of the domain. Since there is a neutron source in this region and the boundary conditions bordering the source region are reflective, slower changes in the flux levels are expected in that part of the domain. Therefore, the implementation of the P_3 approximation in this region is physically sound. As we get closer to the outer borders of the domain, the approximation orders implemented by the computer code get higher. There is no neutron source in the outer region and the absorption becomes an important mechanism in determining the flux levels. Therefore, sudden drops in the flux levels within short distances should be accepted as normal trends in this region. Since the sudden changes in the flux levels usually require a more rigorous treatment of the transport equation, the higher orders used by the computer code are understandable.

In Tables 9.8 and 9.9, the scalar fluxes at $y = 139.0\ cm$ and $y = 80.0\ cm$ for the first energy group are compared to the exact solution as has been done with the previous case. The notation in these tables require some explanation. When an order is noted, this order is the maximum order in the problem domain for that solution. Therefore, when the P_9 approximation is noted, there may be some nodes using P_7, P_5 and P_3 approximations. In a similar manner, some nodes may be using P_3 and P_5 approximations if a P_7 approximation is mentioned.

As seen from Tables 9.8 and 9.9, the P_5 approximation seems to be providing results which are more accurate than the P_7 and P_9 approximations. In other words, as the distribution of the spherical harmonic approximation orders becomes more heterogenous, the accuracy does not improve. One other test of the modular approach was done on the continuity of the scalar fluxes at the interfaces of the nodes where the spherical harmonic orders change from one node to the other. For

5	5	5	9	9	9	9	7	9	9
9	7	9	7	9	9	9	7	7	9
9	7	7	7	9	7	9	9	9	9
9	5	5	5	9	9	9	5	9	5
3	7	7	7	7	7	7	9	9	7
7	7	7	7	7	9	7	9	7	9
5	5	5	5	7	7	7	9	9	7
3	3	3	3	5	7	7	5	7	9
3	3	3	3	5	7	7	5	7	9
3	3	3	3	5	7	3	9	9	7

Figure 9.8: Distribution of the spherical harmonic orders for Gelbard's problem

Table 9.8: Comparisons of the scalar fluxes at y=139.0 cm provided by the modular method

Distance (cm)	P_5	P_7	P_9	Exact
0.0	6.122E-6	6.063E-6	6.087E-6	6.118E-6
10.0	6.072E-6	6.087E-6	6.093E-6	6.062E-6
20.0	5.890E-6	5.959E-6	5.939E-6	5.884E-6
30.0	5.571E-6	5.749E-6	5.769E-6	5.561E-6
40.0	5.104E-6	5.175E-6	5.170E-6	5.070E-6
50.0	4.420E-6	4.400E-6	4.434E-6	4.408E-6
60.0	3.609E-6	3.633E-6	3.609E-6	3.615E-6
70.0	2.750E-6	2.737E-6	2.694E-6	2.773E-6
80.0	1.948E-6	1.905E-6	1.893E-6	1.980E-6
90.0	1.295E-6	1.201E-6	1.203E-6	1.317E-6
100.0	8.256E-7	7.996E-7	7.842E-7	8.225E-7
110.0	4.978E-7	5.484E-7	5.569E-7	4.934E-7
120.0	3.133E-7	3.173E-7	3.242E-7	3.038E-7
130.0	2.437E-7	2.138E-7	2.061E-7	2.261E-7

Table 9.9: Comparisons of the scalar fluxes at y=80.0 cm provided by the modular method

Distance (cm)	P_5	P_7	P_9	Exact
0.0	1.887E-3	1.876E-3	1.875E-3	1.954E-3
10.0	1.901E-3	1.895E-3	1.894E-3	1.951E-3
20.0	1.905E-3	1.899E-3	1.899E-3	1.937E-3
30.0	1.882E-3	1.874E-3	1.874E-3	1.900E-3
40.0	1.770E-3	1.767E-3	1.767E-3	1.810E-3
50.0	1.618E-3	1.648E-3	1.650E-3	1.605E-3
60.0	1.113E-3	1.094E-3	1.091E-3	1.224E-3
70.0	8.234E-4	8.368E-4	8.397E-4	7.374E-4
80.0	3.257E-4	3.145E-4	3.081E-4	3.562E-4
90.0	1.691E-4	1.814E-4	1.809E-4	1.512E-4
100.0	6.245E-5	6.641E-5	6.674E-5	6.050E-5
110.0	2.295E-5	2.225E-5	2.232E-5	2.375E-5
120.0	9.699E-6	9.786E-6	1.033E-5	9.748E-6
130.0	5.466E-6	4.927E-6	5.082E-6	5.371E-6

that purpose, the scalar flux at $y = 0.0\ cm$ is plotted in Figure 9.9. It can be seen from that figure that all of the scalar fluxes display a continuous character through the interfaces of the nodes which use different orders of the spherical harmonic orders. Another result which is very obvious is that the scalar fluxes for various approximations coincide with each other very closely.

The fourth problem solved by using the nodal method was a criticality problem. This problem is a four group, fast reactor type problem and it was taken from Kobayashi et al. [18]. As seen from Figure 9.10, the problem domain is divided into four regions. The lower left corner is the reactor core and the surrounding regions are the blanket regions. The sides of the problem bordering the core region use the reflective boundary conditions while the outer boundaries use the vacuum boundary conditions. The core is a multiplicative region while the multiplication in the blanket is very low. The characteristics of the core and the blanket materials are given in the Table 9.10. As it was done with Gelbard's problem, this problem has also been solved by the conventional and the modular approach. The configuration for solving this problem was chosen to be 8x8 nodes. The convergence criterion for the outer iteration was $1.0E-5$. The results of this problem have been compared to Kobayashi's results. The comparisons of the multiplication factors are given in Table 9.11. The integrated fluxes for various regions are tabulated in Tables 9.12 and 9.13. The spherical harmonic distribution in the nodes for the modular approach are given in Figure 9.11.

As can be seen from Table 9.11, the multiplication factors computed by the nodal method are in good agreement with Kobayashi's multiplication factors. The differences between the nodal method results and Kobayashi's results are smaller

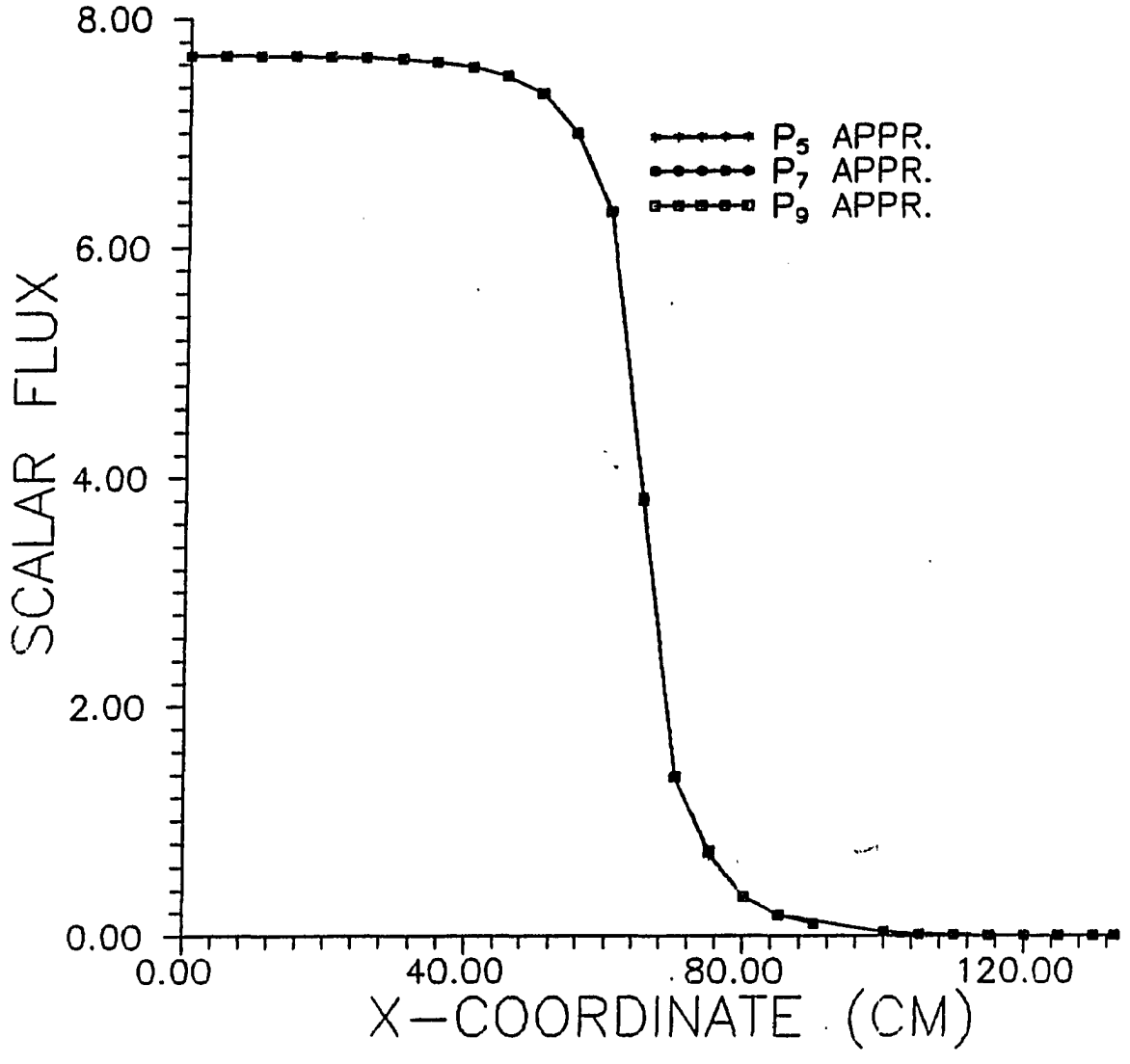

Figure 9.9: The scalar flux at y=0.0 as provided by the modular approach

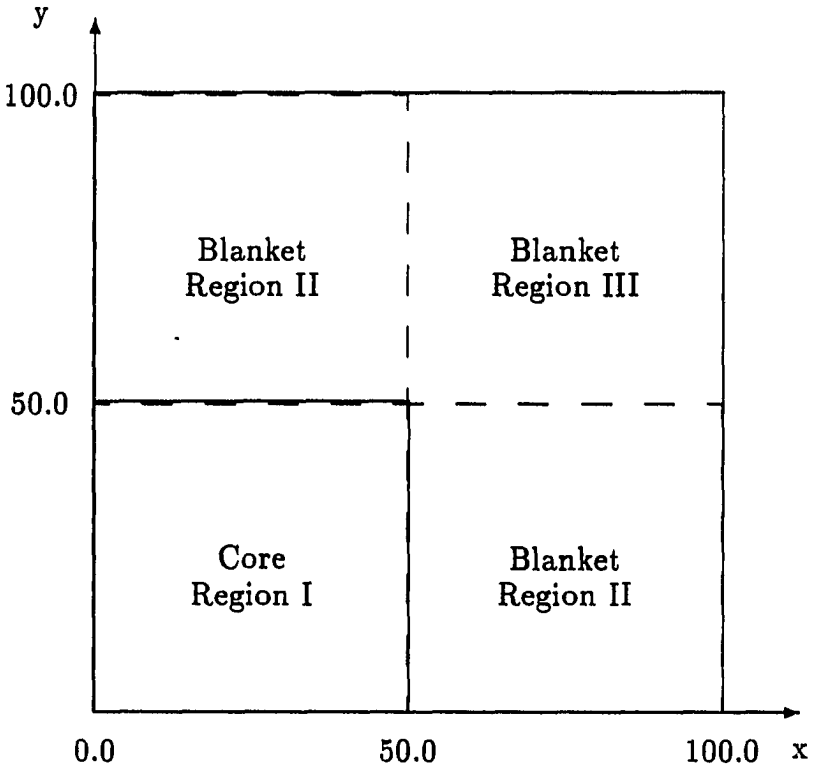

Figure 9.10: The geometry and dimensions for Kobayashi's problem

than 0.07 %. If Tables 9.12 and 9.13 are compared, it is seen that the judgment for the multiplication factor is true also for the integrated fluxes. The modular results also compare to Kobayashi's results favorably. One important point in the modular results is that the computer code did not go to orders higher than the fifth order although the allowed maximum order was higher. Therefore, we can assume that the problem can be adequately solved by a fifth order approximation.

The fifth and the last problem solved to test the nodal method is also a criticality problem. The IAEA benchmark problem, which is also known as the EIR-2 benchmark problem, is a one group problem with anisotropic scattering [49]. The

Table 9.10: The neutronic parameters for Kobayashi's problem

Material	g	Σ_t	χ_g	$\upsilon\Sigma_{fg}$	$\Sigma_{s,1\to g}$	$\Sigma_{s,2\to g}$	$\Sigma_{s,3\to g}$	$\Sigma_{s,4\to g}$
CORE	1	0.0994728	0.577	9.94141	0.0629328	0.0	0.0	0.0
	2	0.135722	0.362	8.41624	0.02963	0.124152	0.0	0.0
	3	0.1782531	0.061	9.60889	0.0029	0.0067	0.1670531	0.0
	4	0.2647604	0.0	1.46382	0.0	0.0003	0.0032	0.2545504
BLANKET	1	0.1249375	0.577	4.83123	0.0696275	0.0	0.0	0.0
	2	0.164042	0.362	0.0	0.04736	0.153532	0.0	0.0
	3	0.2677556	0.061	0.0	0.0512	0.00739	0.2289256	0.0
	4	0.3415301	0.0	0.0	0.0	0.00004	0.00399	0.3324201

5	5	5	5	5	5	5	5
5	5	5	5	5	5	5	5
5	5	5	5	5	5	5	5
5	5	5	5	5	5	5	5
3	3	3	3	5	5	5	5
3	3	3	3	5	5	5	5
3	3	3	3	5	5	5	5
3	3	3	3	5	5	5	5

Figure 9.11: Distribution of the spherical harmonic orders for Kobayashi's problem

Table 9.11: Comparisons of multiplication factors to Kobayashi's results

	Nodal Method	Kobayashi
P_1	1.04475	1.04449
P_3	1.05016	1.04961
P_5	1.05034	1.04958
P_7	1.05038	1.04959
Modular	1.05020	- -

Table 9.12: The integrated fluxes provided by the nodal method for various regions of the core

Appr. Order	Group	Region I	Region II	Region III
P_1	1	1.000	5.424E-2	3.998E-3
	2	4.038	6.224E-1	1.153E-1
	3	3.269	7.130E-1	1.666E-1
	4	1.087	3.207E-1	8.726E-2
P_3	1	1.000	5.040E-2	4.265E-3
	2	4.021	6.018E-1	1.140E-1
	3	3.247	6.957E-1	1.636E-1
	4	1.073	3.137E-1	8.608E-2
P_5	1	1.000	4.984E-2	4.253E-3
	2	4.016	6.003E-1	1.138E-1
	3	3.243	6.943E-1	1.634E-1
	4	1.071	3.131E-1	8.595E-2
P_7	1	1.000	4.977E-2	4.262E-3
	2	4.015	6.001E-1	1.138E-1
	3	3.242	6.940E-1	1.663E-1
	4	1.071	3.128E-1	8.588E-2
Modular	1	1.000	5.028E-2	4.253E-3
	2	4.023	6.014E-1	1.139E-1
	3	3.246	6.950E-1	1.635E-1
	4	1.072	3.133E-1	8.600E-2

Table 9.13: The integrated fluxes provided by Kobayashi for various regions of the core

Appr. Order	Group	Region I	Region II	Region III
P_1	1	1.000	5.512E-2	4.040E-3
	2	4.046	6.234E-1	1.149E-1
	3	3.275	7.120E-1	1.656E-1
	4	1.084	3.186E-1	8.681E-2
P_3	1	1.000	5.141E-2	4.263E-3
	2	4.031	6.034E-1	1.138E-1
	3	3.258	6.957E-1	1.632E-1
	4	1.077	3.128E-1	8.553E-2
P_5	1	1.000	5.113E-2	4.262E-3
	2	4.029	6.028E-1	1.138E-1
	3	3.255	6.955E-1	1.632E-1
	4	1.076	3.126E-1	8.550E-2
P_7	1	1.000	5.107E-2	4.260E-3
	2	4.028	6.027E-1	1.137E-1
	3	3.255	6.954E-1	1.632E-1
	4	1.076	3.126E-1	8.549E-2

Table 9.14: Neutronic parameters for the EIR-2 benchmark problem [49]

Material	Σ_a	$\upsilon\Sigma_f$	Σ_t	Σ_{s0}	Σ_{s1}	Σ_{s2}
1	0.07	0.079	0.60	0.53	0.27	0.10
2	0.28	0.0	0.48	0.20	0.02	0.01
3	0.04	0.043	0.70	0.66	0.30	0.20
4	0.15	0.0	0.65	0.50	0.15	0.10
5	0.01	0.0	0.90	0.89	0.40	0.10

boundary conditions are vacuum conditions all around the core region. Although the scattering cross sections are given up to the third order as can be seen in Table 9.14, this problem has been solved for the isotropic case. The results used for comparison have also been obtained for the isotropic scattering case. The geometry for the problem is given in Figure 9.12. The problem has been solved by using a 6x6 configuration. The outer iteration convergence criterion was chosen to be $1.0E-06$. M. Mordant has solved this problem by using three different computer codes [50]. The results presented in Table 2 in his paper are compared to the multiplication factor obtained by using the P_5 approximation. The P_1 and P_3 multiplication factors which are not in the Table 9.15 are 0.99996 and 1.00891 respectively. From the comparison given in Table 9.15, it is seen that the multiplication factor computed through the nodal method is very close to the results provided by Mordant. The largest difference between the nodal method result and those provided by Mordant is less than 0.04 %.

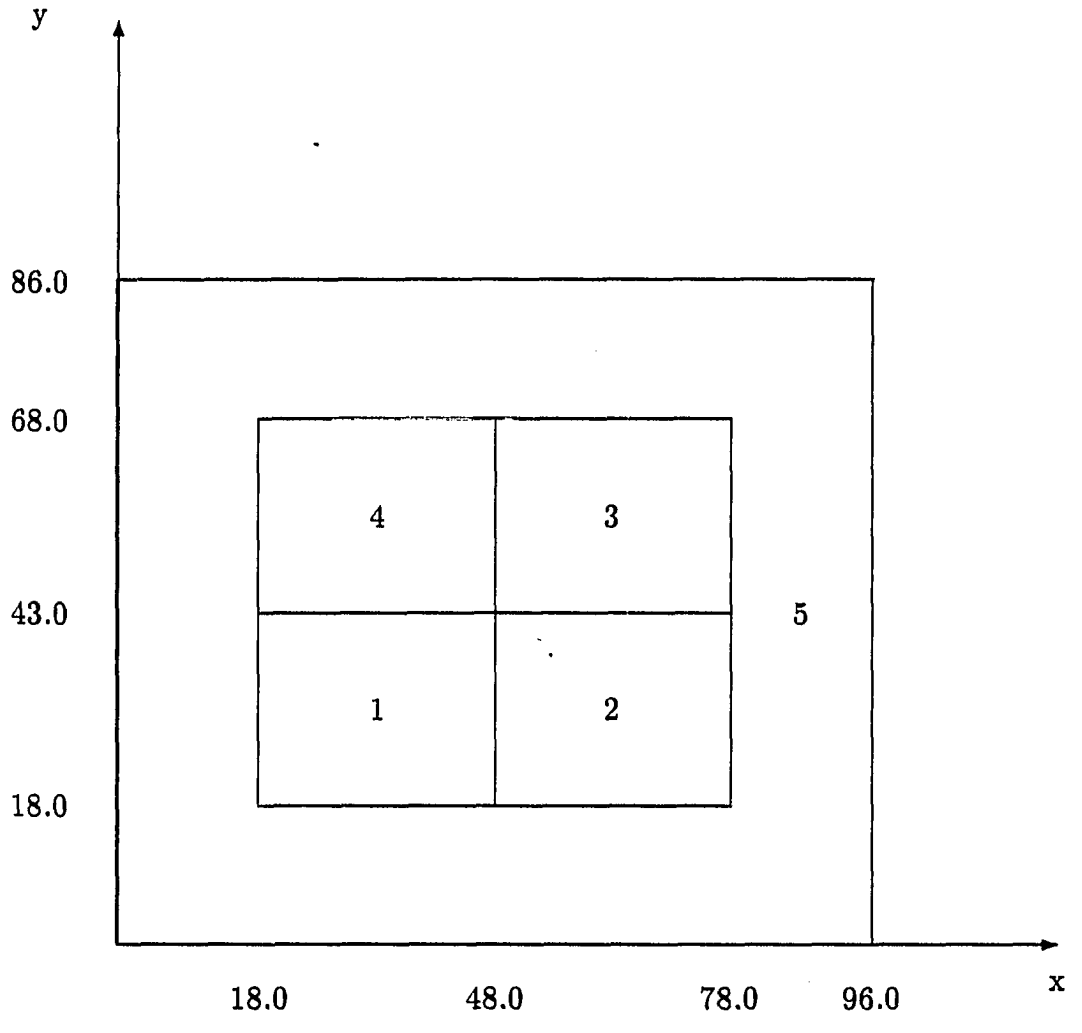

Figure 9.12: The geometry and dimensions for EIR-2 benchmark problem

Table 9.15: Comparisons of the multiplication factors for the EIR-2 problem [50]

Code	Mesh	Approximation	Multiplication Factor
NODAL METHOD	6x6	P_5	1.00917
SURCU	64x64	(1,1,1)	1.00882
SURCU	64x64	(2,2,2)	1.00890
TWODANT	120x120	S_8	1.00886
TWOTRAN-NODAL	64x74	S_8	1.00889
ZEPHYR-CD-D01	72x80	S_{ext}	1.00880
ZEPHYR-CD-D01	Fine mesh limit		1.00889
Error (+/- 2σ)			+/- 0.00004

10 SUMMARY AND CONCLUSIONS

The purpose of this research was to develop a modular nodal method for solving the neutron transport equation by using the spherical harmonic approximation. The project has been carried out for two-dimensional Cartesian geometry. In the development of the modular nodal method, the second order form of the even-parity neutron transport equation was used for manipulating the spherical harmonic differential equations. The second order spherical harmonic differential equations were put into a form such that they could be automatically generated with a computer code for any order. The boundary conditions for the spherical harmonic approximation have been manipulated to the same form as the partial currents used in diffusion equation applications. An algorithm for generating these boundary conditions automatically for rectangular regions was also developed. The simultaneous set of governing equations and boundary conditions were decoupled from each other by implementing an iterative scheme for solution. This resulted in a new form of the governing equations such that they all have a form analogous to the neutron diffusion equation. The modular nodal method was developed by using this final form of the governing equations and the boundary conditions.

In the development of the nodal method, the spherical harmonic moments were expanded into fourth order Legendre polynomials. A least squares minimiza-

tion scheme was used for determining the coefficients of the expansions for the spherical harmonic moments. The boundary conditions were implemented in an integral sense. In addition, the nodes with different orders for the spherical harmonic approximations were interfaced. An algorithm was developed for determining the spherical harmonic approximation order in each individual node.

The results of this dissertation can be evaluated by observing the following features of the developed method. One of the conditions a numerical method should satisfy is numerical stability of the method. The other condition which should be satisfied is the accuracy of the numerical scheme. In addition, if iterative schemes are employed by a numerical method, they should converge to a solution. A fourth condition which must be satisfied is that the modular method must comply with the physics of the problems and provide accurate results.

The stability of the numerical method was studied through Fletcher's problem. In that study, it was shown that the scalar flux values converge to some limiting values as the nodal sizes decrease. While the differences between the scalar flux values for the 4x4 and 5x5 nodal configurations were on the order of 0.1, the same quantity was 0.001 for the 6x6 and 8x8 nodal configurations. In addition, the results of the 4x4 nodal configuration were within a range reflecting the physics of the problem. Therefore, we can say that the stability condition were satisfied by the method.

The second test was the accuracy test. The accuracy was studied for five test problems. In Fletcher's problem, the scalar flux results agreed with Fletcher's results with a difference on the order of 1.0% while that difference increased significantly at the corner of the diagonal for the source region. For Natelson's problem,

the scalar flux results were within the 1.0% range of Kobayashi's results. For Gelbard's problem, the results were practically the same as the reference solutions except for P_3 approximation. For Kobayashi's criticality problem, the differences between the nodal method and Kobayashi's multiplication factors were less than 0.07%. The multiplication factor calculated for the EIR-2 benchmark problem were within 0.04% away from the results published by Mordant. These results show that the method passes the accuracy test although some questions arose from the comparison to Fletcher's problem.

Another consideration was to check how the implemented iterative schemes performed. The outer iteration, or the source iteration, and the middle iteration schemes converged for all test problems. The inner iteration seemed to have convergence problems for the spherical harmonic approximation orders higher than P_7. Since the P_7 approximation was high enough to solve most problems successfully, this did not pose any difficulty for these test problems.

The modular approach was tested for Gelbard's and Kobayashi's problems. The method has been successful in implementing automatic ordering of the spherical harmonic approximation in accordance with geometry for the specific problem. The method provided reasonably accurate results comparable to P_5 solutions although higher orders were used in some portions of the domain. One other important point is that the scalar flux was observed to be continuous at the interfaces where the spherical harmonic approximations were changed.

As a result of the discussion above, we can say that the modular nodal method is successful in meeting the goals of this research project. As with any research, many new questions appear. The inner iterative scheme requires more attention for

solving the convergence problem for high order spherical harmonic approximations. Also we need to further study the accuracy of the modular implementation.

11 SUGGESTIONS FOR FUTURE WORK

It is suggested that further study be conducted for the following areas.

1. The convergence properties of the inner iteration, where the simultaneous spherical harmonic differential equations are solved iteratively, should be studied in more depth and the convergence problems for some of the high orders of the spherical harmonics approximation should be resolved.

2. The convergence properties of the middle iteration, where the nodes are decoupled from each other and solved iteratively, can be studied and the convergence rate of that iteration enhanced.

3. The modular approach uses a relatively primitive scheme for choosing spherical harmonic orders for the nodes. Therefore, nodes implementing low order approximations can be seen among nodes using higher orders of the spherical harmonic approximation. A more sophisticated scheme can be devised for automatic ordering purpose. In addition, further work can be carried out for improving the accuracy of the modular method.

4. The current method can handle only isotropic scattering. Anisotropic scattering capability should be added to the method. This requires major modifications both in the nodal formulation and in the computer code.

5. The method can be extended to the three dimensional problems. This extension requires considerable amount of work in two areas. One of these is the manipulation of the spherical harmonic equations in three dimensions. A recurrence relation should be developed for generating three dimensional second order spherical harmonic equations automatically as was done in this dissertation for two dimensional problem. The other area is manipulation and generation of the boundary conditions in an automatic manner. If the least squares minimization approach is used for developing the nodal equations, these equations can be developed by using the three dimensional nodal method as the reference method.

12 BIBLIOGRAPHY

[1] C. Mark. The Spherical Harmonics Method I, CRT-340. Atomic Energy of Canada, Ltd., Ontario, 1944.

[2] C. Mark. The Spherical Harmonics Method II, CRT-338. Atomic Energy of Canada, Ltd., Ontario, 1944.

[3] R. E. Marshak. Note on the Spherical Harmonic Method As Applied to the Milne Problem for a Sphere. Physical Review, 71, No. 7, 443 (1947).

[4] B. Davison. Neutron Transport Theory. Oxford, New York, 1957.

[5] G. C. Pomraning and M. Clark. Nucl. Sci. Engr., 16, 147 (1963).

[6] J. A. Davis. Variational Vacuum Boundary Conditions for a P_N Approximation. Nucl. Sci. Engr., 25, 189 (1966).

[7] V. S. Vladimirov. Mathematical Problems in the One-Velocity Theory of Particle Transport. Atomic Energy of Canada, Ltd., Ontario, 1963.

[8] S. Kaplan and J. A. Davis. Canonical and Involutory Transformations of the Variational Problems of Transport Theory. Nucl. Sci. Engr., 28, 166 (1967).

[9] B. Anderson. FLIP, An IBM-704 Code to Solve the PL and Double-PL Equations in Slab Geometry. WAPD-TM-134, 1959.

[10] E. Gelbard. TRIP, A Two Dimensional P-3 Program in XY Geometry for the IBM-704. WAPD-TM-217, 1960.

[11] R. Gast. A P-9 Multigroup Method for Solution of Transport Equation in Slab Geometry. WAPD-232, 1960.

[12] P. Daitch. CEPTR, An IBM-704 Code to Solve P-3 Approximation to the One Velocity Transport Equation in Cylindrical Geometry, MPC-20, 1959.

[13] J. K. Fletcher. Further Work on the Solution of the Static Multigroup Neutron Transport Equation Using Spherical Harmonics. TRG Report 2849. UKAEA, 1976.

[14] J. K. Fletcher. The Solution of the Time-Independent Multi-group Neutron Transport Equation Using Spherical Harmonics. Ann. Nucl. Energy, 4, 401 (1977).

[15] J. K. Fletcher. The Solution of the Multigroup Neutron Transport Equation Using Spherical Harmonics. Nucl. Sci. Engr., 84, 33 (1983).

[16] J. K. Fletcher. A Solution of the Multigroup Neutron Transport Equation Using Spherical Harmonics. Transport Theory and Statistical Physics, 15, Nos. 1&2, 157 (1986).

[17] J. K. Fletcher. Recent Developments of the Transport Theory Code MARC/PN. Progress in Nuclear Energy, 18, No. 1/2, 75 (1986).

[18] K. Kobayashi, H. Oigawa and H. Yamagata. The Spherical Harmonics Method for the Multigroup Transport Equation in XY Geometry. Ann. Nucl. Energy, 13, No. 12, 663 (1986).

[19] G. G. Bilodeau and et al. PDQ An IBM-704 Code to Solve the Two Dimensional Few Group Neutron Diffusion Equations. WAPD-TM-70, 1957.

[20] D. L. Delp, D. L. Fischer, J. M. Harriman and M. J. Stedwell. FLARE A Three Dimensional Boiling Water Reactor Simulator. GEAP-4598, 1964.

[21] N. K. Gupta. Nodal Methods for Three Dimensional Simulators. Progress in Nuclear Energy, 7, 127 (1981).

[22] M. R. Wagner. Nodal Synthesis Method and Imbedded Flux Calculations. Trans. Am. Nucl. Soc., 18, 152 (1974).

[23] F. Bennewitz, H. Finnemann and H. Moldaschl. Solution of The Multidimensional Neutron Diffusion Equation by Nodal Expansion. Proc. Conf. Computational Methods in Nuclear Engineering. USAEC CONF-750413, 1975.

[24] R. A. Shober, R. N. Sims and A. F. Henry. Two Nodal Methods for Solving Time-Dependent Group Diffusion Equations. Nucl. Sci. Engr., 64, 582 (1977).

[25] R. D. Lawrence and J. J. Dorning. A Nodal Green's Function Method for Multidimensional Neutron Diffusion Calculations. Nucl. Sci. Engr., 76, 218 (1980).

[26] M. R. Wagner and K. Koebke. Progress in Nodal Reactor Analysis. Proceedings of A Topical Meeting on Advances in Reactor Calculations, ANS, Salt Lake City, Utah, 1983.

[27] R. D. Lawrence. Progress in Nodal Methods for the Solution of the Neutron Diffusion and Transport Equations. Progress in Nuclear Energy, 17, No. 3, 271 (1986).

[28] A. F. Rohach. A Polynomial Nodal Model Using Legendre Expansions. Ann. Nucl. Energy. 13, No. 2, 57 (1986).

[29] A. F. Rohach. A Legendre Polynomial Nodal Model for 2-D Diffusion Problems. Ann. Nucl. Energy, 13, No. 10, 549 (1987).

[30] A. F. Rohach. A Legendre Polynomial Nodal Model for 3-D Diffusion Problems. Ann. Nucl. Energy, 14, No. 12, 653 (1987).

[31] A. F. Rohach. Department of Nuclear Engineering, private communications, 1987.

[32] M. R. Wagner. A Nodal Discrete-Ordinates Method for the Numerical Solution of the Multidimensional transport equation. Proc. Conf. Computational Methods in Nuclear Engineering, ANS, Williamsburg, VA, 1979.

[33] R. D. Lawrence and J. J. Dorning. A Discrete Nodal Integral Transport Theory Method for Multidimensional Reactor Physics and Shielding Calculations. Proc. Conf. Advances in Reactor Physics and Shielding, ANS, Sun Valley, Idaho, 1980.

[34] W. F. Walters and R. D. O'Dell. Nodal Methods for Discrete-Ordinates Transport Problems in XY Geometry. Proc. Conf. Advances in Mathematical Methods for the Solution of Nuclear Engineering Problems, Munich, 1980.

[35] R. F. Pevey. ORNL/CSD/TM-182. Oak Ridge National Laboratory, 1982.

[36] I. Dilber and E. E. Lewis. Variational Nodal Methods for Neutron Transport. Nucl. Sci. Engr., 91, 132 (1985).

[37] M. Feiz. Development of a Polynomial Nodal Model to the Multigroup Transport Equation in One Dimension. Ph.D. Dissertation, The Iowa State University, 1986 (unpublished).

[38] M. Feiz and A. F. Rohach. Development of A Legendre Polynomial Nodal Model for the Multigroup Transport Theory P_N Approximation. Ann. Nucl. Energy. 15, No. 8, 389 (1988).

[39] A. F. Henry. Nuclear Reactor Analysis. MIT Press, Cambridge, Mass., 1975.

[40] G. I. Bell and S. Glasstone. Nuclear Reactor Theory. Van Nostrand Reinhold, New York, 1970.

[41] J. J. Duderstadt and L. J. Hamilton. Nuclear Reactor Analysis. John Wiley & Sons, New York, 1976.

[42] E. E. Lewis and W. F. Miller. Computational Methods of Neutron Transport. John Wiley & Sons, New York, 1984.

[43] P. M. Morse and H. Feshbach. Methods of Theoretical Physics. McGraw-Hill, New York, 1953.

[44] K. Kobayashi. An Acceleration Method of the Iteration Calculation Using the Pade Approximation in the Spherical Harmonics Method. Ann. Nucl. Energy, 15, No. 5, 235 (1988).

[45] H. Greenspan, C. N. Kelber and D. Okrent. Computing Methods In Reactor Physics. Gordon and Breach Science Publishers, New York, 1968.

[46] MACSYMA. Symbolics, Inc., Cambridge, Mass., 1983.

[47] M. Natelson. Variational Derivation of Discrete Ordinate-Like Approximations. Nucl. Sci. Engr., 43, 131 (1971).

[48] E. M. Gelbard and B. Crawford. ANL-7416 (Suppl. 2), 1977.

[49] A. Kavenoky, J. Stepanek, F. Schmidt. Transport Theory and Advanced Reactor Calculations. IAEA-TECDOC-254, 1981.

[50] M. Mordant. Phase-Space Finite Elements Encoded in Zephyr for XY and RZ Transport Calculations. Progress in Nuclear Energy, 18, No. 1/2, 27 (1986).

13 ACKNOWLEDGEMENTS

The author thanks his major professor Dr. Alfred F. Rohach for his interest, support and suggestions during this research project. In addition to that, he also expresses his thanks to all of the Nuclear Engineering faculty for their contribution to his graduate study at the department. In addition to the work at the department, the opportunity provided by Dr. Joe Gray at the NDE center contributed to author's education significantly. The author is also indebted to his wife, Oya, for her support and for her sacrifices she made by postponing her own career and by staying away from home. The author also wishes to thank his parents Emine and Mehmet Emin Inanc for their support all through his life. The special thanks go to the Turkish taxpayers who made the author's graduate study possible through their financial support.

14 APPENDIX

The expressions given below are for calculating the coefficients used in the recurrence relations for generating the second order spherical harmonic differential equations.

$$A_1 = -\left[(4l^3 + 10l^2 + 2l - 4) + (4l - 2)m^2\right]$$

$$A_2 = -\left[(4l^3 + 2l^2 - 6l) + (4l + 6)m^2\right]$$

$$A_3 = 32l^3 + 48l^2 - 8l - 12$$

$$B_1 = -\left[(4l^3 + 2l^2 - 6l) - (8l^2 + 8l - 6)m + (4l + 6)m^2\right]$$

$$B_2 = -\left[(4l^3 + 10l^2 + 2l - 4) + (8l^2 + 8l - 6)m + (4l - 2)m^2\right]$$

$$C_1 = (1 + \delta(2 - m))(3 + 2l)$$

$$C_2 = (2l^5 - 9l^4 + 4l^3 + 21l^2 - 18l) - (8l^4 - 24l^3 - 10l^2 + 54l - 18)m + (12l^3 - 18l^2 - 32l + 33)m^2 - (8l^2 - 18)m^3 + (2l + 3)m^4$$

$$C_3 = (1 + \delta(2 - m))(1 - 2l)$$

$$C_4 = -(1+\delta(2-m))(2l+3)$$

$$C_5 = -(2l^5+3l^4-4l^3-3l^2+2l)+(8l^3+4l^2-8l+2)m+$$
$$(4l^3+2l^2-12l+5)m^2-(8l-4)m^3-(2l-1)m^4$$

$$C_6 = -(2l^5+7l^4+4l^3-7l^2-6l)+(8l^3+20l^2+8l-6)m+$$
$$(4l^3+10l^2-4l-15)m^2-(8l+12)m^3-(2l+3)m^4$$

$$C_7 = (1+\delta(2-m))(2l-1)$$

$$C_8 = (2l^5+19l^4+60l^3+65l^2-2l-24)+(8l^4+56l^3+110l^2+30l-50)m+$$
$$(12l^3+54l^2+40l-35)m^2+(8l^2+16l-10)m^3+(2l-1)m^4$$

$$D_i = 2C_i \quad for \quad i = 1,2,3,4,5,6,7,8$$

$$\acute{A}_i = A_i \quad for \quad i = 1,2,3$$

$$\acute{B}_i = B_i \quad for \quad i = 1,2$$

$$\acute{C}_i = C_i \quad for \quad i = 1,2,3,4,5,6,7,8$$

$$\acute{D}_i = D_i \quad for \quad i = 1,3,4,7$$

$$\acute{D}_i = -D_i \quad for \quad i = 2,5,6$$